DISSERTATIONS IN
HEALTH SCIENCES

Aki T. Heikkinen

Interplay of Passive and Active Drug Disposition in in vitro Models of Drug Absorption and Distribution

Publications of the University of Eastern Finland
Dissertations in Health Sciences

UNIVERSITY OF
EASTERN FINLAND

AKI T. HEIKKINEN

Interplay of Passive and Active Drug Disposition in in vitro Models of Drug Absorption and Distribution

To be presented by permission of the Faculty of Health Sciences,
University of Eastern Finland for public examination
in auditorium ML2, Medistudia building, University of Eastern Finland, Kuopio,
on Friday 4th of June 2010, at 12 noon.

Publications of the University of Eastern Finland
Dissertations in Health Sciences
15

School of Pharmacy
Faculty of Health Sciences
University of Eastern Finland
Kuopio
2010

Kopijyvä Oy,
Kuopio, 2010

Series Editors:

Professor Veli-Matti Kosma, MD, PhD
Department of Pathology
Institute of Clinical Medicine
School of Medicine
Faculty of Health Sciences

Professor Hannele Turunen, PhD
Department of Nursing Sciences
Faculty of Health Sciences

Distribution:

Eastern Finland University Library/Sales of Publications
P.O.Box 1627, FI-70211 Kuopio, FINLAND
http://www.uef.fi/kirjasto

ISBN: 978-952-61-0138-5
ISBN: 978-952-61-0139-2 (PDF)
ISSN: 1798-5706
ISSN: 1798-5714 (PDF)
ISSNL: 1798-5706

Authors address: School of Pharmacy
Faculty of Health Sciences
University of Eastern Finland
P.O.Box 1627,
FI-70211 Kuopio, Finland
aki.t.heikkinen@gmail.com

Supervisors: Professor Jukka Mönkkönen, PhD
School of Pharmacy
Faculty of Health Sciences
University of Eastern Finland
Kuopio, Finland

Timo Korjamo, PhD
R&D, Translational Sciences
Orion Corporation, Orion Pharma
Espoo, Finland

Reviewers: Professor Olavi Pelkonen, MD, PhD
Institute of Biomedical Sciences
Department of Pharmacology and Toxicology
University of Oulu
Oulu, Finland

Sibylle Neuhoff, PhD
Simcyp Limited
Sheffield, UK

Opponent: Associate Professor Anna-Lena Ungell, PhD
AstraZeneca R&D *[Bioau]*, Research Area CV/GI
Mölndal, Sweden

Heikkinen, Aki T. Interplay of Passive and Active Drug Disposition in *in vitro* Models of Drug Absorption and Distribution. Publications of the University of Eastern Finland. Dissertations in Health Sciences, 15. 2010. 105 p.

ABSTRACT

Permeation through the intestinal epithelia is a major barrier for oral drug delivery, which is the most often utilized administration route. Therefore, there is considerable interest in developing ways to reliably predict epithelial permeation early on in the drug discovery - development process. Consequently, several *in vitro* assays are utilized to gain insight into the mechanisms involved in permeation as well as to screen the compounds for their transport characteristics. However, the predictive value of these *in vitro* methods relies to a great extent on the appropriate interpretation and thorough understanding of the *in vitro* data.

In vitro permeation experiments with cultured cell monolayers have been applied successfully for the prediction of the extent of intestinal absorption of compounds which are primarily transported via the passive transcellular route. However, simple extrapolation from the apparent *in vitro* permeability to the *in vivo* intestinal absorption is less reliable when paracellular permeation or active transporters are significantly involved in permeation through the epithelia. A key characteristic of active transport is its saturability, especially in the intestine where the drug concentrations are high. Thus, successful prediction of the active transport must account for the concentration dependency. Simple membrane based assays as well as cell monolayer permeation experiments have been applied for studies of concentration dependent transporter function. However, the reported *in vitro* determined kinetic parameters describing the transporter saturation are inconsistent. Consequently, the extrapolation to the *in vivo* setting remains challenging.

The main focus of the present study was the interplay of active and passive drug disposition in *in vitro* cellular permeation models. The effects of the experimental conditions on the apparent permeability and active transport were examined. Furthermore, drawbacks of the data analysis approaches traditionally applied in permeation experiments were investigated. Additionally, the pH and the protein concentration were shown to alter the observed P-glycoprotein ATPase activation kinetics in a membrane based assay. These results provide further insights into the dynamics of the drug disposition kinetics in epithelial permeation as well as on the confounding factors involved in *in vitro* experimental settings. Moreover, the compartmental model based analysis applied for the *in vitro* permeation data seems to be a promising approach for determining transporter kinetics.

National Library of Medicine Classification: QV 38, WB 350, WI 400, WI 402, QS 532.5.E7, QU 120

Medical Subject Headings: Pharmaceutical Preparations; Pharmacokinetics; Administration, Oral; Intestinal Absorption; Epithelium; Epithelial Cells; Intestinal Mucosa; Permeability; Biological Transport; Cells, Cultured; Cell Membrane; Hydrogen-Ion Concentration; Proteins; P-Glycoprotein; Adenosine Triphosphatases; Research Design; *In vitro*

Heikkinen, Aki T. Lääkeaineiden passiivinen ja aktiivinen kulkeutuminen lääkeaineimeytymisen ja –jakautumisen *in vitro* malleissa. Itä-Suomen yliopiston julkaisuja. Terveystieteiden tiedekunnan väitöskirjat, 15. 2010. 105 p.

TIIVISTELMÄ

Lääkeaineen kyky kulkeutua ruoansulatuskanavan epiteelisolukon läpi on eräs merkittävimmistä suun kautta annosteltujen lääkeaineiden imeytymistä rajoittavista tekijöistä. Tämän vuoksi useita *in vitro* menetelmiä käytetään jo lääkekehityksen alkuvaiheessa lääkeaineiden läpäisykyvyn ennustamiseksi ja sopivien lääkeainekandidaattien seulomiseksi. Näiden menetelmien ennustearvo kuitenkin perustuu merkittävässä määrin saatujen tulosten oikeaan tulkintaan ja perinpohjaiseen ymmärtämiseen.

Soluviljelmissä kasvatetuilla epiteelisoluilla tehtäviä lääkeaineiden läpäisykokeita on onnistuneesti käytetty ennustamaan lääkeaineiden imeytymistä ruoansulatuskanavasta, kun pääasiallinen imeytymismekanismi on passiiviseen diffuusioon perustuva kulkeutuminen solukalvojen läpi. Toisaalta *in vitro* havaitun läpäisyn kyky ennustaa kliinistä lääkeaineiden imeytymistä on osoittautunut heikommaksi, kun lääkeaineen kulkeutuminen soluvälitilan kautta tai aktiiviset kuljetusprosessit vaikuttavat merkittävästi lääkeaineen imeytymiseen. Eräs aktiivisen kuljetuksen tärkeimmistä ominaisuuksista on saturoituvuus eli riippuvuus lääkeainepitoisuudesta, joka tulisi ottaa huomioon ennustettaessa aktiivisesti kuljetettavien lääkeaineiden imeytymistä. Aktiivisten kuljetusprosessien pitoisuusriippuvuuden tutkimiseen on sovellettu sekä eristetyillä solukalvoilla että elävillä soluilla suoritettavia *in vitro* kokeita. Kirjallisuudessa raportoiduissa pitoisuusriippuvuutta kuvaavissa parametreissa on kuitenkin suurta vaihtelua ja näiden *in vitro* tulosten hyväksikäyttäminen kliinisen lääkeaineiden imeytymisen ennustamisessa on osoittautunut erittäin haastavaksi.

Tässä väitöskirjatyössä keskityttiin pääasiassa passiivisen kulkeutumisen ja aktiivisen kuljetuksen yhteistoimintaan *in vitro* soluläpäisykokeiden aikana. Tutkimuksessa selvitettiin koeolosuhteiden vaikutuksia havaittuun läpäisykykyyn ja aktiiviseen kuljetukseen. Lisäksi pH:n ja proteiinipitoisuuden osoitettiin vaikuttavan havaittuun P-glykoproteiinin ATPaasi -aktivaatiokinetiikkaan eristetyillä solukalvoilla suoritetuissa kuljetusproteiinin aktiivisuuskokeissa. Nämä tulokset antavat lisätietoa passiivisen ja aktiivisen kulkeutumisen dynamiikasta sekä useista häiritsevistä tekijöistä koeasetteluissa. Lisäksi tämän väitöskirjatyön tulokset osoittavat matemaattisiin monitilamalleihin perustuvan tulosanalyysin olevan lupaava lähestymistapa aktiivisten kuljetusproteiinien toiminnan tutkimuksessa.

Yleinen suomalainen asiasanasto: lääkeaineet; lääkkeet; kulkeutuminen; imeytyminen; farmakokinetiikka; ruoansulatuselimet; suolisto; solut; solukalvot; epiteeli; läpäisevyys; pH; proteiinit

It would be so much better if we called most of them models rather than theories. Then we would not have to defend their truth but only their usefulness. Most of us need models in order to think.

G. Scatchard, *Discuss. Faraday Soc.*, 1956, 21, 27

Acknowledgements

The present study was carried out in the Department of Pharmaceutics, University of Kuopio during the years 2005-2009 and finalised in the School of Pharmacy, Faculty of Health Sciences, University of Eastern Finland in 2010.

This research has been funded by the Finnish Foundation for Technology and Innovation (TEKES) and the Graduate School for Pharmaceutical Research (GSPR). Additionally, University of Kuopio, The Finnish Pharmacists' Association and The Finnish Pharmaceutical Society have provided financial support for my PhD studies.

I thank Professor Jukka Mönkkönen, my principle supervisor, Dean of the Faculty of Health Sciences, for believing in me and my research during the whole course of my PhD work. You gave me plenty of freedom to take my research in the direction I found most interesting, but still guided my work when I did not know where to proceed or which track to choose. I also thank Professor Arto Urtti, my second supervisor during the very early days of this work, whose original ideas contributed significantly at the starting point of present study and for the general direction these studies have taken. Unfortunately, the practical issues with schedules prevented me from taking the full advantage of his expertise. I am also greatful to Timo Korjamo, PhD, who replaced Professor Urtti as my second supervisor a couple of years ago. You have given me many useful comments and much guidance during the days you have been officially my supervisor. However, especially I would like to thank you for the invaluable practical and scientific guidance you provided during the early days, when you were not officially my supervisor and were still preparing your own thesis. However busy you were with your own work, you had always time for my not-always-very-intelligent speculations. I hope also you received something back from me during those debates. Moreover, I have to admit that a significant part of the ideas underlying my studies probably came originally from your mind.

I am honoured to have Associate Professor Anna-Lena Ungell as my opponent and Professor Olavi Pelkonen and Sibylle Neuhoff, PhD, as the reviewers of my thesis. Thank you for your expert contributions.

The Master's thesis work of Varpu Lepikkö contributed significantly to paper IV. I thank you for your input. My other Master's thesis student, Outi Kolju, is also acknowledged for her work. Your thesis has served as an excellent source of references for me. I also thank and bow to Mr Markku Taskinen, without your skilful assistance these experiments may never have been completed and one should not overlook your invaluable work in fine tuning the methodologies and keeping the lab running. I also highly appreciate the way you questioned ways of doing things when needed. My little brother Olli Heikkinen, BSc, I owe thanks for the mind broadening discussions during the early phase of the model development for the paper II and, more importantly, listening to (or at least convincingly pretending to) my sometimes never ending

babbling about almost anything. I also thank Ewen MacDonald, PhD, for his efforts to improve the English in my text.

Additionally, I have had the privilege to collaborate with many bright scientists during the years. Eva del Amo, MSc, thanks for bringing an international breeze into our group and especially for the most inspiring collaboration with the P-gp review. Sanna Siissalo, PhD, Jussi Malkki, MSc, and all the other individuals involved with the IVIVC and IVIVRe projects are also acknowledged. Without all you people working for these projects my PhD studies may never have even started. Kirsi Myöhänen, PhD, I thank you for the introducing me to the interesting world of placental perfusion. I must not neglect the impact of Professor Per Artursson, Gunilla Englund, PhD, and Pär Matsson, PhD. I was privileged to conduct lab work for my Master's thesis under your guidance in Uppsala during the fall 2004. Your reassuring words during those days encouraged me to proceed to my PhD.

Marjukka Suhonen, PhD, Jenni Hakkarainen, MSc, and Heidi Kemiläinen, MSc, I thank you for taking me into your coffee group in the early days and all the scientific and non-scientific discussions we had. Additionally, I am grateful to Heidi for making the crucial decision which opened the doors for me. I also thank 'the researchers of an alternative reality' Doctors Riikka Laitinen and Jari Pajander for sharing with me their ever so positive thoughts of life, science and everything while I have been sipping my coffee in regular *Terapiatuoli* sessions during the last year or so. Also all the guys in the floorball teams I have played over the years have to be acknowledged for helping me to hold on both my mental and physical health. Moreover, to *The Apes*, i.e. Anssi, Kimmo, Paavo, Tero, Timo, Toni, Vesa and Ville, I owe a huge thanks for the good times spent during the past decade and especially for helping me to keep 'fit' by arranging annual 'sports' events.

I also want to thank_____(add your name here iff applicable) for being interested enough in my thesis to read it through.

Furthermore, I thank my parents Paula & Matti and my siblings, Esa, Sanna & Olli (him again). Without you, I wouldn't be me.

Last and foremost, I want to express my deepest gratitude to my beloved wife Henna and my son Topi simply for just being there. Words are not enough to express how much you mean to me.

Kuopio, May 2010

Aki Heikkinen

List of original publications

This doctoral thesis is based on the following original publications:

I Heikkinen A.T., Mönkkönen J.: Protein concentration and pH affect the apparent P-glycoprotein ATPase activation kinetics, Int J Pharm 346: 169-172, 2008.

II Heikkinen A.T., Mönkkönen J., Korjamo T.: Kinetics of cellular retention during Caco-2 permeation experiments: Role of lysosomal sequestration and impact on permeability estimates, J Pharmacol Exp Ther 328:882-892, 2009.

III Heikkinen A.T., Mönkkönen J., Korjamo T.: Determination of permeation resistance distribution in *in vitro* cell monolayer permeation experiments. Eur J Pharm Sci 40: 132-142, 2010.

IV Heikkinen A.T., Korjamo T., Lepikkö V., Mönkkönen J.: Effects of experimental setup on the apparent concentration dependency of active efflux transport in *in vitro* cell permeation experiments. Mol Pharmaceutics 7: 605-617, 2010.

Additionally, some parts of the literature review in this thesis are adapted with permission from a previously published review article:

Heikkinen A.T., Korjamo T., Mönkkönen J.: Modeling the drug disposition kinetics in *in vitro* intestinal absorption cell models. Basic Clin Pharmacol Toxicol 106:180-188, 2010.

Contents

Abbreviations

A	Area of the cell monolayer
ABC	ATP binding cassette, a family of transporter proteins
ABL	Aqueous boundary layer, consists of barriers formed by porous support filter (when applicable) and the unstirred water layer (UWL)
A_{Pgp}	P-gp-ATPase activity
$A_{Pgp,0}$	Baseline of the P-gp-ATPase activity
$A_{Pgp,max}$	Maximum achievable P-gp-ATPase activity with a given activator
BCRP	Breast Cancer Resistance Protein, an ABC transporter encoded by ABCG2 gene
Caco-2	Human colon adenocarcinoma cell line
C_{ABL}	Average concentration within ABL
C_{api}	Concentration in the apical compartment
C_{baso}	Concentration in the basal compartment
C_{bulk}	Concentration in the bulk phase
C_{cell}	Total cellular concentration
$C_{cell,free}$	Free cellular concentration
C_{d0}	Concentration in the donor compartment at the beginning of the experiment
C_r	Concentration in the receiver compartment
C_{surf}	Concentration at the cell surface
<C>	Average system concentration
CYP	Cytochrome P450, a family of enzymes involved in drug metabolism
D_{aq}	Aqueous diffusion coefficient
DMSO	Dimethylsulfoxide
$EC_{50,K}$	The intracellular concentration resulting the cellular distribution coefficient (K) to be the average of maximum and minimum values
$EC_{50,Pgp}$	The concentration resulting in half maximum activation of P-gp-ATPase activity
F_A	Fraction absorbed
$_iP$	Inorganic phosphate, released in ATP hydrolysis
IVIVE	*In vitro – In vivo* extrapolation
K	Apparent cellular distribution cefficient, ratio of total and free cellular concentration
K_m	The intracellular free concentration resulting in 50% of the maximum P-gp mediated transport rate
$K_{m,app}$	The initial donor concentration (C_{d0}) resulting in 50% of the maximum effective P-gp mediated transport rate ($V_{max,app}$) in permeation experiments
K_{max}	Apparent maximum of K, approached asymptotically at low concentrations
K_{min}	Apparent minimum of K, approached asymptotically at high concentrations
LLC-PK_1	Porcine kidney cell line
M	Amount

MDCK	Madine Darby canine kidney cell line, strains I and II
MDCKII-MDR1	Transfected MDCK (strain II) cell line constitutively expressing human P-glycoprotein
MRP2	Multidrug resistance-associated protein 2, an ABC transporter encoded by the ABCC2 gene
P	Permeability
P_{ABL}	Permeability through an aqueous boundary layer
P_{api}	Composite permeability through the cell membrane and ABL at apical side
P_{app}	Apparent permeability
$P_{app,Palm}$	Apparent permeability determined using Equation 2.4. Accounts for the loss of sink conditions. 100% recovery assumed.
$P_{app,sink}$	Apparent permeability determined using Equation 2.3. Receiver sink conditions and 100% recovery assumed.
$P_{app,Tran}$	Apparent permeability determined using Equation 2.5. Accounts for the loss of sink conditions. Accounts for the changes in recovery as a first order process.
P_{baso}	Composite permeability through the cell membrane and ABL at basal side
P_i	Permeability of ionized species of the compound through a cell membrane
P_u	Permeability of unionized species of the compound through a cell membrane
PBPK	Physiologically based pharmacokinetics
P-gp	P-glycoprotein, an ABC transporter encoded by ABCB1 gene
Q_{12} and Q_{21}	First order cellular distribution rate coefficients from cytosolic to lysosomal and lysosomal to cytosolic compartment, respectively
SLC	Solute carriers, a family of transporter proteins
TEER	Transepithelial electrical resistance
UGT	Uridine diphosphate glucuronosyltransferase, a family of enzymes involved in drug metabolism
UWL	Unstirred water layer
V_{max}	Maximum P-gp mediated transport rate
$V_{max,app}$	Apparent maximum effective P-gp mediated transport rate in permeation experiments

1 Introduction

There is a constant need for new drugs. The inexorable development of bacterial resistance to current antibiotics creates a never-ending need for novel antibiotics (Walsh, 2003). In addition, treatments for several diseases, such as HIV and different types of cancer, would greatly benefit from new, more efficacious, drugs. However, the development of new drugs is expensive and time consuming (DiMasi et al., 2003), and these costs are translated at least in part into the price that society has to pay for the drug therapy. Therefore, efficacious tools to lower the costs and expedite the drug development process are of profound importance. The costs of drug development increase dramatically during the clinical phases of development. Therefore, although *in vitro* studies are not likely to ever obviate *in vivo* animal and clinical studies in drug development, the ability to produce reliable predictions of the *in vivo* behavior of drugs as early as possible during the drug discovery - development process would save time and resources needed to bring new drug molecules to the market.

The oral route is a convenient and the most often applied route for drug administration. However, the oral bioavailability of drugs may be limited by several factors, including inadequate solubility, slow dissolution and inappropriate stability of the drug within the intestine, poor ability to penetrate the gut wall and extensive metabolism within the gut wall and/or in the liver before reaching the systemic circulation (Dressman et al., 1998). Thus, one important prerequisite for an orally administered drug to reach the target site within the body is the ability to be transported in an intact form across the gut wall from the intestinal lumen to the mesenteric circulation. In addition, in order to reach the target site within the body, the drug often has to penetrate also other barrier tissues, such as the blood brain barrier when the drug target lies in the central nervous system. Therefore, the disposition characteristics of a molecule through the epithelial and endothelial barriers define to a great extent the suitability of the molecule as a drug.

Various *in vitro* approaches have been used to screen and predict the disposition of drugs through the epithelial and endothelial barriers of the body as well as to gain insights into the mechanisms involved. In this thesis, the passive and active drug disposition in *in vitro* models of drug absorption and disposition were explored with the emphasis on understanding the underlying mechanistic interplay. The discussion stems mainly from the viewpoint of intestinal absorption and permeation through the gut wall. However, majority of the results may also have implications to the drug disposition in other epithelial and endothelial barriers of the body.

2 Background of the study

2.1 GUT WALL PERMEATION

The gut wall permeation from intestinal lumen into circulation involves passage through series of barriers. The unstirred water and mucous layers on top of the epithelial cells may serve as rate limiting permeation barriers if the permeability through the epithelial cells is very high (Loftsson and Brewster, 2008). Furthermore, the rate of blood flow flushing the intestinal epithelia may serve as a rate limiting step for high permeability compounds (Cong et al., 2000). However, generally the above mentioned barriers are considered to play only a minor role *in vivo*, and for the majority of compounds the epithelial cells lining the gut wall are considered to be the primary barrier for gut wall permeation (Lennernäs, 2007).

The epithelial cells along the intestine, as well as along the crypt-villus axis, differ in several characteristics relevant for drug permeation (Figure 2.1), such as paracellular space (Fihn et al., 2000; Hollander, 1992) and expression levels of several transporters and drug metabolizing enzymes (Berggren et al., 2007; Englund et al., 2006). Furthermore, the site of absorption within the intestine and the epithelia involved may differ between drugs. Rapidly absorbed molecules are likely to use only the proximal part of the intestine whereas slowly absorbed molecules (whether the slow absorption is attributable to slow dissolution, slow release from the formulation or low permeability) are likely to be absorbed also from the distal parts of the intestine. In addition, only the villi tips are considered to contribute to the effective area for absorption of high permeability compounds whereas low permeability compounds are believed to diffuse further down along the crypt-villus axis and exploit larger absorptive surface area (Artursson et al., 2001; Strocchi and Levitt, 1993). However, this suggestion stems mainly from experimental results on anesthetized animals and, in contrast, a very recent analysis of literature data has casted some doubt on the validity of this hypothesis in awake human beings by suggesting that the whole surface area of epithelia would be available also for high permeability compounds (Avdeef and Tam, 2010). Due to the complexity of the mechanisms involved in the drug permeation through the gut wall, a single *in vitro* model can never fully appreciate all the factors involved. Therefore, rigorous prediction of intestinal absorption requires a thorough understanding of the underlying mechanisms both *in vivo* and *in vitro* (Ungell, 2004).

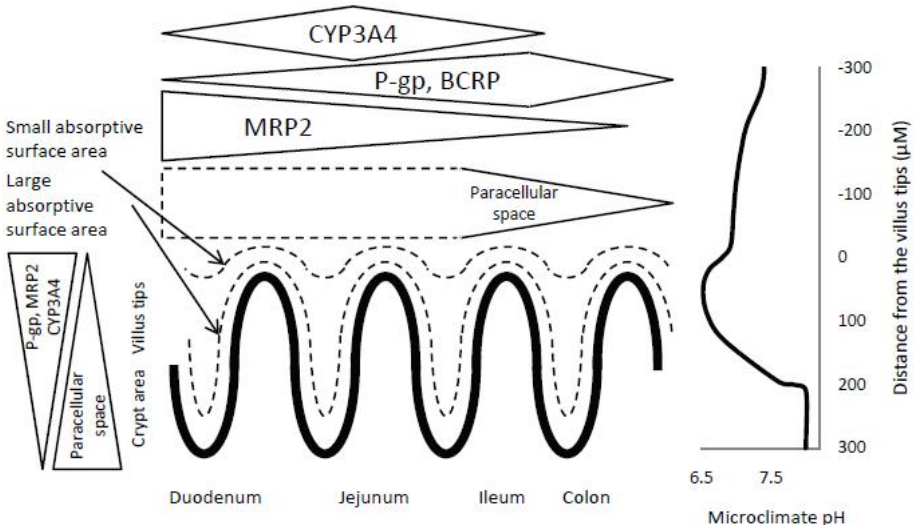

Figure 2.1. The spatial variation of factors affecting the gut wall permeation. The general trends of expression levels of selected transporters and metabolic enzymes are shown. The enterocytes migrate from the crypt area to the villi tips during maturation. Thus, the expression levels vary also along the crypt-villus axis. The paracellular space is tighter at the villi tips compared to crypt region and tighter in colon than in small intestine, whereas the data available suggests only minor differences in paracellular space between different segments of the small intestine (Markov et al., 2010)*. Only villi tips are considered to be available for absorption of high permeability compounds, whereas low permeability compounds have time to diffuse further down between the villi and exploit the larger surface area for absorption. The microclimate pH near the epithelial surface has been reported to vary between different segments of the intestine. Furthermore, microclimate pH varies also along the crypt-villus axis, the profile shown represents experimental data from rat jejunum* (Daniel et al., 1985)*. Compiled from* (Avdeef, 2003; Berggren et al., 2007; Chan et al., 2004; Dahan et al., 2009; Daniel et al., 1985; Englund et al., 2006; Fihn et al., 2000; Hollander, 1992; Matsson, 2007; Mouly and Paine, 2003; Neuhoff, 2005; Paine et al., 1997)

2.2 BARRIERS AND TRANSFER ROUTES INVOLVED IN EPITHELIAL PERMEATION

Barriers and transfer routes involved in epithelial permeation both *in vitro* and *in vivo* are summarized in Figure 2.2.

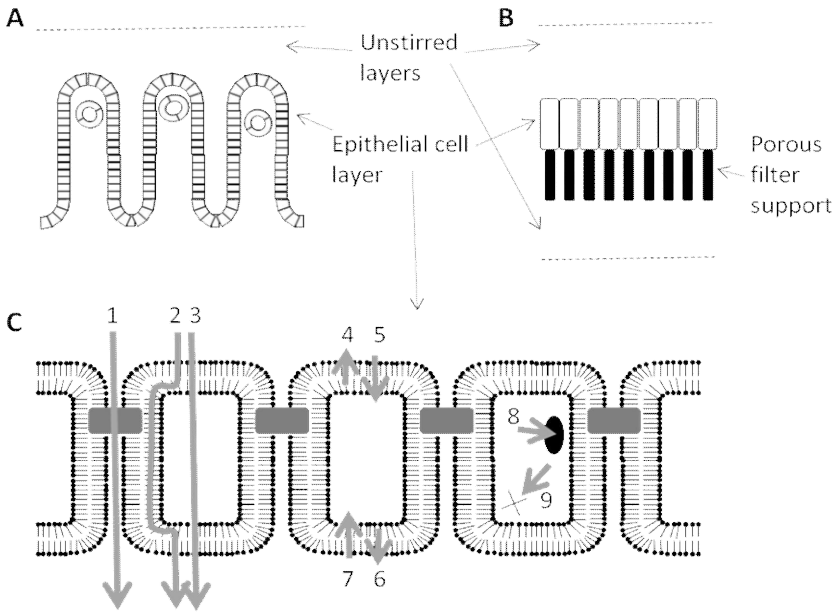

Figure 2.2. Schematic representation of the barriers and transfer routes in in vivo intestinal epithelia (A,C) and in in vitro cell monolayer permeation experiments (B,C). (A) In addition to the epithelial cell layer, the permeation barrier consists of the unstirred water and mucus layer at the luminal side in vivo. Additionally, the rate of blood flow flushing the basal side of the enterocytes may serve as the rate limiting step of the in vivo absorption of high permeability compounds. (B) The cell monolayer, the unstirred water layer on both sides as well as the porous filter support at the basal side form the permeation barrier in in vitro permeation experiments. (C) The transfer through epithelial cell layer may involve: (1) paracellular diffusion; (2) lateral diffusion via cell membrane; (3) transcellular diffusion through the cell membranes and the cytosol; (4,6) active efflux and (5,7) uptake through apical and basal cell membranes, respectively; (8) specific and unspecific binding/sequestration to the cellular structures and (9) intracellular metabolism.

2.2.1 Unstirred water layer/Aqueous boundary layer

Even when the bulk solution of a vessel is well stirred, there usually is a stagnant layer adjacent to the membrane surface. Consequently, when a drug permeates through the membrane, a concentration gradient can be formed to the vicinity of the surface (Barry and Diamond, 1984). This additional diffusion barrier is known as the unstirred water layer (UWL). UWL is not a clearly defined boundary; the concentration changes

gradually from the surface value to the bulk value (Pohl et al., 1998). However, for operational purposes the situation is often modeled as a completely unstirred region adjacent to the membrane followed by the bulk phase with a uniform concentration (Figure 2.3). The operational UWL thickness is defined by

$$\frac{dC}{dx} = \frac{C_{bulk} - C_{surf}}{h} \qquad \textit{Equation 2.1}$$

dC/dx is the concentration gradient adjacent to the membrane surface and is modeled as constant throughout the operational UWL thickness h. C_{bulk} and C_{surf} refer to the concentrations in the bulk phase and at the surface of the membrane, respectively.

The UWL thickness in the human intestine has been estimated to be approximately 100 µm under physiological conditions and is attributed mainly to the mucous layer covering the epithelia (Lennernäs, 2007). However, this estimate does not take into account the folded structure of intestinal epithelia and it has been suggested that if one considers the folded structure, the thickness of UWL would be approximately 300 µm (Sugano, 2009a).

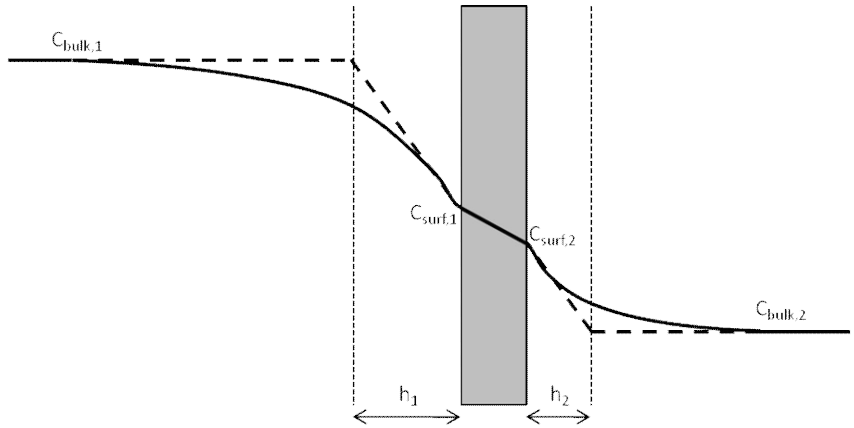

Figure 2.3. Schematic representation of the concept of unstirred layers as a permeation barrier. Solid curve represents a hypothetical concentration profile during steady state permeation; C_{bulk} and C_{surf} refer to the concentrations in the bulk phases and at the surfaces of the membrane (gray box), respectively. Dashed curve is the operational concentration profile and h_1 and h_2 are the operational thicknesses of the unstirred layer on both sides of the membrane. Compiled from (Barry and Diamond, 1984; Korjamo et al., 2009; Pohl et al., 1998).

The role of UWL as an intestinal absorption barrier *in vivo* is somewhat controversial in the recent literature. The estimated human *in vivo* jejunal effective permeability of two high-permeability compounds, D-glucose and antipyrine was not significantly affected by a fourfold change in single-pass perfusion rates (Fagerholm and Lennernäs, 1995). Consequently, it was concluded that UWL is not a significant absorption barrier *in vivo*

but, rather, the permeation rate of both high and low permeability compounds is controlled by the epithelial cell layer (Fagerholm and Lennernäs, 1995; Lennernäs, 2007). On the other hand, simulation studies aiming for explaining the observed enhancement of solubility limited intestinal absorption by bile micelle solubilisation, dose strength increase and particle size reduction have pointed to a clinically significant role of UWL as an absorption barrier for high permeability compounds *in vivo* (Sugano, 2009a; Sugano, 2010). Furthermore, the role of UWL as an *in vivo* absorption barrier has also been supported by kinetic modeling of the absorption of a P-glycoprotein substrate digoxin in the rat intestinal perfusion studies (Liu et al., 2006). This discrepancy could be explained by the superimposition of UWL and the intestinal mucuous layer. If the mucous layer would be sufficiently robust not to be significantly distracted by the flow of the perfusion media in intestinal perfusion experiments, the above mentioned observation by Fagerholm and Lennernäs would lead only to the conclusion that the putative unstirred layer above the mucous layer is not playing any role in the permeation barrier, but would not reveal anything about the role of the UWL caused by the undisturbed mucous layer. However, there is no experimental data available about the behavior of mucous layer in these kinds of experiments. Nonetheless, it is generally accepted that the contribution of UWL is significant *in vitro* (Adson et al., 1995; Avdeef et al., 2005; Korjamo et al., 2009; Yu and Sinko, 1997) and should thus not be neglected. UWL complicates the experimental determination of actual permeability through the biological permeation barrier of interest, especially of high permeability compounds, and thus makes the comparison of permeation data from different laboratories difficult. Moreover, UWL may hinder the determination of mechanisms involved in the permeation of the biological barrier as well as the elucidation of structure permeability relationships during drug discovery (Balakrishnan et al., 2007; Korjamo et al., 2009; Youdim et al., 2003).

In the current literature, the aqueous boundary layer (ABL) is sometimes used as a synonym for UWL. However, in *in vitro* cell monolayer permeation setting, also the support filter on which *in vitro* cell monolayers are cultured forms a permeation barrier. The disposition of a molecule through the support filter is attributed to the aqueous diffusion within the pores of the filter. Thus, the filter can be considered as an aqueous boundary for permeation, similarly to UWL. Consequently, in this thesis, the terminology of Balakrishnan and coworkers (2007) is adapted: the ABL consists of the UWL and also the porous support filter when applicable (i.e. at the basal side when cell monolayers are grown on support filters).

2.2.2 Passive cellular permeation

The epithelial permeation of rapidly absorbed compounds is considered to primarily occur passively via the transcellular route, whereas also other permeation routes and mechanisms may play an important role in the permeation of slowly absorbed compounds (Artursson et al., 2001). Passive transcellular permeation involves penetration across the apical cell membrane followed by diffusion through the cell cytosol and, finally, permeation across the basal cell membrane. Furthermore, very lipophilic compounds distribute exceedingly into the cell membranes and, thus, the involvement of diffusion via lateral cell membrane has also been hypothesized (Raub et al., 1993). Although several processes are involved, the permeation through the apical cell membrane is generally considered to be the rate limiting step of passive transcellular permeation *in vivo* (Lennernäs, 2007).

The majority of drug molecules are weak acids or bases. Thus, under physiological conditions, the drug molecules often exist in both ionized and neutral forms. Ionized and neutral forms have their own distinct characteristics in terms of distribution between lipid and aqueous phases and behavior in electrochemical gradients. Consequently, the neutral form is generally considered to be able to passively permeate through lipid membranes, whereas the passive permeability of ionized form is considered insignificant or even non-existent; a concept commonly known as the pH partition hypothesis (Shore et al., 1957). Therefore, the pH conditions at the surface of the intestinal epithelium may play a significant role in the permeation of the drugs through the gut wall. There is a considerable variation in the pH conditions within the intestine and consequently, the proportion of ionized and neutral forms may vary markedly between different locations. However, it is generally considered that the slightly acidic microclimate pH (Figure 2.1) at the surface of the intestinal epithelia is not directly regulated by the luminal pH (Avdeef, 2003; Legen and Kristl, 2003; Shiau et al., 1985).

In addition to the transcellular route, drugs may permeate the intestinal epithelia by diffusing via the paracellular space. However, the paracellular space is restricted by the tight junctions between the cells. Consequently, paracellular permeation is limited by the paracellular pore size, porosity and the paracellular path length (Avdeef, 2010). The paracellular permeation route is accessible for both ionized and neutral compounds. However, because of the negative charge of the cell surface, it has been suggested that paracellular permeability of neutral compounds would be lower than that of cations and higher than that of anions of same size (Adson et al., 1995; Karlsson et al., 1999; Linnankoski et al., 2009; Pade and Stavchansky, 1997). The paracellular pores have been estimated to have a radius of ≤10 Å and comprise only a fraction of about 10^{-5} of

the surface area of the epithelium of human small intestine (Linnankoski et al., 2009). On the other hand, the characteristics of paracellular route *in vitro* may vary significantly between cell lines and laboratories (Avdeef, 2010). Nonetheless, this permeation route is considered to play a significant role in the epithelial permeation only for relatively small hydrophilic compounds with poor cell membrane permeability (Artursson et al., 2001).

2.2.3 Active transport

Although the passive transfer through the cell membranes is a major determinant of the epithelial permeability, the involvement of active transporters in drug transport through the cell membranes has been recognized during recent decades (Al-Awqati, 1999). The solute carriers (SLC) and ATP binding cassette (ABC) transporters are the two major gene families among the cell membrane transporters involved in drug transport (Giacomini et al., 2010). The eukaryote ABC transporters are solely efflux transporters that utilize the energy of ATP to transport the drugs out of the cells independent of the direction of the substrate concentration gradient (Chang, 2003). On the contrary, the SLC family includes transporters which facilitate the transport of the substrates along the concentration gradient as well as secondary active transporters which exploit ion gradients for concentrative transport (Steffansen et al., 2004). Thus, depending on the location and transport direction of the transporter involved, transporters may regulate the intestinal absorption by either enhancing or inhibiting the gut wall permeation. However, SLC transporters are generally considered to facilitate intestinal absorption (Steffansen et al., 2004) whereas the majority of drug transporting ABC transporters, such as P-glycoprotien (P-gp), breast cancer resistance protein (BCRP) and multidrug resistance associated protein 2 (MRP2) impair intestinal absorption (Chan et al., 2004). The passive diffusion rate is linear with respect to drug concentration gradient, whereas the active transport is saturable. Consequently, the involvement of active transporter may result in nonlinearity in the intestinal absorption kinetics. At low doses, the transporter significantly contributes to (either increases or decreases) the absorption, whereas at high doses the absorption is primarily dictated by passive permeation. Furthermore, the inhibition or induction of drug transporters may result in drug-drug and food-drug interactions (Balayssac et al., 2005; Steffansen et al., 2004; Zhang et al., 2009).

2.2.4 Gut wall metabolism

In addition to the barriers for drug transfer, the permeation of a drug from the intestinal lumen into the mesenteric circulation may be restricted by metabolism within the enterocytes, mediated primarily by cytochrome P450 (CYP) and uridine diphosphate (UDP) glucuronosyl transferase (UGT) enzymes. Although the liver is the

primary site of drug metabolism, metabolism in the enterocytes has been shown to significantly contribute to the first pass metabolism of some drugs, such as the short-acting benzodiazepine midazolam (Paine et al., 1996; Thummel et al., 1996). Moreover, there is a significant overlap in the substrate specificities of the transporters and metabolic enzymes resulting in a complex interplay of active transport and metabolism during the permeation through the gut wall (Pang, 2003; Siissalo et al., 2010). Probably the best recognized of these is the interplay of P-gp with CYP3A4 (Knight et al., 2006).

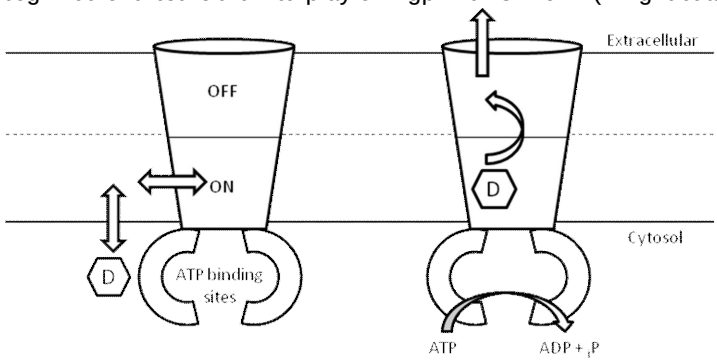

Figure 2.4. Schematic of the putative structure and translocation cycle of P-gp. The two transmembrane domains form together a funnel shaped binding pocket through the cell membrane. The transported substrate (D) reaches the ON-binding site located within the cell membrane presumably via the inner leaflet of the membrane. P-gp utilizes the energy from ATP hydrolysis to translocate the substrate to the low affinity OFF-site from where the substrate is released into the extracellular space. Compiled from (Ambudkar et al., 2006; Omote and Al-Shawi, 2006).

2.3 P-GLYCOPROTEIN

P-glycoprotein (P-gp), an efflux transporter, is a transmembrane protein containing two consecutive units which are composed of one ATP binding domain and a transmembrane domain containing six transmembrane helices. In the current literature, the name P-glycoprotein is generally used for this protein and the encoding gene is referred to as MDR1 (multidrug resistance), or as ABCB1 as proposed by The Human Gene Nomenclature Committee. The two transmembrane domains form together a binding pocket for transported substrates within the cell membrane (Figure 2.4). Putatively, the transported substrates bind to the ON-site of the binding pocket located within the inner lipid leaflet of the cell membrane. Subsequently, the ATP binding sites bind and hydrolyze ATP, releasing inorganic phosphate ($_{i}$P) and ADP, which provides the energy for translocation of the transported substrate from the ON-site of the binding pocket to the OFF-site of the binding pocket located at the outer lipid leaflet of the cell membrane from where the transported substrate is released to the extracellular space (Figure 2.4). However, the exact mechanism of P-gp action, i.e. the molecular

details of how ATP hydrolysis is coupled to transport, are still under debate. The recent insights to the molecular mechanism of action of P-gp have been reviewed in detail by Ambudkar et al (2006).

P-gp is often overexpressed in cancer tissues and is one of the mechanisms responsible for the cancer multidrug resistance by extruding several chemotherapeutic agents out from the cancer cells (Polgar and Bates, 2005). P-gp is also highly expressed in several healthy epithelial and endothelial tissues of the body, such as in the apical membrane of the enterocytes, canalicular membrane of the hepatocytes, brush border of proximal tubules of kidney and the apical membrane of the microcapillary endothelia constituting the blood brain barrier (Cordon-Cardo et al., 1989; Thiebaut et al., 1987). The transported substrates of P-gp include a variety of structurally unrelated xenobiotics, including several clinically important drugs, such as digoxin (Englund et al., 2004), some HIV protease inhibitors (Owen et al., 2005) and some anticancer agents (Schellens et al., 2000). Typically, P-gp substrates are relatively hydrophobic compounds that can form hydrogen bonds. Furthermore, the presence of tertiary amino groups and planar aromatic domains is promoting for an interaction with P-gp (Seelig and Landwojtowicz, 2000). However, within these broad criteria, there seems to be no further general structural similarities between P-gp substrates and the detailed molecular mechanism of substrate recognition of P-gp remains unknown (Omote and Al-Shawi, 2006). Because of the wide substrate specificity and the localization at several barrier tissues of the body, a physiological task of P-gp is considered to be the regulation of entry of potentially toxic xenobiotics into vulnerable tissues of the body (Cordon-Cardo et al., 1989). P-gp has been shown to inhibit the intestinal absorption and access into the central nervous system as well as enhancing the hepatic and renal elimination of P-gp substrates (Balayssac et al., 2005; Fromm, 2003). Furthermore, P-gp mediated transport has been suggested to contribute to the regulation of the substrate concentration at the metabolic sites in the hepatocytes (Lau et al., 2004) and enterocytes (Knight et al., 2006). Thus, P-gp may affect the pharmacokinetics of a wide range of compounds at several levels. In this respect, it is important to consider the contribution of P-gp when predicting the *in vivo* pharmacokinetics.

2.3.1 Experimental *in vitro* methods to study the drug - P-glycoprotein interaction

Due to of the evident role of P-gp in pharmacotherapy, the drug molecules are studied for their interaction with P-gp already in the early drug development phase (Balimane et al., 2006; Polli et al., 2001). A number of experimental approaches, including membrane based ATPase and vesicular transport assays as well as cell based cellular uptake and transcellular transport assays, have been established to identify and study

the functional interaction between drug molecules and P-gp. The information obtained from these assays as well as the time and other resources needed to perform the experiments vary with the different experimental approaches. Understanding the strengths and limitations of each methodology is essential for rational use of these assays and for appropriate interpretation of the results. However, although several methods are available, the U.S. Food and Drug Administration states in their draft guidance concerning drug interaction studies that "the transcellular transport assay should be used as a definitive method for identifying P-gp substrates and inhibitors" (FDA, 2006). Some characteristics of the different methods used to assess transporter interactions are summarized in Table 2.1. The membrane based ATPase and vesicular transport assays as well as cell based cellular uptake assays are briefly described below, whereas transcellular transport, i.e. cell monolayer permeation experiments are covered more comprehensively in Chapters 2.4 and 2.5. Similar experimental approaches are available also for studying other ABC transporters in addition to P-gp. Furthermore, vesicular transport, cellular uptake and transcellular transport assays can be modified for studying also other types of transporter proteins (Xia et al., 2007).

Table 2.1. Summary of the characteristics of different in vitro methods to study drug – P-gp interactions

	ATPase	Vesicular transport	Modulation of cellular uptake	Transcellular transport
Throughput	++++	+++	++	+
Membrane or cell based	Membrane	Membrane	Cell	Differentiated cell monolayer
Detection of inhibitors and substrates	Activators and inhibitors can be detected in separate experiments Risk of false positives and false negatives	Substrates and inhibitors can be detected in separate experiments	Detects, but does not distinguish, substrates and inhibitors simultaneously	Substrates and inhibitors can be detected in separate experiments
Detection method required	Independent of the compounds used Fast colorimetric measurement	Dependent on the compound traced	Dependent on the probe compound used, direct fluorometric detection often applied	Dependent on the compound traced
Detection of transport	No	Yes	No	Yes
Optimal drug concentration	Intermediate Dependent on the compound used	Low for substrates High for inhibitors	High	Low for substrates High for inhibitors

2.3.2 ATPase assay

P-gp is an ATP hydrolyzing protein and the energy provided is utilized for extrusion of the transported substrates out of the cell. In the absence of exogenous substrates, P-gp maintains a baseline level ATPase activity, possibly due to putative endogenous substrate(s) present in the lipid membrane (Borgnia et al., 1996). Usually, the presence of transported substrates markedly activates the ATPase activity of P-gp. This characteristic can be used to pinpoint the P-gp substrates by measuring the ATP hydrolysis rate. In addition, inhibitors of substrate activated P-gp-ATPase activity can be detected. In practice, the experiments are performed using the cell membrane fraction from P-gp expressing cells (Sarkadi et al., 1992; Xia et al., 2007) or with P-gp reconstituted into artificial lipid membranes (Borgnia et al., 1996). Cell membranes from transfected insect cells expressing human P-gp are often exploited in these studies. P-gp is incubated in the presence of ATP and the P-gp-ATPase activity is quantified by measuring the rate of $_{i}P$ release. P-gp must be in orientation exposing the ATP binding domains to the incubation medium in order to ATP to be accessible to P-gp. However, it is usually not known in detail in which proportion the lipid bilayer is oriented as right-side-out vesicles with ATP binding domain of P-gp located inside the vesicles (not accessible to ATP), or as inside-out vesicles or open lamellae with the ATP binding domain exposed to the incubation medium (Glavinas et al., 2008). Therefore, the exact amount of active P-gp in the assay is often not known and, thus, the ATPase activity per amount of P-gp cannot always be quantified accurately.

An additional characteristic hampering the use of ATPase activation studies in quantitative prediction of transport is the fact that these predictions must be based on an assumption of constant and substrate independent stoichiometry between ATPase activity and the transport rate. Indeed, results with a limited number of compounds support the correlation between ATPase activity and transport rate. However, the reported coupling ratios (molecules of ATP hydrolyzed per molecule transported) vary significantly for different substrates (Ambudkar et al., 1997; Ambudkar et al., 1999; Omote and Al-Shawi, 2002; Shapiro and Ling, 1998). However, the exact determination of the transport rate is challenging, especially of high permeability compounds. Thus, it can be speculated that variations in reported coupling ratios may reflect the variation in the experimental errors in the estimation of transport rates rather than a true substrate dependency of the coupling ratio. Consequently, the validity of the assumption of substrate independent stoichiometry remains to be clarified.

Although the above mentioned drawbacks in the use of P-gp-ATPase rate as a surrogate for transport of rate of substrates, this methodology has been successfully used to shed light into functional polymorphism (Sakurai et al., 2007) and species

differences of P-gp function (Xia et al., 2006). The ATPase assay has also been exploited to study the concentration dependency of the interaction between P-gp and substrates (Adachi et al., 2001; Xia et al., 2006). One postulated advantage of ATPase assay in such studies is the knowledge of the substrate concentration at the close vicinity of the binding site. The incubation medium in the ATPase experiments mimics the aqueous cytosol and, thus, the observed concentration dependency of ATPase activation is assumed not to be confounded by transmembrane movement rate of the substrate (Glavinas et al., 2008). Additionally, the straightforwardness of the assay, the possibility for use in the high throughput mode and the possibility to characterize the function of one specific transporter have made the ATPase assay an attractive and widely used screening method for P-gp interactions in the pharmaceutical industry (Feng et al., 2008; Glavinas et al., 2008; Polli et al., 2001; Xia et al., 2007). The goal of screening is to detect compounds susceptible either to P-gp mediated transport or to P-gp mediated interactions as P-gp inhibitors. Therefore, one needs to take into account that both false negatives and false positives with respect to experimentally detectable transport of the substrate are possible when using P-gp-ATPase measurements (Polli et al., 2001; Xia et al., 2007). Some of the highly P-gp-ATPase activating compounds are not detectably transported by P-gp whereas some compounds that are evidently transported by P-gp, such as cyclosporin A, do not exhibit any detectable activation of P-gp-ATPase. High ATPase activation without detectable P-gp mediated transport is associated with compounds with high lipid membrane permeability. The compounds may be transported by P-gp *per se*, but the passive diffusion is much faster than the P-gp mediated transport rate. Consequently, for these compounds the P-gp mediated transport can be difficult or impossible to detect experimentally. However, these types of compounds may act as competitive inhibitors of P-gp mediated transport in living cells (Polli et al., 2001). The evident P-gp mediated transport without P-gp-ATPase activation has been speculated to be due to their slow P-gp mediated translocation rate resulting in such a slow rate of ATP hydrolysis that it does not result in any detectable activation of the baseline level P-gp-ATPase activity (Glavinas et al., 2008).

2.3.3 Vesicular transport assay

Vesicular transport assays can be used either to trace the P-gp mediated transport of the compound of interest or to explore the modulation (inhibition) of P-gp mediated transport of a known P-gp substrate (Glavinas et al., 2008). Similar vesicular preparations to those utilized in P-gp-ATPase experiments can also be used for vesicular transport experiments. In these experiments, the accumulation of the experimental compound into the vesicles is measured and the difference in the accumulation rates in the absence and presence of ATP is attributed to P-gp mediated

transport. Similarly to the ATPase assay, the lipid bilayer in the preparation used should primarily be in the inside-out vesicle conformation because the P-gp in the right-side-out vesicles and open lamellae does not contribute to compound accumulation. Although the presence of these undesirable conformations in the membrane usually does not compromise the ability to detect transporter function, they may complicate the data analysis if a quantitative analysis is being performed (Glavinas et al., 2008). The advantage of this method compared to the ATPase assay is the fact that with this method, the actual P-gp mediated transport of the substrate is being determined. Furthermore, similarly to ATPase experiments, the drug concentration in the aqueous phase in close vicinity to P-gp is assumed not to be confounded by transmembrane disposition, thus simplifying the interpretation of the concentration dependency of the observed interaction (Glavinas et al., 2008). On the other hand, this method requires an individual detection method for each substrate, making the experiments more laborious and expensive. Furthermore, rigorous measurement of the P-gp mediated transport rate of high passive permeability substrates may be experimentally challenging, because the active transport is likely to be masked by the passive disposition (Xia et al., 2007). Consequently, vesicular transport assay is often applied as a screening tool for transporter inhibitors (Glavinas et al., 2008; Pedersen et al., 2008).

2.3.4 Modulation of cellular uptake assays

The modulation of uptake of known P-gp substrates into living cells can be used to study interactions between P-gp and drug molecules. The acetomethyl ester of calcein (calcein-AM) is a lipophilic P-gp substrate with high passive permeability through the cell membranes. The intracellular esterases rapidly cleave the ester bond inside the cell converting non-fluorescent calcein-AM into highly fluorescent calcein which is not able to permeate through the cell membranes. The P-gp mediated transport inhibits the influx of calcein-AM. Consequently, P-gp inhibition increases the cellular calcein-AM concentration leading to an increase in accumulation of calcein which can be readily detected. In addition to the calcein-AM assay, which is widely used as a screening tool for P-gp inhibitors (Feng et al., 2008; Polli et al., 2001), also other highly fluorescent probe P-gp substrates, such as daunorubicin and rhodamine 123, have been employed (Litman et al., 2003; Schwab et al., 2003).

The advantages of the cellular uptake assay include easy and fast experimental setup once the setup is optimized and the cells needed have been cultivated reproducibly. The assay potentially detects both substrates and inhibitors simultaneously, which can be regarded as an advantage in the screening setting. However, the downside of this methodology is the fact that the results do not provide information of the transfer of

the compound studied and, thus, it is impossible to differentiate substrates from inhibitors. In comparison with the membrane based ATPase and vesicular transport assays, the time and resources needed to cultivate the cells for the experiments represent further drawback to using cellular uptake assays in screening. Furthermore, the studied inhibitor has to permeate through the cell membrane in order to reach the intracellular binding site of P-gp. This may seriously complicate the data interpretation in concentration dependency studies (Litman et al., 2003). It should also be borne in mind that the specificity of the cellular uptake assay, alike any other cell culture assay, for a particular transporter is dependent on the expression levels of transporters in the cells used, as well as on the specificity of the probe substrate.

2.4 *IN VITRO* CELL PERMEATION EXPERIMENTS

In vitro cell permeation experiments are routinely used during drug development process for screening the intestinal absorption potential of compounds as well as for more detailed predictions of intestinal absorption (Artursson et al., 2001; Badhan et al., 2009; Balimane and Chong, 2005). Furthermore, these experiments are used for screening the transporter interactions that might complicate the pharmacokinetic behavior of the compound and also for a more thorough exploration of the mechanisms involved in drug disposition (Artursson et al., 2001; Balimane and Chong, 2005; Polli et al., 2001).

Several *in vitro* cell models, such as Caco-2 (a human colonic adenocarcinoma cell line), canine kidney derived MDCK (both strains I and II) and porcine kidney derived LLC-PK_1 have been used in *in vitro* cell permeation studies (Artursson et al., 2001; Balimane and Chong, 2005; Braun et al., 2000; Matsson et al., 2005). Although all the transfer routes relevant to intestinal absorption may, in principle, be present in *in vitro* cell models, the relative contribution of different routes tends to differ from the *in vivo* situation. Thus, none of the cell models established truly fully resembles the *in vivo* intestinal absorption barrier. The features of differentiated Caco-2 monolayer cultured on porous support filters mimic some of the characteristics of human intestinal epithelia. The cell membrane composition is assumed to be similar (Hidalgo, 2001; Ungell, 2004), and also the expression pattern of drug transporters is, although only qualitatively, similar (Englund et al., 2006; Hilgendorf et al., 2007). On the other hand, the paracellular space is tighter (Artursson et al., 2001; Avdeef and Tam, 2010) and the expression levels of drug metabolizing CYP enzymes are lower in wild type Caco-2 than in the human enterocytes *in vivo* (Crespi et al., 2000; Engman et al., 2001; Ungell, 2004). Compared to Caco-2, an advantage of MDCK and LLC-PK_1 cell lines is their faster growth and differentiation in culture. The expression levels of endogenous transporters in these cell lines is considered to be low, but not completely absent

(Braun et al., 2000; Goh et al., 2002). Thus, these cell lines are considered to be suitable and are widely used, after transfection with transporter encoding genes, for studying the function of selected transporters (Balimane and Chong, 2005).

Most of the cellular permeation experiments used to model intestinal absorption are performed using the Transwell system where the cell monolayers are cultured on porous membranes. Typically, the drug is applied to the apical liquid compartment (representing the luminal side of the enterocytes). Then, the appearance of the drug to the basal liquid compartment (representing the circulation within the capillaries embedded in the *lamina propria*) is monitored as a function of time and the apparent permeability (P_{app}) through the cells is determined by relating the observed transport rate to the concentration gradient driving the transport (Hubatsch et al., 2007). Additionally, the involvement of active transporters may readily be probed by performing the experiments also in the opposite, i.e. basal to apical, direction. Also the possible concentration and pH dependencies of the drug transfer can be easily tested (Neuhoff et al., 2003; Polli et al., 2001). Furthermore, in more detailed mechanistic studies, both the disappearance from the donor and the appearance into the receiver compartment as well as retention within the cell monolayer may be determined (Bartholome et al., 2007). However, one of the restrictions for multiple measurements in a single experiment is the limited liquid compartment volume and consequent inevitable depletion of the compound into samples as well as the end point nature of the cellular sampling. Furthermore, the experimental data from the cellular compartment is at most a single value of the total cellular amount and, thus, does not provide any direct information about the intracellular localization.

2.5 MATHEMATICAL MODELS OF DRUG DISPOSITION KINETICS IN CELL PERMEATION EXPERIMENTS

Several mathematical and computational models to describe and predict the drug disposition during permeation experiments have been proposed. Most often the analysis of permeation experiment data involves the determination of P_{app} and, thus, utilization of a single barrier model. However, considering the cell monolayer as a single barrier is in some cases a major oversimplification. Thus, also several more mechanistic models describing the drug disposition with more thorough spatial detail have been proposed.

2.5.1 Single barrier models

Although there are several individual barriers and transfer routes involved in the drug disposition in cell permeation studies (Figure 2.2), the data analysis is often based on the assumption of a single permeation barrier separating the donor and receiver

compartments. These models are derived from Fick's first law of diffusion, assuming a linear concentration gradient across the barrier (Equation 2.2). In practice, these models describe the flux through the whole barrier ($\Delta M/\Delta t$) with a single parameter, usually referred to as the apparent (P_{app}) or effective (P_{eff}) permeability to acknowledge the fact that this parameter is not reflecting only the intrinsic permeability coefficient but, rather, it represents a composite value reflecting all the permeation barriers and routes involved.

$$\frac{\Delta M}{\Delta t} = P_{app} A(C_d - C_r) \qquad \textit{Equation 2.2}$$

C_d and C_r refer to concentration in the donor and receiver compartments, respectively, and A is the area available for transport.

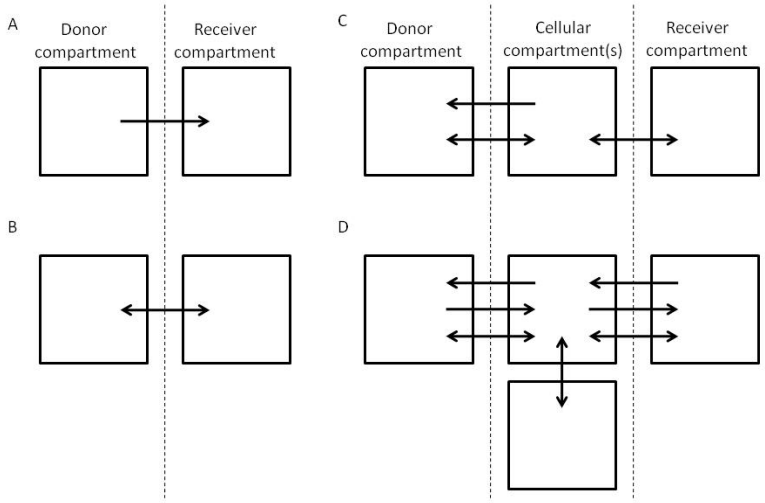

Figure 2.5. Box-model representation of single barrier (A,B) and compartmental (C,D) models to describe the drug disposition kinetics in the cell monolayer permeation experiments. (A) Drug disposition is modeled as a unidirectional process (one headed arrow) from donor to receiver compartment through a single barrier (dashed line). (B) Drug disposition is modeled as a bidirectional process (double headed arrow) through a single barrier between donor and receiver compartments. (C) The cell monolayer is described as a single kinetic compartment between the donor and receiver compartments. Drug disposition through the barriers at the donor and receiver sides of the cellular compartment may be described as a combination of unidirectional and bidirectional processes referring to passive diffusion and active transport, respectively. (D) The detail embedded in the compartmental models may be increased by including additional intracellular compartments and independent transport processes between different compartments.

Schematically the single barrier models can be categorized into unidirectional and bidirectional models (Figure 2.5 A,B). The former group approximates the flux to be

unidirectional from the donor to the receiver compartment without being affected by the receiver concentration. The latter models take into account the increase of the receiver concentration as well as the decrease of the donor concentration, thus allowing for the determination of permeability also when the concentration gradient decreases significantly during the experiment.

2.5.1.1 Unidirectional single barrier models

The most often used model to analyze permeation experiment data is given in Equation 2.3.

$$\frac{\Delta M}{\Delta t} = P_{app,sink} A C_{d0} \qquad \textit{Equation 2.3}$$

In this model, the Equation 2.2 is simplified by assuming the concentration gradient driving the flux to be constant over the experiment and equal to the donor concentration at the beginning of the experiment (C_{d0}). This assumption is bound to be violated to some extent by the flux of the compound. However, the consequent error is generally considered insignificant if the concentration at the receiver compartment is less than 10% of the donor concentration, i.e. so called sink conditions are maintained (Hubatsch et al., 2007). Thus, this permeability estimate will be referred to as $P_{app,sink}$ in this thesis. The sink conditions in the receiver compartment will be maintained if the flux of the compound through the barrier is sufficiently slow. Furthermore, the sampling protocol often includes replacement of the withdrawn sample with fresh buffer, thus enabling prolonged sink conditions also with high permeability compounds. In such cases, the concentration gradient may be diminished considerably due to reduction of the donor concentration. Therefore, it has been recommended that the donor concentration should be recalculated after every sampling by subtracting the cumulative amount transported to the receiver compartment at each time interval in order to obtain the P_{app} value that describes correctly the disposition of the compound (Hubatsch et al., 2007). Additionally, the amount of the compound withdrawn from the system and the possible changes in the liquid volumes due to sampling have to be taken into account in the calculations.

In addition to the sink condition assumption, the compound is assumed to be fully recoverable from the liquid compartments, i.e. there should not be 'loss' of drug due to any mechanism, such as degradation, metabolism or binding to the apparatus or the cell structures. Significant violations of 100% recovery assumption as well as violation of sink conditions are known to cause a bias in estimated P_{app} values (Hubatsch et al., 2007). However, there is no consensus about what represents adequate recovery (Polli

et al., 2004), partly because the tolerable error in P_{app} estimates depends on the purpose of the study.

2.5.1.2 Bidirectional single barrier models

Since the sink conditions may not be maintained with high permeability compounds, models have been proposed to estimate P_{app} under nonsink conditions.

Assuming the total amount of the compound in the system (M) is constant within a sampling interval and is fully recoverable from the liquid compartments, a model that does not require sink conditions to be maintained can be derived from Equation 2.2 (Palm et al., 1999). In this bidirectional single barrier model, the single parameter describing the drug disposition can be determined by fitting Equation 2.4 to the measured receiver concentrations. This permeability estimate will be referred to as $P_{app,Palm}$ in this thesis.

$$\mathbf{C_R(t) = \frac{M}{V_R + V_D} + \left(C_R(0) - \frac{M}{V_R + V_D} \right) e^{-P_{app,Palm} A \frac{V_R + V_D}{V_R V_D} t}} \qquad \textit{Equation 2.4}$$

V_R and V_D are the volumes of the receiver and the donor compartment, respectively. $C_R(0)$ is the concentration in the receiver compartment at the beginning of the sampling interval and $C_R(t)$ is the concentration in the receiver compartment at time t from the beginning of the sampling interval. In practice, depending on the experimental protocol, the sampling necessitates recalculation of, $C_R(0)$ (Palm et al., 1999) or V_D and V_R (Korjamo et al., 2008), and M at each sampling interval. This model assumes 100% recovery and, thus, it is likely to show errors in the P_{app} determination if mass balance problems are present (Hubatsch et al., 2007).

Another proposed bidirectional single barrier model, i.e. applicable to nonsink conditions, to describe the drug disposition in cell permeation experiments requires the measurement of the concentration in both donor and receiver compartments at each sampling time (Tran et al., 2004). In this model, the permeability estimate, referred to as $P_{app,Tran}$ in this thesis, is calculated for each sampling interval separately according to Equation 2.5.

$$\mathbf{P_{app,Tran} = -\left(\frac{V_r V_d}{(V_r + V_d) A t} \right) \ln \left\{ \frac{1 - C_R(t) / < C(t) >}{1 - C_R(0) / < C(0) >} \right\}} \qquad \textit{Equation 2.5}$$

This model uses the difference between the receiver concentration and the 'average system concentration' (<C>, Equation 2.6), which is calculated at each sampling time, as the thermodynamic force term. This model describes the rate of change in the apparent mass balance as a first order process and takes into account the reduced concentration gradient. Consequently, it was originally proposed that this model would provide

exact permeability estimates even when the sink conditions and 100 % mass balance were not maintained (Tran et al., 2004).

$$< \mathbf{C(t)} >= \frac{\mathbf{V_r C_r(t) + V_d C_d(t)}}{\mathbf{V_r + V_d}} \qquad \textit{Equation 2.6}$$

Both of the above mentioned bidirectional models describe the drug disposition with a single parameter, namely P_{app}, and take into account the decrease in the concentration gradient assuming that the donor and receiver concentrations will be equal at equilibrium, i.e. the concentration gradient across the cell monolayer is predicted to approach zero. However, in cases where the transport through the cell monolayer is polarized, such as when active transport is involved, or in cases where weak acids or bases are studied in the presence of a pH gradient, the concentrations in the donor and receiver compartments will not be equal at equilibrium, i.e. the concentration gradient will approach some non-zero value, which is dependent upon the direction and extent of the polarization of the transport. Thus, these models do not adequately take into account the change in the concentration gradient when the transport is significantly polarized; ultimately leading errors in the permeability estimates in such cases. Nonetheless, both of these models have been utilized in studies reported in the literature where symmetric bidirectional transport does not apply, namely for weak acids and bases in the presence of a pH gradient across the cell monolayer (Palm et al., 1999; Thiel-Demby et al., 2009).

2.5.1.3 Applications of the single barrier models

The use of single *in vitro* determined P_{app} value for the prediction of intestinal absorption *in vivo* is based on several assumptions, i.e. 1) the cell model applied is able to adequately mimic the permeation characteristics of the *in vivo* intestinal epithelia for the whole length of the absorptive area, 2) the gastrointestinal transit time is similar for all compounds and 3) the *in vivo* absorption is limited only by the permeation through epithelia. Indeed, when solubility and stability issues do not limit absorption, and absorption through the epithelia is mainly governed by passive diffusion, a correlation between *in vitro* P_{app} through *in vitro* cultured cell monolayers and fraction absorbed (F_A) in human can be obtained (Artursson et al., 2001; Fagerholm, 2007b). However, these predictions generally tend to be less reliable for low permeability compounds than for high permeability compounds (Fagerholm, 2007b; Matsson et al., 2005). Furthermore, there may be substantial inter-laboratory variation in the observed P_{app} values due to different cell culture and experimental conditions may be substantial (Hayeshi et al., 2008a). Thus, *in vitro* data from various sources cannot be used in a single correlation, but rather, independent correlations need to be developed for each

cell system and experimental setup. Additionally, it has been recently suggested that equally reliable predictions of F_A of passively absorbed drugs could be simply calculated from the physicochemical properties of the molecule (Linnankoski et al., 2008).

Although the F_A of passively absorbed drugs may be predicted fairly well from *in vitro* cell permeation derived P_{app}, the correlation between *in vitro* and *in vivo* permeation rates is qualitative rather than quantitative because the relative contribution of different transfer routes, such as paracellular space and active transporters, tend to differ between the *in vitro* and the *in vivo* situations (Artursson et al., 2001; Matsson et al., 2005). Additionally, the effective area for absorption may differ in the *in vitro* and *in vivo* settings and the spatial variation in several factors, such as pH, paracellular space and the expression levels of transporters and metabolizing enzymes along the intestine (Figure 2.1) will undoubetly affect the permeation *in vivo*. Therefore, a single *in vitro* determined P_{app} value cannot totally predict the *in vivo* intestinal absorption, especially when complex concentration dependent phenomena, such as metabolism or active transport, are involved. Therefore, a rigorous *in vitro - in vivo* extrapolation (IVIVE) of intestinal absorption requires a more complex mechanistic approach.

Although a simple single barrier analysis of absorptive direction permeability assay at a single concentration gives an estimate of the overall absorption potential of the molecule from intestinal lumen into portal vein, the problem is that it usually does not reveal any details about the mechanism of drug disposition. However, the single barrier analysis has been applied for mechanistic investigation of drug disposition. Adson and co-workers (Adson et al., 1995) were able to uncouple the contributions of hydrodynamic barriers from the cellular barriers and, furthermore, to distinguish the paracellular transfer route from the transcellular route. In practice, these studies derive their conclusions from the P_{app} estimates determined under various experimental conditions. Similar experimental approaches have been applied by several others to quantify the role and the distribution of the unstirred layers (Karlsson and Artursson, 1991; Korjamo et al., 2008) and to explore the transfer route of the ionized species of weak electrolytes (Avdeef et al., 2005; Palm et al., 1999) as well as elucidating the active transport mechanisms from the passive transcellular diffusion (Korjamo et al., 2007; Polli et al., 2001; Troutman and Thakker, 2003b). Theoretically, any of the above mentioned single barrier models could be used for determination of P_{app} in mechanistic studies as long as the assumptions of the model applied are adequately met. However, often these assumptions are violated, at least to some extent. The extent of these violations and, thus, also the consequent errors may vary between different experimental conditions (e.g. concentration, pH etc). Therefore, the effects of the

experimental conditions of interest on the P_{app} may be biased and, consequently, the interpretation of the data and conclusions may be confounded. Thus, critical examination of the applicability of the assumptions involved in the P_{app} estimation should not be overlooked. This is further examined in chapters 6 and 8.

One of the most often applied approaches to probe the transfer mechanisms in cell permeation studies is to conduct the permeation experiments in both absorptive (apical to basal) and secretory (basal to apical) directions (sometimes referred as bidirectional permeation experiments in the literature (Neuhoff et al., 2003), which should not be confused with the term 'bidirectional single barrier model' used in this text) to reveal the apparent polarization of the transport (Polli et al., 2001). Usually clear polarization of the transport, i.e. >2 fold difference in P_{app} in opposite directions, is interpreted as involvement of active transport (FDA, 2006) if there is no pH gradient present in the experiments. However, more detailed investigation (concentration dependency, use of specific inhibitors, transfected cell lines etc) is often required to confirm this conclusion and to identify the transporter(s) involved. Moreover, because of the saturable nature of transporter function, the substrate concentration used is of importance in these experiments. Consequently, performing these kinds of studies with only a single concentration provides qualitative or, at best, 'semi-quantitative' information about the active transport involved (Del Amo et al., 2009; Kalvass and Pollack, 2007).

After intestinal administration, the intestinal drug concentrations *in vivo* may be relatively high and thus the saturation of transporters and metabolic enzymes in the enterocytes is a distinct possibility. Thus, a general approach to predict the involvement of saturable processes *in vivo* should be able to predict the concentration dependency of these processes. One often applied approach to study the saturation of transporter function in *in vitro* cell permeation experiments is based on unidirectional single barrier model and on the assumption of additive passive diffusion and active transporter mediated transport (Equation 2.7) (Kalvass and Pollack, 2007; Korjamo et al., 2007; Sun and Pang, 2008; Troutman and Thakker, 2003a).

$$\mathbf{P_{app} AC_{d0} = P_{pass} AC_{d0} \pm V_{max,app} A \frac{C_{d0}}{K_{m,app} + C_{d0}}} \qquad \textit{Equation 2.7}$$

Where P_{pass} is the passive diffusion driven apparent permeability, $V_{max,app}$ is the maximal achievable effective transporter mediated flux rate and $K_{m,app}$ is the initial donor concentration that will yield an effective transporter mediated flux rate which is 50 % of $V_{max,app}$. The sign of the active component of Equation 2.7 indicates the direction of active transport relative to the total flux. Often in the literature the parameters describing the kinetics of active transport are referred to as V_{max} and K_m, which infers to

interpretation of these parameters according to the original Michaelis-Menten enzyme kinetics. However, in this model, the concentration dependency of the transporter function is directly related to the initial concentration at the bulk phase of the donor compartment whereas the binding site of transporters lie at the surface of the cells (uptake) or within the cells (efflux). Therefore, although the Michaelis-Menten theory might adequately describe the transporter function *per se*, the donor concentration derived $V_{max,app}$ and $K_{m,app}$ parameters do not reflect only the transporter function. Rather, they are composite parameters, describing the concentration dependency of the interplay between passive and active transport mechanisms. Indeed, $V_{max,app}$ and $K_{m,app}$ values have been observed to be biased by passive permeability, unstirred water layers as well as the transporter expression level (Balakrishnan et al., 2007; Bentz et al., 2005; Korjamo et al., 2007; Sun and Pang, 2008) and also to show direction dependency (Troutman and Thakker, 2003a). Consequently, these parameters are not readily applicable for the prediction of transporter saturation *in vivo* (Bolger et al., 2009; Del Amo et al., 2009). Similarly, simulation studies have revealed that concentration dependence of intracellular metabolic enzymes cannot be adequately incorporated into single barrier models (Sun and Pang, 2008). Thus, more sophisticated models are needed. The effects of the experimental setup, and of the consequent changes in the passive drug disposition, on the apparent transporter kinetics are further discussed in chapter 8.

2.5.2 Compartmental models

The determination of P_{app} using a single barrier model is the cornerstone of the permeation experiment data analysis. However, it is clear that single barrier models cannot fully describe the drug disposition and the mechanisms involved in permeation experiments. Therefore, several more mechanistic compartmental models have been developed to explain and predict the experimental data. In general, compartmental models describe the transfer of a compound between several kinetic compartments (Figure 2.5). The degree of complexity of the proposed compartmental models varies from fairly simple three-compartment models, which describe the transfer as a one-dimensional process with a set of differential equations and the cell layer as a single kinetic compartment in between donor and receiver compartments (Gonzalez-Alvarez et al., 2005; Kalvass and Pollack, 2007; Kapitza et al., 2007; Korjamo et al., 2007), to multi-compartment models which describe the cell layer as several compartments and may incorporate a more complex spatial dependency of molecule movement as well as formation and movement of the metabolites within the system modeled (Bentz et al., 2005; Tam et al., 2003; Tran et al., 2005; Zhang et al., 2006).

Compartmental models are usually composed of a group of ordinary differential equations defining the rates of compound movement between kinetic compartments. Additionally, it is important to account for possible discontinuation in functions due to the mass and volume removed in the sampling (Sun et al., 2008). In some cases, these differential equation groups can be solved analytically with certain approximations (Kalvass and Pollack, 2007; Komin and Toral, 2009). However, often these differential equation groups are not analytically solvable and, thus, numerical methods need to be employed to simulate the time course of drug disposition. Therefore, utilization of these kinds of models requires a considerable amount of computing power though this should not pose a problem with modern computers.

2.5.2.1 Applications of compartmental models

One of the first published compartmental models of the drug disposition in *in vitro* cell permeation was applied for the quantitative analysis of the interplay of passive diffusion through the cell membranes and the efflux transporter P-gp mediated transport through the apical cell membrane (Ito et al., 1999). In that study, Ito and co-workers showed that a rather simple, but still mechanistically feasible, three compartment model was better able to describe the experimental drug disposition than a single barrier model. Additionally, this study suggested that the permeability through the apical cell membrane of two low permeability compounds, digoxin and vinblastine, was significantly lower than through the basolateral cell membrane, consistent with the low fluidity of the exofacial leaflet of the apical cell membrane (Lande et al., 1995).

In the above mentioned study by Ito et al (1999) the experimental data was only available from a single concentration and, consequently, the P-gp mediated transport was described as linear, concentration independent process. This model has been further refined by several investigators to further justify the biochemically feasible location and binding site of the P-gp in the model (Gonzalez-Alvarez et al., 2005) and to include Michaelis-Menten type concentration dependent P-gp function to explain unexpected experimental observations and to gain insights into the dynamics of concentration dependent efflux transport (Kalvass and Pollack, 2007; Korjamo et al., 2007; Tran et al., 2005). Furthermore, the same three compartment base structure of the model has been further developed to describe a more complex interplay between several concentration dependent processes, such as different transporters, metabolism and the putative concentration dependent paracellular transfer to simulate the possible outcomes of the interplay as well as to determine parameters describing the individual processes involved (Bourdet et al., 2006; Sun and Pang, 2008; Sun et al., 2008; Tam et al., 2003).

In the above mentioned models, the cell monolayer was modeled as a single kinetic compartment without any intracellular concentration gradients. However, also more detailed models describing intracellular kinetics have been suggested; such as models accounting for the distribution of the compound between cell membranes and cytosol, the distribution into the intracellular lipid and mitochondrial and lysosomal accumulations driven by electrostatic and pH gradients (Zhang et al., 2006; Zhang et al., 2010). These models may be able to mimic the time course of observed drug disposition in the liquid compartments as well as the total cellular retention during the experiments. However, in practice, the parameter values cannot be rigorously estimated by fitting these models into the experimental data from cell permeation experiments because the experimental data does not contain detailed enough information about the cellular localization of the compound. Therefore, utilization of these models is based on *a priori* estimates of the input parameter values.

When the parameter values of a model are to be determined by fitting the model to the experimental data, the model complexity is in practice limited by the resolution of the experimental data. Consequently, such models are likely to ignore some of functionally minor mechanisms and to describe some of the mechanisms under composite parameters. Thus, compartmental models could often be considered as 'semi-mechanistic' (Dahl et al., 2009). Nonetheless, the compartmental models enable the mathematical description of complex systems with parameters bearing some mechanistic significance, as well as estimation of these parameters and also the determination of the statistical uncertainty of the estimates (Ito et al., 1999).

2.6 PHYSIOLOGICALLY BASED MODELS OF *IN VIVO* INTESTINAL ABSORPTION

Several physiologically based pharmacokinetic (PBPK) models have been applied for predicting the *in vivo* pharmacokinetics (Pelkonen et al., 2008). Such models allow simulation and prediction of the effects of variation of several mechanistic details, such as in the expression levels and population variability of transporters and metabolic enzymes. Furthermore, it has been proposed that PBPK models could be exploited for simulation of pharmacokinetic studies in populations in which *in vivo* clinical studies could not feasibly be performed (Jamei et al., 2009b). However, the details of the mechanisms involved in the pharmacokinetics are often unreachable when approached from 'top-down' from the clinical data (Jamei et al., 2009a). Therefore, several *in vitro* approaches have to be applied and the data obtained have to be combined elaborately in order to construct a feasible prediction from 'bottom-up' that accounts for all the clinically significant phenomena involved. Building such a model is a challenging and ambitious task. However, in the recent years, marked advances in the field of

physiologically based IVIVE have been achieved (Agoram et al., 2001; Badhan et al., 2009; De Buck and Mackie, 2007; Jamei et al., 2009a; Rostami-Hodjegan and Tucker, 2007). Furthermore, computer software, such as GastroPlus™ (Simulations Plus Inc, Lancaster, CA, USA), Simcyp® Population-based ADME Simulator (Simcyp Ltd, Sheffield, UK) and PK-Sim® (Bayer Technology Services GmbH, Leverkusen, Germany), utilizing these models have become commercially available. Various approaches to incorporate the intestinal absorption with varying degrees of mechanistic detail in the PBPK models have been published (Huang et al., 2009). The first intestinal absorption models ignored the structure of the gastrointestinal tract and, thus, lacked mechanistic detail. However, an increased insight into absorption mechanisms has led to incorporation of a more physiological description of the factors involved in absorption (reviewed by Boobis et al., 2002). An early version of this kind of physiologically based intestinal absorption model (Compartmental Absorption and Transit, CAT) proposed by Yu and Amidon (1999) described the gut wall as a single barrier and the permeability parameters were originally derived from *in situ* absorption studies in human. However, as in the *in vitro* situation, also in the *in vivo* setting, the single barrier model of the gut wall cannot adequately describe the dynamics of the involvement of efflux transporters and intestinal metabolism. Consequently, recent models have included the enterocytes as an additional compartment between intestinal lumen and circulation and these models now contain several transporters and metabolic enzymes in mechanistically and biochemically reasonable locations (Agoram et al., 2001; Badhan et al., 2009; Jamei et al., 2009b; Tubic et al., 2006). Despite the evident advances in the physiologically based IVIVE, several issues still remain and more and more reliable and useful predictions are still being sought for. A practical and reliable approach for IVIVE of concentration dependent active transport of molecules through the cell membranes in the relevant tissues is one of aspects still lacking from the current predictions, partly because of the lack of suitable *in vitro* input data (Badhan et al., 2009). Such a lack of data possibly results in imprecise predictions for compounds whose pharmacokinetics are significantly affected by transporters. One of the requirements for successful exploitation of *in vitro* data in *in vivo* predictions is a thorough understanding of the *in vitro* method being applied. Therefore, the studies in this thesis were conducted in order to gain insights into selected *in vitro* methods used to study the permeation and transporter kinetics. Furthermore, a rational approach was sought for handling the *in vitro* component of IVIVE of transporter mediated transport. A major emphasis was placed upon intestinal absorption and P-gp mediated transport. However, the general principles are applicable for other barrier tissues and also for other transporters.

3 Aims of the study

The general objective of the studies conducted in this thesis was to gain further insights into the dynamics of active and passive disposition processes in *in vitro* models for drug permeation and active transport in order to improve the predictive value of *in vitro* methods. The specific aims were:

1. To assess the effects of the experimental setup on the observed concentration dependent function of P-gp (I, IV)

2. To assess the validity of single barrier assumption based analysis of cell permeation data under various experimental conditions (II, IV)

3. To establish a rational approach to describe and determine the active and passive drug disposition kinetics in *in vitro* permeation experiments (II, III, IV)

4 General experimental procedures

4.1 CHEMICALS

(+/-)Verapamil hydrochloride was from ICN Biomedicals (Aurora, OH), (+/-) ibuprofen, (+/-) propranolol hydrocloride and quinidine from Sigma (St. Louis, MO), testosterone from Fluka (Buchs, Switzerland), bafilomycin A1 was from LC Laboratories (Woburn, MA) and the P-gp inhibitor GF120918 (Hyafil et al., 1993) was a kind gift from GlaxoSmithKline (Research Triangle Park, NC). ^{3}H-ibuprofen (5 Ci/mmol), ^{3}H-testosterone (76 Ci/mmol) and ^{3}H-quinidine (20 Ci/mmol) were from American Radiolabeled Chemicals (St. Louis, MO) and ^{3}H-propranolol (20.6 Ci/mmol) from Perkin Elmer (Boston, MA, USA). The cell culture reagents were from BioWhittaker (Cambrex Bio Science, Verviers, Belgium) and EuroClone (UK). All the chemicals were of analytical grade or better.

Some properties of the model compounds are summarized in Table 4.1.

Table 4.1. Properties of model compounds used

Compound	pKa	D_{aq} [c]	MW
Monensin	acid 4.26 [a]	5.1	693
Quinidine	base 4.32, 8.51 [b]	7.2	324
Verapamil	base 9.07 [b]	5.9	491
Testosterone	NA	7.5	288
Propranolol	base 9.53 [b]	7.9	259
Metoprolol	base 9.56 [b]	7.8	268
Ibuprofen	acid 4.45 [b]	7.9	260

[a] Calculated by the ACDLABSACD/pKa program (Version 6.00)

[b] Experimental values taken from (Avdeef and Box, 1995; Avdeef, 2003)

[c] Aqueous diffusion coefficient at 37 °C was calculated with equations presented in (Avdeef et al., 2005)

NA, Not applicable

4.2 CELL CULTURE

MDCKII-MDR1 (The Netherlands Cancer Institute, Amsterdam, The Netherlands) and Caco-2 (ATCC HTB-37, Manassas, VA) cells were cultured and prepared for permeation experiments as described earlier (Korjamo et al., 2005; Korjamo et al., 2007). For permeability experiments, the cells were seeded onto uncoated polycarbonate filters (Catalog number 3401, pore size 0.4 µm, diameter 12 mm; Corning Life Sciences, Corning, NY). MDCKII-MDR1 (passages 34-43) and Caco-2 (passages 42-55) were used for permeation experiments at 4 and 21-24 days post-seeding, respectively.

Before the experiments, the cell monolayers were washed and preincubated for 30 minutes at 37 °C in a humidified incubator in the appropriate transport buffer. The integrity of the monolayers was checked by a transepithelial electrical resistance measurement, only data from inserts with resistance higher than 150 Ωcm^2 (MDCKII-MDR1) or higher than 300 Ωcm^2 (Caco-2) were included in the analysis.

4.3 SAMPLE ANALYSIS

In the analysis, the ^3H-labelled samples were mixed with OptiPhase HiSafe 3 scintillation cocktail (PerkinElmer Wallac) and the radioactivity was quantified using a MicroBeta liquid scintillation counter (PerkinElmer Wallac, Turku, Finland).

4.4 COMPARTMENTAL MODELS

Several compartmental models were constructed and applied in this thesis. Schematic box-model figures of these models are presented in Figure 4.1 and the differential equations describing the mass transfer are shown below.

4.4.1 Model 1a: Three-compartment model

Model 1a describes the passive permeation through the permeation barriers at the apical and basal sides of the cell monolayer as well as instantaneous intracellular distribution.

The time profile of free concentration at the apical (C_{api}) and basal (C_{baso}) chambers and in the cell monolayer ($C_{cell,free}$) are defined as

$$\frac{dC_{api}}{dt} = \frac{A}{V_{api}}\left[-P_{api}\left(C_{api} - C_{cell,free}\right)\right] \qquad \textit{Equation 4.1}$$

$$\frac{dC_{cell,free}}{dt} = \frac{A}{V_{cell}K}\left[P_{api}\left(C_{api} - C_{cell,free}\right) - P_{baso}\left(C_{cell,free} - C_{baso}\right)\right] \qquad \textit{Equation 4.2}$$

$$\frac{dC_{baso}}{dt} = \frac{A}{V_{baso}}\left[P_{baso}\left(C_{cell,free} - C_{baso}\right)\right] \qquad \textit{Equation 4.3}$$

P_{api} and P_{baso} are the composite permeability coefficients across the ABL and cell membrane at the apical and basal sides, respectively. V_{api} and V_{baso} refer to volumes of apical and basal chambers, respectively. The stepwise decline in chamber volumes due to sampling was accounted for when applicable. The cellular volume (V_{cell}) for modeling was calculated from the nominal filter area and the height of the cell monolayer estimated from cross sectional microscopy of cells which were cultured with the same protocol as the cells used for permeation experiments (10 µm for MDCKII-MDR1 and 20 µm for Caco-2).

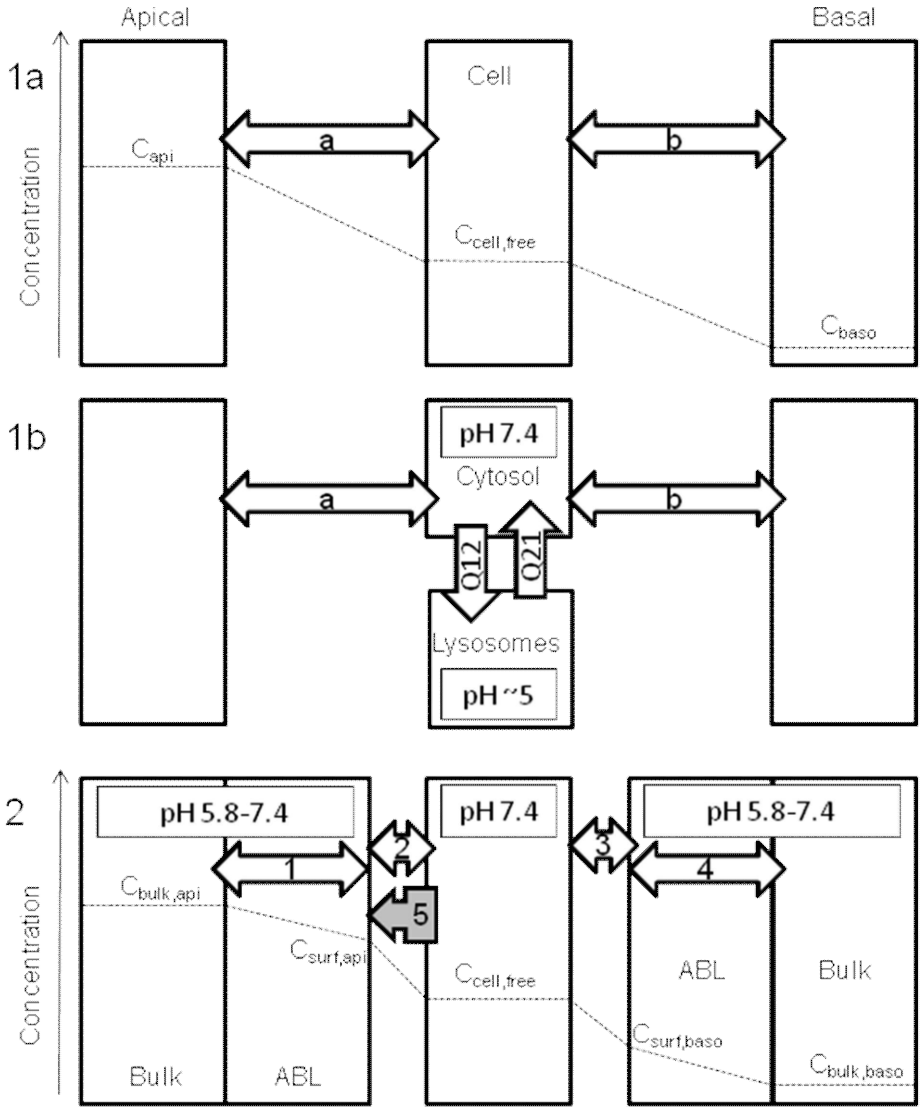

Figure 4.1. Box model representation of models 1a, 1b and 2. In models 1a and 1b, the aqueous boundary layer (ABL) and cell membrane on both sides of the cell monolayer are described as single barriers (a,b). In model 1b, the cytosol to lysosome and lysosome to cytosol distribution rates are described with rate coefficients Q_{12} and Q_{21}, respectively. Model 2 accounts for the ABLs and cell membranes individually (1-4) and allows the inclusion of P-gp mediated efflux through the apical cell membrane (5) into a mechanistically feasible location. The experiments were conducted at various extracellular pHs and the ionization of the compounds was accounted for in the model 2. The dashed lines show schematically the approximation of the concentration gradient from the donor to the receiver compartment in the apical to basal direction experiments at pH 7.4.

The instant cellular distribution was described with cellular distribution coefficient K, which is defined as the ratio of total to the free cellular concentration.

$$\mathbf{K} = \frac{\mathbf{C_{cell}}}{\mathbf{C_{cell,free}}}$$ *Equation 4.4*

Cellular retention was found to be saturable (see the results in capters 6 and 8) and the concentration dependence of the cellular distribution coefficient K was approximated using a simple sigmoidal function assuming a non-saturable component and a single saturable binding site.

$$\mathbf{K} = \mathbf{K_{max}} - (\mathbf{K_{max}} - \mathbf{K_{min}})\frac{\mathbf{C_{cell,free}}}{\mathbf{EC_{50,K}} + \mathbf{C_{cell,free}}}$$ *Equation 4.5*

$EC_{50,K}$ refers to the intracellular free concentration resulting in the K of average of upper (K_{max}) and lower (K_{min}) limits.

4.4.2 Model 1b: Four-compartment model

The lysosomal sequestration of basic compounds may affect also the rate of cellular retention in addition to the extent. In model 1b, the distribution between the 'cytosolic' and 'lysosomal' compartments was described with first order rate coefficients Q_{12} and Q_{21}.

Mass transfer in apical and basal compartments was described identically in models 1a and 1b. Thus, Equation 4.1 and Equation 4.3 describe the concentration profile in apical and basal compartments, respectively, also in model 1b.

The mass transfer in the cellular 'cytosolic' compartment:

$$\frac{\mathbf{dM_{cyto}}}{\mathbf{dt}} = \mathbf{P_{api}A}\left(\frac{\mathbf{M_{api}}}{\mathbf{V_{api}}} - \frac{\mathbf{M_{cyto}}}{\mathbf{V_{cell}K}}\right) - \mathbf{P_{baso}A}\left(\frac{\mathbf{M_{cyto}}}{\mathbf{V_{cell}K}} - \frac{\mathbf{M_{baso}}}{\mathbf{V_{api}}}\right) - \mathbf{Q_{12}}\frac{\mathbf{M_{cyto}}}{\mathbf{K}} + \mathbf{Q_{21}M_{lyso}}$$ *Equation 4.6*

Cellular 'lysosomal' compartment:

$$\frac{\mathbf{dM_{lyso}}}{\mathbf{dt}} = \mathbf{Q_{12}}\frac{\mathbf{M_{cyto}}}{\mathbf{K}} - \mathbf{Q_{21}M_{lyso}}$$ *Equation 4.7*

M refers to the amount of the compound in apical (api), basal (baso), cytosolic (cyto) and lysosomal (lyso) compartments.

4.4.3 Model 2: Five-compartment model

Model 2 accounts separately for ABLs and cell membranes, as well as for the concentration dependent P-gp mediated transport when applicable. The total permeation barrier in the cell permeation experiments was differentiated into four distinct barriers between the compartments; apical ABL, apical cell membrane, basal cell membrane and basal ABL (including both porous support filter and the basal

UWL). Although the basal ABL consists of UWL and the support filter, the contribution of ABL on both sides of the cell monolayer was handled similarly in the five compartment model. Thus, the contributions of the filter support and UWL within the basal ABL are not distinguished in the model.

The time profile of average free concentration at apical ($C_{bulk,api}$, $C_{ABL,api}$) and basal ($C_{bulk,baso}$, $C_{ABL,baso}$) bulk and ABL compartments, respectively, and in the cell monolayer ($C_{cell,free}$) are defined as

$$\frac{dC_{bulk,api}}{dt} = \frac{A}{V_{bulk,api}}\left[-P_{ABL,api}\left(C_{bulk,api} - C_{surf,api}\right)\right] \qquad \textit{Equation 4.8}$$

$$\frac{dC_{ABL,api}}{dt} = \frac{A}{V_{ABL,api}} * \left[P_{ABL,api}\left(C_{bulk,api} - C_{surf,api}\right) - \left(f_u P_u + f_i P_i\right)C_{surf,api} + \left(f_{u,cell} P_u + f_{i,cell} P_i\right)C_{cell,free} + J_{P-gp}\right] \qquad \textit{Equation 4.9}$$

$$\frac{dC_{cell,free}}{dt} = \frac{A}{V_{cell} K}\left[\left(f_u P_u + f_i P_i\right)\left(C_{surf,api} + C_{surf,baso}\right) - 2\left(f_{u,cell} P_u + f_{i,cell} P_i\right)C_{cell,free} - J_{P-gp}\right] \qquad \textit{Equation 4.10}$$

$$\frac{dC_{ABL,baso}}{dt} = \frac{A}{V_{ABL,baso}} * \left[\left(f_{u,cell} P_u + f_{i,cell} P_i\right)C_{cell,free} - \left(f_u P_u + f_i P_i\right)C_{surf,baso} - P_{ABL,baso}\left(C_{surf,baso} - C_{bulk,baso}\right)\right] \qquad \textit{Equation 4.11}$$

$$\frac{dC_{bulk,baso}}{dt} = \frac{A}{V_{bulk,baso}}\left[P_{ABL,baso}\left(C_{surf,baso} - C_{bulk,baso}\right)\right] \qquad \textit{Equation 4.12}$$

P-gp mediated transport rate '*in situ*', is defined as

$$J_{P\text{-}gp} = V_{max}\frac{C_{cell,free}}{K_m + C_{cell,free}} \qquad \textit{Equation 4.13}$$

or in the presence of the P-gp inhibitor GF120918 and for the passively transported compounds

$$J_{P\text{-}gp} = 0 \qquad \textit{Equation 4.14}$$

$P_{ABL,api}$ and $P_{ABL,baso}$ are the permeabilities across the apical and basal ABLs, respectively. Current data did not allow for the determination of separate permeability values in apical and basal cell membranes. Thus, in the final model fitting, separate values for P_u and P_i were obtained but equal values in both cell membranes were used. f_u, f_i, $f_{u,cell}$ and $f_{i,cell}$ refer to unionized and ionized fraction in the extracellular and in the intracellular compartments, respectively, calculated assuming constant intracellular pH of 7.4, which is in the range of the measured intracellular pH values both in Caco-2 (Liang et

al., 2007; Nielsen et al., 2003) and MDCK (Bogner et al., 1992), whereas transport buffer pH (5.8 – 7.4) of a given experiment was used for the extracellular compartments.

The model structure would allow for the addition of paracellular flux between the ABL compartments bypassing the cell membranes and the intracellular space. However, attempts to fit both the membrane permeability of ionized species and the paracellular permeability simultaneously resulted in obscure parameter estimates (data not shown). Furthermore, addition of paracellular permeability of 2 $*10^{-6}$ cm/s into the model, based on the mannitol permeability, did not significantly affect the parameter estimation (results not shown). Thus, for simplicity, paracellular flux was neglected.

The operational ABL volumes separately on both sides are

$$\mathbf{V_{ABL}} = \frac{\mathbf{D_{aq}}}{\mathbf{P_{ABL}}}\mathbf{A} \qquad \textit{Equation 4.15}$$

D_{aq} is the estimated aqueous diffusion coefficient at 37°C (Table 4.1).

Consequently bulk phase volumes are

$$\mathbf{V_{bulk}} = \mathbf{V_{tot}} - \mathbf{V_{ABL}} \qquad \textit{Equation 4.16}$$

V_{tot} refers to the total volume of the corresponding chamber (V_{api} or V_{baso}). When the sample volumes are not replaced to the chambers the volumes decline stepwise during the experiments. This was accounted for in the modeling when applicable.

The concentrations at the cell surfaces ($C_{surf,api}$ and $C_{surf,baso}$) were estimated from the bulk concentration (C_{bulk}) and the average concentration in ABL compartment (C_{ABL}) on the respective side of the cell monolayer assuming a linear concentration gradient within the ABLs (Figure 4.1)

$$\mathbf{C_{surf}} = \mathbf{2C_{ABL}} - \mathbf{C_{bulk}} \qquad \textit{Equation 4.17}$$

The initial conditions for the differential equations in apical to basal direction experiments are

$$\mathbf{C_{bulk,\,api}} = \mathbf{C_{ABL,\,api}} = \textbf{Initial donor concentration} \qquad \textit{Equation 4.18}$$

$$\mathbf{C_{bulk,baso}} = \mathbf{C_{ABL,\,baso}} = \mathbf{C_{cell,free}} = \mathbf{0} \qquad \textit{Equation 4.19}$$

Whereas in the experiments in the basal to apical direction, the initial conditions are

$$\mathbf{C_{bulk,\,api}} = \mathbf{C_{ABL,\,api}} = \mathbf{0} \qquad \textit{Equation 4.20}$$

$$\mathbf{C_{bulk,baso}} = \mathbf{C_{ABL,\,baso}} = \mathbf{C_{cell,free}} = \textbf{Initial donor concentration} \qquad \textit{Equation 4.21}$$

5 Protein concentration and pH affect the apparent P-glycoprotein ATPase activation kinetics[1]

Abstract. Reliable predictions of the role of P-glycoprotein in the pharmacokinetics are needed already at the early stage of drug development. In order to obtain meaningful *in vitro–in vivo* scaling factors, it is essential to know the factors affecting the *in vitro* results. In this study, the apparent P-glycoprotein–ATPase activation kinetics was determined using the cell membrane fraction of human MDR1-transfected insect cells. The apparent affinities to P-glycoprotein of basic verapamil and quinidine were higher at pH 7.4 than at pH 6.8. However, this shift in pH did not have a significant effect on the apparent affinity of acidic monensin. The protein concentration used in the assay did not affect the apparent activator affinities, but was inversely related to the maximum activation achieved. Thus, pH and protein concentration should be taken into account when interpreting the Pgp–ATPase data.

[1] Adapted with permission of Elsevier B.V. from: Heikkinen A.T., Mönkkönen J.: Protein concentration and pH affect the apparent P-glycoprotein ATPase activation kinetics, Int J Pharm 346: 169-172, 2008.

5.1 INTRODUCTION

The P-gp-ATPase activation method has been used for determining kinetic parameters describing the concentration dependent P-gp function (Adachi et al., 2001; Xia et al., 2006). However, the kinetic parameters obtained with the P-gp-ATPase method vary between laboratories. In this study the effect of pH and protein concentration to the P-gp-ATPase activation assay were examined. The results show that these factors result in variation in P-gp-ATPase activity measurements and thus may partly explain the variation in the parameters that has been reported.

5.2 MATERIALS AND METHODS

The P-gp-ATPase assay was performed using the cell membrane fraction from High Five cells expressing human P-gp (GENTEST/BD Biosciences, Woburn, MA, USA). The assay was performed according to the manufacturer's protocol with modifications in protein concentration and in buffer pH. 50 µl of membrane suspension (20, 40 or 60 µg of protein/well) in ATPase buffer containing 50 mM Tris, 50 mM MES, 2 mM EGTA, 2 mM dithiothretiol, 50 mM potassium chloride and 5 mM sodium azide, pH 6.8 or pH 7.4 as indicated, was preincubated with or without test compound for 5 min at 37 °C. 10 µl of 30 mM ATP magnesium salt in ATPase buffer was added (final ATP concentration was 5 mM). After 20 min of incubation at 37 °C, 30 µl 10 % of SDS solution supplemented with Antifoam A was added to stop the reaction. Subsequently, 150 µl of detection solution containing 8 % of ascorbic acid, 3 mM of zinc acetate and 7 mM of ammonium molybdate was added and these mixtures were incubated at 37 °C for 20 min. The absorbance of each mixture was measured at 660 nm using Victor^2 (Perkin Elmer/Wallac, Turku, Finland).

The P-gp-ATPase activity (A_{Pgp}) was calculated according to the equation

$$A_{Pgp} = \frac{({}_iP_{(t)} - {}_iP_{(0)}) - ({}_iP_{(t)bg} - {}_iP_{(0)bg})}{t * n} \qquad \textit{Equation 5.1}$$

where ${}_iP_{(t)}$ and ${}_iP_{(0)}$ are the amount of liberated phosphate at time t and 0, respectively, and ${}_iP_{(t)bg}$ and ${}_iP_{(0)bg}$ are the amount of liberated phosphate in the presence of 100 µM sodium orthovanadate at time t and 0, respectively. The activities were normalized to the protein amount n. ${}_iP_{(t)bg}$ was not affected by any of the studied molecules (data not shown) indicating that studied molecules did not interfere with the background (bg) ATP hydrolysis or with the detection of liberated phosphate.

To estimate the maximum activation with particular activator ($A_{Pgp,max}$) and the activator concentration resulting in half-maximum activation ($EC_{50,Pgp}$), the data were fitted to the Equation 5.2

$$A_{Pgp} = A_{Pgp,0} + (A_{Pgp,max} - A_{Pgp,0}) * \frac{C}{C + EC_{50,Pgp}}$$ *Equation 5.2*

where A_0 is the P-gp-ATPase activity at activator concentration C = 0. GraphPad Prism, version 4.03 (GraphPad Software Inc., San Diego, CA) was used for data fitting.

All the experiments were performed using the same membrane lot to avoid the possible effect of membrane lot to lot variation.

5.3 RESULTS AND DISCUSSION

The apparent $EC_{50,Pgp}$ of the basic compounds verapamil and quinidine were lower at pH 7.4 than at pH 6.8 with all protein concentrations used (Figure 5.1). Most of the known P-gp substrates are weak bases and their distribution between aqueous and lipid phases varies according to pH at the physiological pH range. As the binding site of P-gp lies inside the lipid bilayer (Figure 2.4), it is expected that basic substrates reach the binding site more readily at higher pH, resulting in lower $EC_{50,Pgp}$ values. However, the reversed effect was not clearly seen with the acidic monensin. This is probably due to the fact that the pH area used was too far away from the pKa of monensin (Table 4.1), thus the concentration at the binding site of P-gp was not significantly affected. Further, pH shift did not affect the P-gp-ATPase activation of the neutral compounds digoxin and testosterone (data not shown), suggesting that the pH shift did not affect on the P-gp function *per se*.

In addition to $EC_{50,Pgp}$, the pH shift slightly affected A_{max} values of verapamil and monensin. According to the Sigma product information sheet of MgATP, the pKa of ATP is 6.5. Thus, also the ionization state of ATP is affected when pH in changed from 6.8 to 7.4. The affinity to P-gp of different forms of ATP may vary and could cause the observed shift in $A_{Pgp,max}$ parameters. However, if this was the reason the effect would be seen independent of the activator used. With quinidine, digoxin and testosterone there was no sign of pH effect on $A_{Pgp,max}$ (digoxin and testosterone data not shown). Thus, the reason for the variable $A_{Pgp,max}$ values of verapamil and monensin in different pH environments remains unclear.

The protein concentration used in the assay did not significantly affect $EC_{50,Pgp}$, suggesting that the concentration of activators at the binding site was not significantly affected by the variation in the protein concentration used.

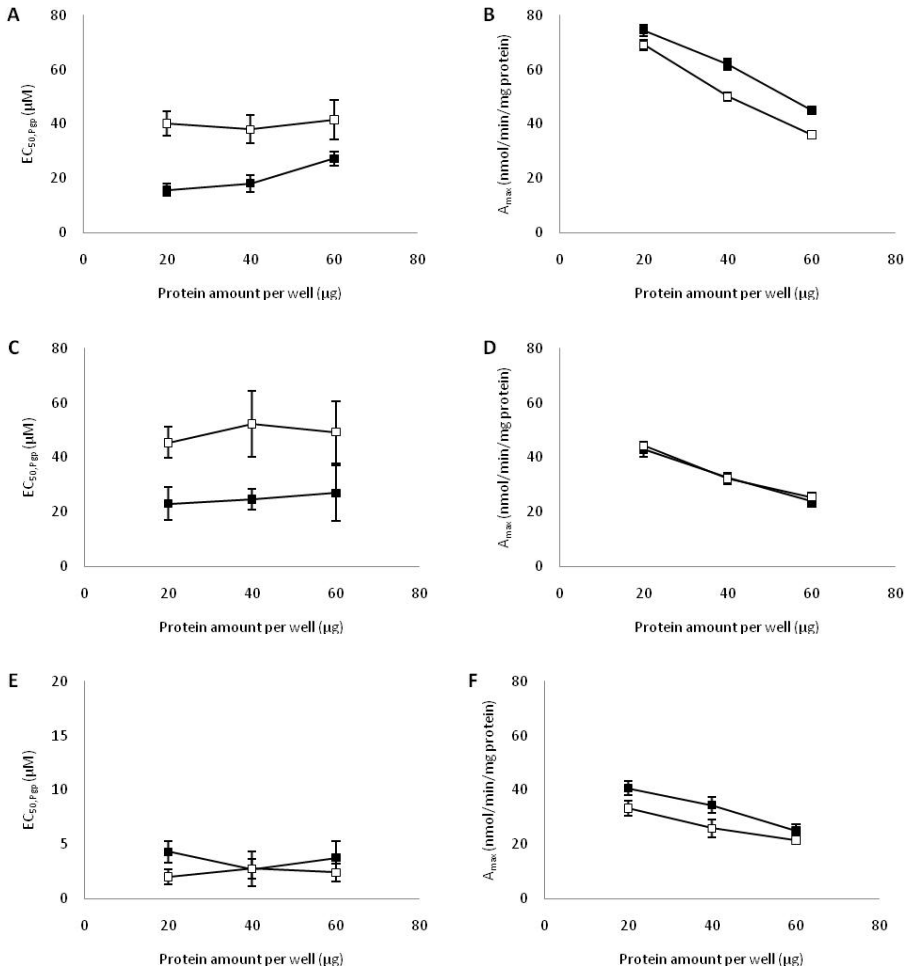

Figure 5.1. Apparent $EC_{50,Pgp}$ (A,C,E) and A_{max} (B,D,F) values of verapamil (A,B), quinidine (C,D) and monensin (E,F) at pH 6.8 (open symbols) and at pH 7.4 (closed symbols) when assays were performed using 20, 40 or 60 μg of protein/well. Symbols represent the parameters fitted on data from 4 measurements at 5 to 7 concentrations per compound ± SE of fitted parameters.

Surprisingly, the A_{max} and the protein concentration were inversely related (Figure 5.1). However, the basal P-gp-ATPase activity (3.7 ± 1.5 nmol/min/mg protein) was not detectably affected by the protein concentration. The ATP concentration remained above 3 mM during all incubations. 3 mM initial ATP concentration was enough to give practically maximum P-gp-ATPase activity (Figure 5.2), suggesting that apparently lower P-gp-ATPase activity with higher protein concentrations is not due to ATP depletion. P-gp-ATPase activity has been shown to be inhibited by ADP, and also substrate inhibition of P-gp-ATPase by high ATP concentrations has been suggested

(Sharom et al., 1995). End product inhibition due to ADP accumulation could explain the apparently lower P-gp-ATPase activities when higher protein concentrations are used.

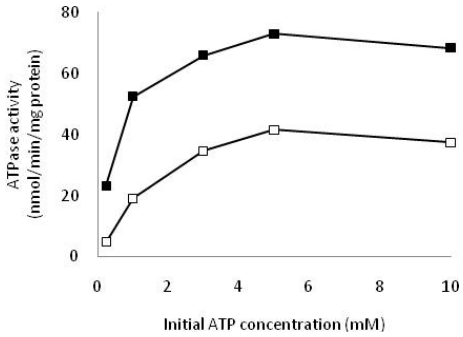

Figure 5.2. Kinetics of the P-gp-ATPase activity at pH 7.4 in the presence of 500 µM verapamil. P-gp-ATPase activity was measured at various ATP concentrations using 20 (closed symbols) and 60 (open symbols) µg protein/well. Symbols represent the average of two measurements.

5.4 CONCLUSIONS

In P-gp-ATPase assay, the possible effect of pH on activators lipid distribution should be taken into account when analyzing ionizable compounds.

Apparent P-gp-ATPase activity is lower when high protein concentrations are used, possibly due to ADP accumulation during the incubation.

6 Kinetics of cellular retention during permeation experiments[2]

Abstract. The permeability estimation from cell monolayer permeation data is usually based on 100 % recovery assumption. However, poor recovery is often seen in such experiments in practice, but often neglected in data interpretation. In the present study, the cellular retention kinetics during Caco-2 permeation experiments of three passively transported compounds (basic propranolol, acidic ibuprofen and neutral testosterone) were determined. Further, the effects of cellular retention kinetics on apparent permeability were evaluated and the role of lysosomal sequestration in cellular retention of propranolol was explored. The cellular retention profiles were observed to be direction and concentration dependent, which may cause erroneous directionality and concentration dependence in permeability estimates. Further, the lysosomal sequestration was demonstrated to contribute to the extent and kinetics of the cellular retention of propranolol.

[2] Adapted with permission of the American Society for Pharmacology and Experimental Therapeutics from: Heikkinen A.T., Mönkkönen J., Korjamo T.: Kinetics of cellular retention during Caco-2 permeation experiments: Role of lysosomal sequestration and impact on permeability estimates, J Pharmacol Exp Ther 328:882-892, 2009.

6.1 INTRODUCTION

Typically, in *in vitro* permeation experiments the permeability estimates are based on the appearance kinetics of the test compound to the receiver compartment. Additionally, samples from both donor and receiver sides are often collected at the final time point of the experiment to determine the recovery of the test compound. The analysis and interpretation of permeation data are often based on the assumption that the cell monolayer behaves as a single barrier for the solute transfer and that the whole mass of the studied compound is in donor and receiver compartments, i.e. the recovery is 100 %. However, physiologically the permeation barrier in cell monolayer experiments consists of various serial and parallel barriers (Figure 2.2) and, further, reduced recovery is often observed in permeability experiments (Polli et al., 2001). Incomplete recovery is attributed to metabolism, drug binding to the plastic surfaces and/or to cellular retention of drug (Fisher et al., 1999; Palmgren et al., 2006; Östh et al., 2002). The possible bias in permeability estimates caused by poor recovery is generally acknowledged but still often neglected in the data interpretation.

The mechanisms causing poor recovery and, consequently, the kinetics of apparent loss of test compound in permeation experiments may be specific to compound, experimental apparatus and permeation barrier (Tran et al., 2004; Östh et al., 2002). Thus, accurate universal correction terms for poor recovery in permeation experiments cannot be applied. However, in some reported studies the poor recovery have been taken into account by correcting the calculations with experimental recovery at a single time point, practically either at the end of the experiment (Youdim et al., 2003) or after initial 'cell loading' period in the beginning of the experiment (Korjamo et al., 2008; Tran et al., 2004).

In Caco-2 cells, drug metabolism is limited due to low expression levels of cytocrome P450 metabolizing enzymes (Engman et al., 2001; Korjamo et al., 2006; Prueksaritanont et al., 1996). Further, an earlier study in our lab have suggested that in the presence of buffer the loss of various drugs to cell culture plastics is minimal whereas the cellular retention may be substantial (Palmgren et al., 2006). Therefore, retention into the cellular structures is likely to be the primary cause of poor recovery for many compounds in cell-based permeation experiments.

Cellular retention may be caused by partitioning into the cellular lipids due to high lipophilicity (Sawada et al., 1999), specific or nonspecific binding to the cellular protein or due to electrostatic binding to the charged structures of the cell (Duvvuri and Krise, 2005a). Furthermore, one major mechanism causing the compound sequestration into the intracellular organelles is ion trapping of weak bases into the organelles with acidic interior (Kaufmann and Krise, 2007). Several intracellular organelles possess acidic

interior and intraorganelle pH may be as low as 4.5 in lysosomes, whereas cytosolic pH lies near neutrality (Asokan and Cho, 2002). It has been shown that basic compounds with suitable pKa are sequestered into the acidic organelles, provided that the membrane permeability of the ionized and unionized forms differ substantially (Duvvuri et al., 2004). Further, lysosomes are the most acidic organelles in the cells and, therefore, most of the pH-partitioning based sequestration of basic compounds is likely to be due to lysosomal sequestration. In addition, it is challenging to experimentally distinguish the true lysosomal sequestration from the possible sequestration into the other acidic vesicles, such as endosomes, in the cells. Therefore, for simplicity in this text term 'lysosome' is used to cover also the other acidic vesicles than lysosomes.

In this study, the cellular retention kinetics of basic propranolol, acidic ibuprofen and neutral testosterone during Caco-2 permeation experiments were explored and modelled. Further, the role of lysosomal sequestration in cellular retention of propranolol was demonstrated. Finally, the effects of cellular retention kinetics on estimates of apparent permeability through the Caco-2 cell monolayer were evaluated.

6.2 METHODS

6.2.1 Permeability and cellular retention experiments.

The physicochemical properties of the model compounds are given in Table 4.1. One basic (propranolol), acidic (ibuprofen) and neutral (testosterone) compound were selected for the experiments. All the model compounds are known to be transported symmetrically through Caco-2 monolayers when no pH gradient is present. Consequently, the permeation is assumed to be primarily governed by passive diffusion. Furthermore, these compounds are not significantly metabolized during Caco-2 permeation experiments (Engman et al., 2001; Korjamo et al., 2008).

HBSS buffered with 25 mM Hepes, pH 7.4, with or without 100 nM bafilomycin A1, a specific inhibitor of vacuolar type H^+ -ATPase (Bowman et al., 1988), that inhibits the acidification of lysosomes (Yoshimori et al., 1991), was used as the transport buffer. The donor solutions were prepared in transport buffer and spiked with the respective ^{3}H-labelled compound (1 µCi/ml). The initial donor concentrations were 1 µM, 50 µM and 300 µM for propranolol and ibuprofen and ~10 nM (blank transport buffer spiked with ^{3}H-testosterone), 1 µM and 50 µM for testosterone. The stock solutions of unlabeled compounds were prepared in dimethylsulfoxide (DMSO) and the DMSO concentration did not exceed 1 % in final donor solutions.

The permeability and cellular retention experiments were conducted in both apical to basal and basal to apical directions on an orbital shaker with orbit diameter of 3 mm at 320 rpm (Titramax 101, Heidolph, Schwabach, Germany) at 37 °C in a humidified incubator. The experiments were started by replacing the preincubation buffer with

fresh transport buffer into the receiver compartment and donor solution into the donor compartment (500 µl in apical and 1500 µl in basal compartment), both with or without 100 nM bafilomycin A1 as indicated. Due to the end point nature of the cellular retention measurements separate cell monolayers were used for each time point. At each time point (5, 15, 30, 60 and 90 minutes) 100µl samples were withdrawn from both chambers from three inserts. Promptly, these three inserts were washed with ice cold transport buffer and the cells were lysed with 300 µl transport buffer supplemented with 1 % Triton X 100 at least for 30 minutes at 37 °C in a humidified incubator. The cell lysates were carefully mixed and 100 µl samples were withdrawn for liquid scintillation counting.

6.2.2 Kinetic modelling.

The compartmental models were constructed, and data fitting and simulations were done with WinNonlin software (version 5.0.1, Pharsight Corporation, CA, USA).

In data fitting, 6 data sets (apical, basal and cellular amounts at every sampled timepoint) of corresponding test compound were simultaneously used; 3 concentrations (1, 50 and 300 µM for ibuprofen and propranolol and 0.01, 1 and 50 µM for testosterone) in both directions. All the experiments were conducted twice in triplicate. Thus, 6 individual experimental values for each time point were used in data fitting. In the fitting procedure, various weighting schemes were tested (no weighting, 1/predicted and 1/predicted^2). The weighting scheme of 1/predicted^2 was selected based on residual blots and estimated standard errors of parameter estimates. Other settings for minimization of the error were the default WinNonlin settings.

6.2.2.1 Model 1a: Modeling the permeation and rapid cellular binding

The compartmental model published earlier (Korjamo et al., 2007) was used as the basis of the compartmental models (Figure 4.1).

All the test compounds included in this study have relatively high transcellular permeability. Therefore, the contribution of paracellular flux of these compounds to the total transport is insignificant. Thus, paracellular space was omitted from the models.

The diffusion barriers at both sides of the cell monolayer consist of ABL and the cell membrane. However, at the basal side the ABL includes also support filter in addition to UWL. Furthermore, the UWL is not likely to be evenly distributed to apical and basal sides because of the differences in compartment geometries (Ho et al., 1999; Korjamo et al., 2008). Additionally, the apical and basolateral membranes of epithelial cells have distinct lipid composition (Simons and van Meer, 1988) and, consequently, they may also have distinct permeation characteristics. Thus, it would be purely coincidental if the permeabilities through the apical and basal barriers of the cell monolayer (P_{api} and P_{baso}, respectively) would be equal. Therefore, it was assumed that

permeabilities are direction and concentration independent, but not necessarily equal for apical and basal barriers. Thus, P_{api} and P_{baso} were fitted separately.

The cellular retention was concentration dependent (Figure 6.1). Therefore, a simple sigmoid equation (Equation 4.5) was employed to model the concentration dependence of the cellular distribution coefficient (K). The differential equations for mass transfer are presented in the Chapter 4.4.

6.2.2.2 Model 1b: Modeling the lysosomal sequestration kinetics

It was assumed that bafilomycin A1 affects the propranolol kinetics only by decreasing the pH gradient between cytosol and lysosomes. This is almost impossible to show experimentally, but the assumption is reasonable because the presence of bafilomycin A1 did not detectably affect the behaviour of ibuprofen or testosterone (data not shown). Therefore, bafilomycin A1 was assumed not to affect the cytosolic compartment. Further, fitting of too many parameters simultaneously results in obscure parameter estimates. Thus, the fitted permeability and cell-buffer distribution parameters (P_{api}, P_{baso}, K_{max}, K_{min} and $EC_{50,K}$) were fixed to the values obtained from the data fitting of model 1 in the presence of bafilomycin A1.

Subsequently, the distribution between cytosolic and lysosomal compartments was described with Q_{12} and Q_{21}, first order rate coefficients from cytosolic to lysosomal and lysosomal to cytosolic compartments, respectively. However, because of the possible concentration dependence of distribution kinetics, both, Q_{12} and Q_{21}, were fitted separately for each concentration and direction. Schematic presentation of model 1b is shown in Figure 4.1 and the differential equations for mass transfer in model 1b are presented in the Chapter 4.4.

6.2.2.3 Simulations.

Model 1 was used to simulate the transfer and cellular retention of virtual test compound in permeability experiment. In the simulations, P_{api} and P_{baso} were set to be $500*10^{-6}$ cm/s and $200*10^{-6}$ cm/s, respectively. The cell-buffer distribution coefficient was set to 4, 100 or 400. These values are in the range of the fitted parameter values (Table 6.1).

6.2.3 Estimation of permeability coefficients.

The apparent permeability through Caco-2 cell monolayer was estimated using three different single barrier models described in chapters 2.5.1.1 (Equation 2.3/$P_{app,sink}$) and 2.5.1.2 (Equation 2.4/$P_{app,Palm}$ and Equation 2.5/$P_{app,Tran}$). In addition to the experimental data, simulated data at the same 'sampling' times than experimental data were used in permeability estimations. Because the simulated data does not include experimental

variation, the variation in the permeability estimates of the simulated data is neither caused nor masked by experimental variation.

Theoretically, the permeability is the reciprocal of the permeation resistance and the total permeation resistance of serial barriers is the sum of the individual resistances of barriers (Flynn et al., 1974). Thus, the apparent permeability was also calculated from permeabilities through apical and basal barriers.

$$P_{app} = \frac{1}{1/P_{api} + 1/P_{baso}} \qquad \textit{Equation 6.1}$$

6.3 RESULTS

6.3.1 Cellular retention during permeation experiments.

Ibuprofen was not significantly retained in the cell monolayer whereas cellular retention of testosterone and propranolol was substantial (Figure 6.1 and Figure 6.2). Further, in the presence of bafilomycin A1 the cellular retention of propranolol was significantly reduced, whereas bafilomycin A1 did not affect the cellular retention of ibuprofen and testosterone (data not shown).

Although, the fraction of the test compound retained in the cell monolayer varied significantly between the test compounds, some similarities in cellular retention profiles were observed (Figure 6.1 and Figure 6.2). Firstly, the fraction of the test compound retained in the cell monolayer was lower with the higher concentrations, resulting in apparently saturable cellular retention. Secondly, in apical to basal direction the test compounds accumulated into the cells fairly rapidly and after initial accumulation phase the amount retained in cells started to decline, whereas in basal to apical direction experiments the test compounds gradually accumulated into the cells for the whole duration of the experiments (90 minutes).

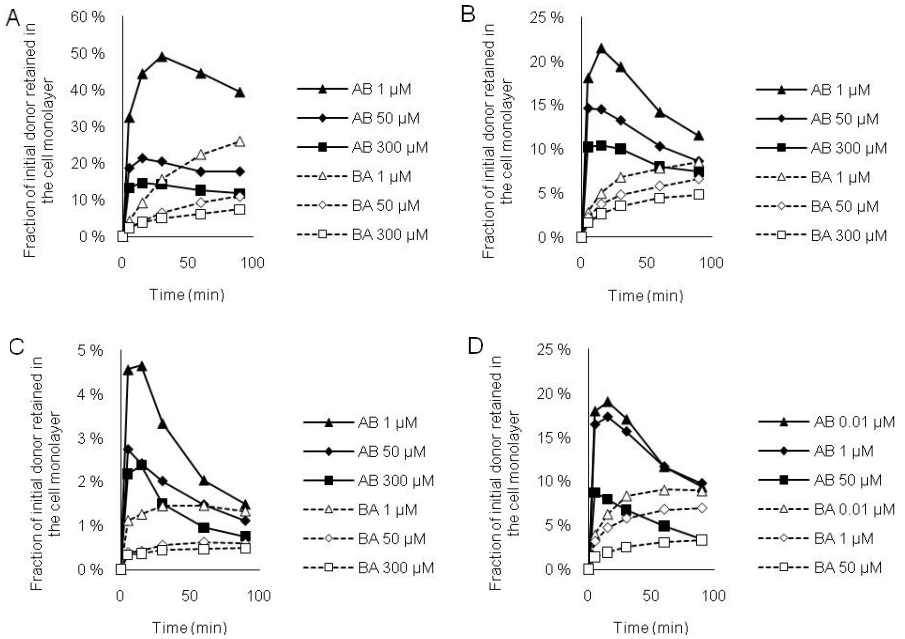

Figure 6.1. The fraction of initial donor amount of (A) propranolol, (B) propranolol in the presence of 100 nM bafilomycin A1, (C) ibuprofen and (D) testosterone retained in the cell monolayer during Caco-2 permeation experiments (note the different scales of the vertical axes). Closed and open symbols represent the apical to basal and basal to apical direction experiments, respectively. Triangles, diamonds and squares denotes to low, intermediate and high concentration, respectively. The symbols represent the average of six measurements. The error bars are omitted for clarity, but the coefficient of variation was generally 10 % or less.

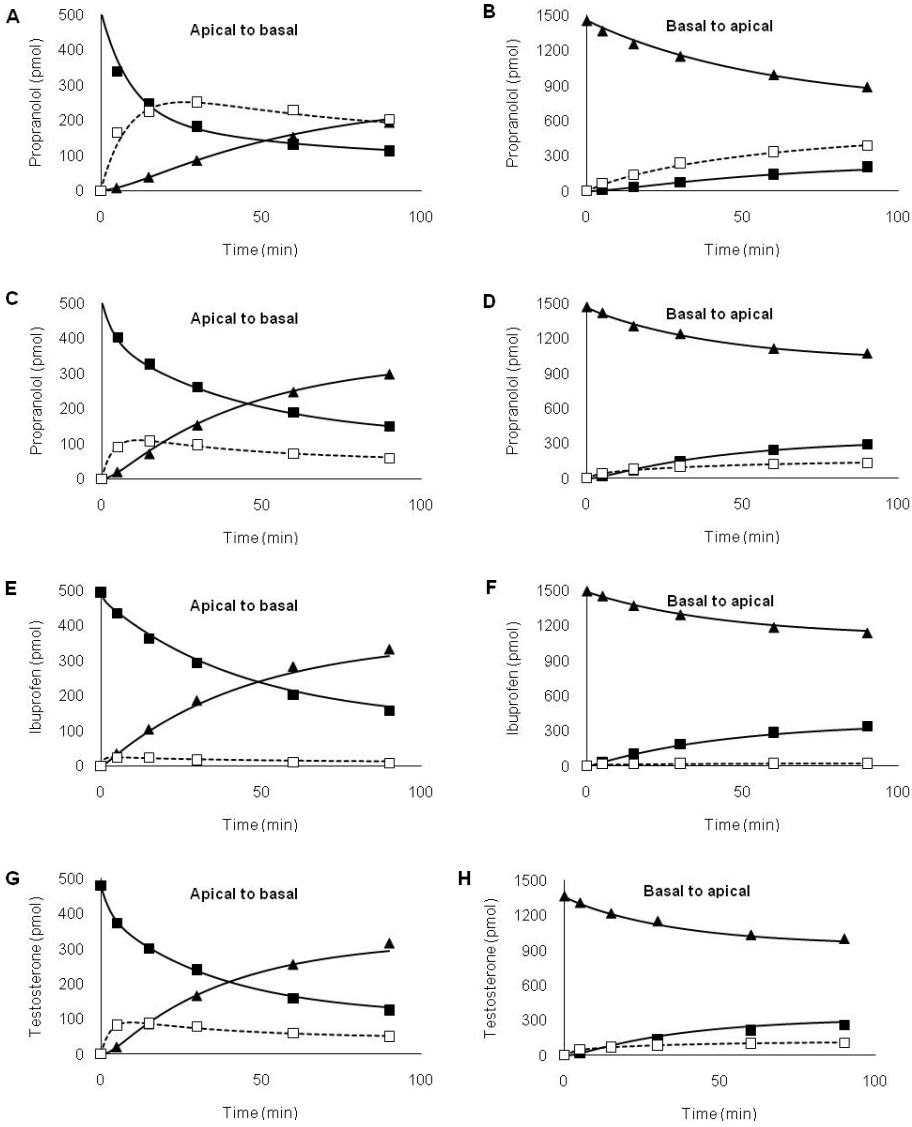

Figure 6.2. The time course of 1 µM (A, B) propranolol, (C, D) propranolol in the presence of 100 nM bafilomycin A1, (E, F) ibuprofen and (G, H) testosterone transfer in Caco-2 permeation experiments. The symbols (solid squares and triangles for apical and basal compartments, respectively, and open squares for cell monolayer) represent the average of 6 measurements and the solid and dashed lines represent the fitted results of model 1 (C to H) and model 2 (A and B). The error bars are omitted for clarity, but the coefficient of variation was generally 10 % or less. The fitted curves mimic the observed data equally well also with the other concentrations used (data not shown).

6.3.2 Kinetic modelling of the solute transfer and cellular retention.

The transfer and cellular retention data were fitted to model 1a and, additionally, propranolol data were fitted to model 1b. The fitted parameters are presented in Table 6.1 and Table 6.2.

Model 1a (cellular compartment modelled as a single kinetic compartment) was found to mimic the transfer and the cellular retention of ibuprofen and testosterone, and also of propranolol when bafilomycin A1 was present. However, the predicted cellular retention profile of propranolol without bafilomycin A1 did not follow the same profile than the observed data (Figure 6.3). Especially in apical to basal direction at 50 µM and 300 µM the amount retained into the cells did not decline as fast as model 1 predicted. Thus, the propranolol data were fitted also to model 1b which includes lysosomes as a distinct kinetic compartment. In the model 1b the cytosol-to-lysosome distribution rate coefficients were fitted individually for each experiment and the precision of rate coefficient estimates was fairly poor, especially for basal to apical direction experiments (Table 6.2). However, the Q_{12} to Q_{21} ratios (estimated as secondary parameters in WinNonlin) could be estimated more precisely and they showed clear concentration dependency (Figure 6.4). Further, the model 1b was better to mimic the cellular retention profile (Figure 6.3) as well as disappearance from donor and appearance to receiver than model 1. In addition, the fitted values for P_{api} were consistently higher than the respective fitted values for P_{baso}.

Table 6.1. The fitted parameters (± SE) for propranolol in the presence of 100 nM bafilomycin A1, ibuprofen and testosterone in model 1a

Compound	Propranolol + bafilomycin A1	Ibuprofen	Testosterone
P_{api} (cm/s*10^{-6})	530 ±8	406 ±16	523 ±12
P_{baso} (cm/s*10^{-6})	200 ±2	183 ±4	241 ±3
P_{app} (cm/s*10^{-6}) [a]	145 ±1	126 ±2	165 ±1
K_{max} (dimensionless)	100 ±1	20 ±1	109 ±1
K_{min} (dimensionless)	44 ±1	6.2 ±0.2	30 ±1
EC_{50} (µM)	11 ±1	2.4 ±0.5	0.8 ±0.1

[a]Apparent permeability was estimated as a secondary parameter in WinNonlin, $P_{app}=1/(1/P_{api}+1/P_{baso})$

Table 6.2. The fitted parameters (± SE) for propranolol in model 1a and model 1b.

	Model 1a	Model 1b
P_{api} (cm/s*10^{-6})	598 ± 18	530[b]
P_{baso} (cm/s*10^{-6})	200 ± 3	200 [b]
P_{app} (cm/s*10^{-6}) [a]	150 ± 2	145 [b]
K_{max} (dimensionless)	414 ± 14	100 [b]
K_{min} (dimensionless)	70 ± 2	44[b]
EC_{50} (µM)	1.8 ± 0.2	11 [b]
Q_{12}, 1 µM AB (1/s*10^{-2})	NA	300 ± 40
Q_{21}, 1 µM AB (1/s*10^{-2})	NA	1.0 ± 0.2
Q_{12}, 50 µM AB (1/s*10^{-2})	NA	140 ± 70
Q_{21}, 50 µM AB (1/s*10^{-2})	NA	2.6 ± 1.4
Q_{12}, 300 µM AB (1/s*10^{-2})	NA	2.1 ± 0.3
Q_{21}, 300 µM AB (1/s*10^{-2})	NA	0.06 ± 0.01
Q_{12}, 1 µM BA (1/s*10^{-2})	NA	300 ± 30
Q_{21}, 1 µM BA (1/s*10^{-2})	NA	0.8 ± 0.1
Q_{12}, 50 µM BA (1/s*10^{-2})	NA	320 ± 390
Q_{21}, 50 µM BA (1/s*10^{-2})	NA	6 ± 7
Q_{12}, 300 µM BA (1/s*10^{-2})	NA	50 ± 30
Q_{21}, 300 µM BA (1/s*10^{-2})	NA	2 ± 1
AIC [c]	1307	1056

[a]Apparent permeability was estimated as a secondary parameter in WinNonlin, $P_{app}=1/(1/P_{api}+1/P_{baso})$.

[b]Values taken from Model 1a in the precence of 100 nM bafilomycin A1 (Table 6.1).

[c]Akaike information criterion. NA, not applicable.

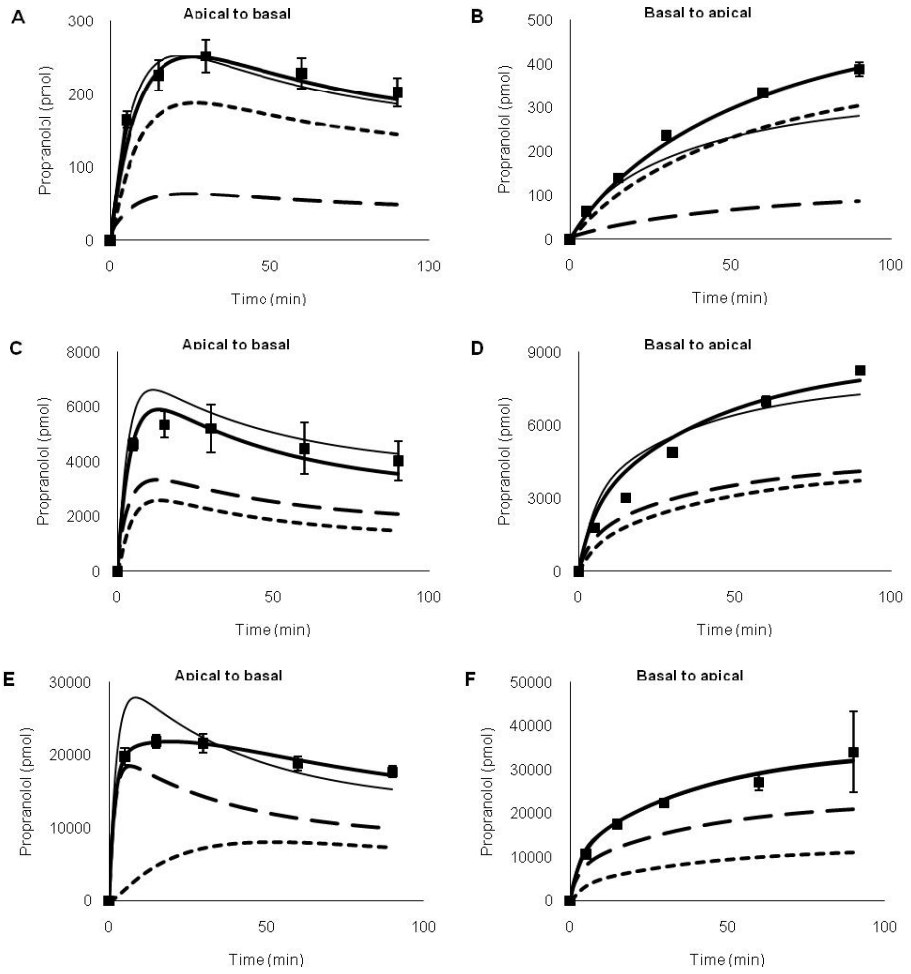

Figure 6.3. The time course of cellular retention of (A, B) 1 µM, (C, D) 50 µM and (E, F) 300 µM propranolol in Caco-2 permeation experiments (note the different scales of the vertical axes). The symbols represent the average of 6 measurements (± standard deviation). The thin and thick lines represent the fitted results of model 1a and model 1b, respectively. The dashed and dotted lines represent the predicted time course of propranolol in cytosolic and lysosomal compartments in model 1b, respectively.

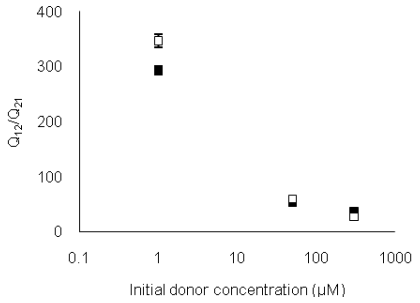

Figure 6.4. The concentration dependence of lysosomal sequestration of propranolol. The closed and open symbols refer to the estimated ratio of flux rates between cytosolic and lysosomal compartments (± standard error) in apical to basal and basal to apical direction experiments, respectively.

6.3.3 Estimation of permeability coefficients.

Model 1a was used to simulate data for permeability estimation. The permeabilities estimated from simulated data using Equation 2.3 ($P_{app,sink}$) increased initially and started to decline in the later phases (Figure 6.5 A). Further, the $P_{app,sink}$ values were lower with higher K, i.e. with higher cellular retention. However, the $P_{app,sink}$ values in apical to basal and basal to apical directions at same cellular retention level were identical. Further, $P_{app,sink}$ was constantly lower than the theoretical P_{app} (calculated using Equation 6.1) and also lower than the permeabilities estimated using Equation 2.4 ($P_{app,Palm}$) or Equation 2.5. ($P_{app,Tran}$).

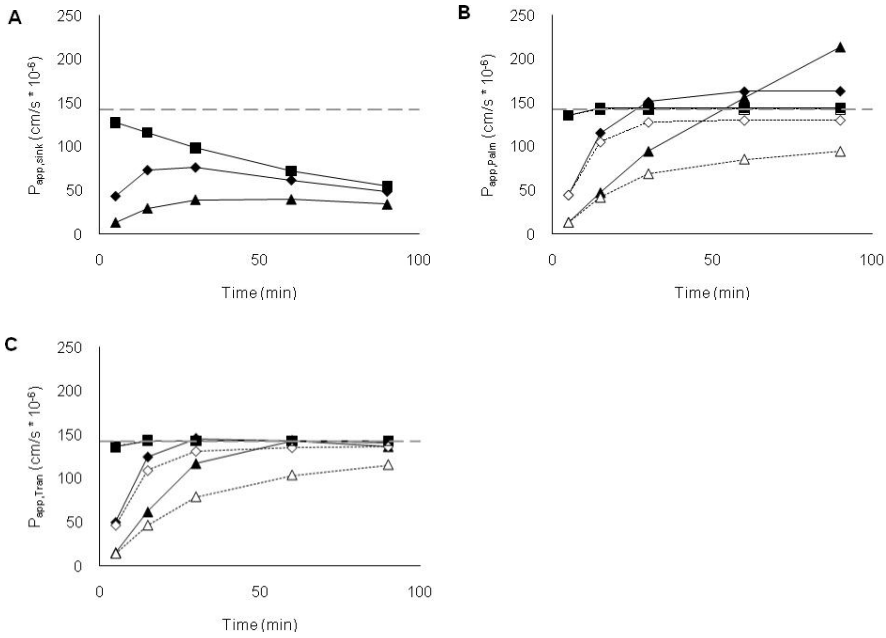

Figure 6.5. The apparent permeabilities estimated from the simulated data using model 1 in apical to basal direction (closed symbols, solid line) and basal to apical direction (open symbols, dash line). $P_{app,sink}$, $P_{app,Palm}$ and $P_{app,Tran}$ are presented in panels A, B and C, respectively. Grey dash line refers to the theoretical P_{app} calculated from P_{api} and P_{baso} using equation $P_{app}=1/(1/P_{api}+1/P_{baso})$. In the simulation P_{api} and P_{baso} were set to 500 and 200 cm/s10^{-6}, respectively and K was set to 4 (squares), 100 (diamonds) or 400 (triangles). There were no direction difference in $P_{app,sink}$ at the same cellular retention, thus, only apical to basal direction is shown.*

$P_{app,Palm}$ and $P_{app,Tran}$ showed similar trends. They both take the decreased concentration gradient into account and render accurate permeability estimates when there is no significant cellular retention. However, cellular retention affects both $P_{app,Palm}$ and $P_{app,Tran}$. They both increased initially and reached eventually a stable level and the time to reach the stable level was longer with higher cellular retention (Figure 6.5). Both

$P_{app,Palm}$ and $P_{app,Tran}$ were consistently higher in A to B direction than in B to A direction (Figure 6.5 B,C). These discrepancies were higher with higher cellular retention. Further, at stable level $P_{app,Palm}$ in A to B direction was always higher, and in B to A direction always lower, than the theoretical P_{app}, whereas $P_{app,Tran}$ remained generally below or at the level of P_{app} in both directions.

Similar trends in permeability estimates were seen when data were simulated using model 1b. However, the times to $P_{app,sink}$ reach the maximum value and $P_{app,Palm}$ and $P_{app,Tran}$ to reach the stable level were delayed when the sequestration to lysosomal compartment was slow (data not shown).

The permeability estimates using experimental data showed similar trends than permeability estimates of simulated data (Figure 6.6).

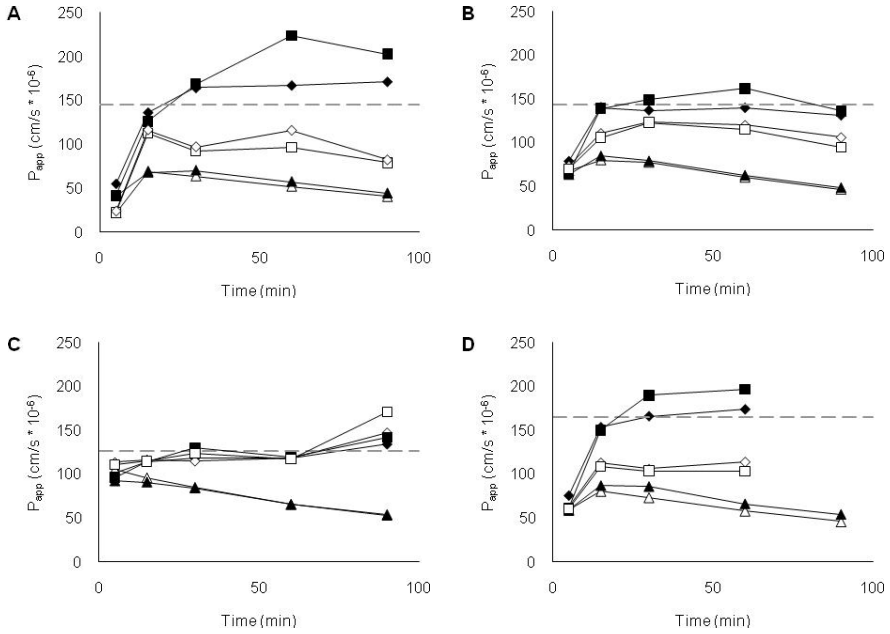

Figure 6.6. The apparent permeabilities of (A) 50 µM propranolol, (B) 50 µM propranolol in the presence of 100 nM bafilomycin A1, (C) 50 µM ibuprofen and (D) 1 µM testosterone estimated from the experimental data in apical to basal direction (closed symbols) and basal to apical direction (open symbols). The symbols (triangles for $P_{app,sink}$, squares for $P_{app,Palm}$ and diamonds for $P_{app,Tran}$) represent the average permeabilities and the error bars are omitted for clarity. At late time points, the testosterone (D) concentrations at the donor and receiver side are close to equilibrium. Consequently, the experimental errors cause significant variation in $P_{app,Palm}$ and in $P_{app,Tran}$. Therefore, $P_{app,Palm}$ and in $P_{app,Tran}$ are presented only up to 60 minutes for testosterone. Grey dashed line refers to the theoretical P_{app} calculated from the fitted values of P_{api} and P_{baso} (Table 6.1).

6.4 DISCUSSION

This study demonstrates the errors caused by cellular retention in permeability estimates. Further, propranolol was observed to be significantly sequestered into the lysosomes during Caco-2 permeation experiments. The inhibition of lysosomal sequestration has recently been reported to increase the apparent Caco-2 permeability ($P_{app,sink}$) of amodiaquine (Hayeshi et al., 2008b). These results suggest that the lysosomal sequestration of basic compounds may significantly contribute to the cellular retention of basic compounds and, thus, cause substantial errors in permeability estimates. However, it has to be noted that all basic compounds may not be susceptible to lysosomal sequestration (Duvvuri et al., 2004).

The fittings of model 1a suggest that cell monolayer behaves as a single kinetic compartment for testosterone and ibuprofen, whereas for propranolol also a slow intracellular compartment may be needed to describe the cellular retention. However, in the presence of bafilomycin A1 a single intracellular compartment was adequate to describe also the cellular retention profile of propranolol, although it is possible that bafilomycin A1 does not neutralize the lysosomes completely (Yoshimori et al., 1991).

The principal driving force to lysosomal sequestration of weak bases is pH gradient between cytosol and lysosomes (Kaufmann and Krise, 2007). However, lysosomal sequestration of bases has been reported to cause concentration dependent elevation of lysosomal pH (Poole and Ohkuma, 1981). Further, extensive accumulation of weak bases, including propranolol, causes osmotic swelling of lysosomes (Ohkuma and Poole, 1981), which may affect the surface area of the lysosomes. Thus, both the driving force and the area available for flux between cytosolic and lysosomal compartments are likely to be dynamic. Consequently, the distribution kinetics of weak bases between cytosolic and lysosomal compartments is variable, depending, among other factors, on the amount of the base in the system. Because of the complexity of the factors involved, it is not a simple task to rigorously model the lysosomal sequestration kinetics.

Model 1b is an attempt to model the lysosomal sequestration kinetics during Caco-2 permeation experiments. Describing the flux rates between the cytosolic and lysosomal compartments with first order rate coefficients is a rough simplification of the underlying phenomena. The cellular data in this study was based on measurements of total cell lysates and, thus, we have no direct experimental knowledge of the test compounds intracellular localization, which would be needed to develop a more rigorous mechanistic model of the lysosomal sequestration kinetics. The methods to measure the intracellular localization are reviewed elsewhere (Kaufmann and Krise, 2007). However, with the currently available methodology it would be very challenging (if not impossible) to obtain rigorous intracellular localization data in

permeation setting. Anyhow, two conclusions can be drawn from the current analysis. Firstly, the clear concentration dependence seen in Q_{12} to Q_{21} ratio (Figure 6.4), which describes the extent of lysosomal sequestration, suggests that the capacity of lysosomes to sequester propranolol is saturating within the concentration range used. Secondly, although the problems in identifying the lysosomal distribution rate coefficients, the model 2 was able to successfully mimic the total cellular retention profile of propranolol better than model 1. Also the AIC values (Table 6.2) favour the model 1a in describing the propranolol kinetics, suggesting that lysosomes may act as a kinetically slow intracellular compartment and the lysosomal distribution rate may be concentration dependent. Thus, the lysosomal sequestration of weak bases affects not only the extent but also the rate of cellular retention.

The cellular retention profile of test compound is dependent of the direction from where the compound enters the cell monolayer. Compartmental modeling was employed to clarify the factors causing this behaviour. The results suggest that the barrier at the basal side of the cell monolayer resist the flux of compounds more that the barrier at the apical side. This seems reasonable because the barrier at the apical side consists only of cell membrane and unstirred water layer, whereas the barrier at the basal side contains additionally the filter support. Further, it has been suggested that the resistance of unstirred water layer would lie predominantly at the basal side because of the differential hydrodynamics (Ho et al., 1999). However, it has been difficult to obtain experimental evidence in favor of this suggestion (Korjamo et al., 2008).

As expected, using $P_{app,sink}$, the approach that requires sink conditions to be fulfilled constantly underestimates the permeability because the concentrations in both compartments changes significantly during the experiments. Moreover, the estimated permeabilities lower with lower concentration due to higher cellular retention. Further, it is important to note that as the appearance kinetics to the receiver is irrespective of experimental direction and because $P_{app,sink}$ neglects the decline of donor concentration, there are no direction differences in $P_{app,sink}$ estimates at the same cellular retention level.

For high permeability compounds it is expected that $P_{app,Palm}$ would be a better estimate of the permeability than $P_{app,sink}$, since the loss of sink conditions does not cause the $P_{app,Palm}$ estimates to decline in the late phases. Also the actual concentration gradient at the onset of the sampling interval is taken into account. However, $P_{app,Palm}$ underestimated the permeability in B to A direction for the whole time course whereas in A to B direction permeability is underestimated only in the very early stage and overestimated at the late stages. The errors made are higher when high amount of test

compound is retained in the cells (Figure 6.5 and Figure 6.6) The appearance kinetics to the receiver is irrespective of experimental direction. Thus, this discrepancy must be caused by the difference in disappearance kinetics from the donor. The permeabilities through apical barrier are estimated to be 2 to 3 times higher than the permeabilities through basal barrier (Table 6.1), for the compounds used in this study. Consequently, at the apparent steady state permeation (when the $P_{app,Palm}$ has reached the stable level), the free cellular concentration as well as amount retained in the cell monolayer follows the concentration of the apical compartment irrespective of the direction of the experiment. Therefore, at the apparent steady state permeation in A to B experiments the test compound appears to the receiver side faster than disappears from the donor side, whereas the opposite is seen in B to A experiments, ultimately causing the errors seen in $P_{app,Palm}$. Further, it has to be noted that with compounds which are significantly retained in the cell monolayer the time to reach the apparent steady state permeation may be delayed significantly. Therefore, at the steady state permeation the concentrations at the donor and receiver may already be near to equilibrium and, thus, the concentration change within a sampling interval is small. Consequently, already minor experimental variation causes significant variation in $P_{app,Palm}$ causing the behaviour of estimated permeabilities to be erratic.

Usually in cell permeation experiments only the appearance rate is measured whereas disappearance rate is not observed in detail. Such data does not contain information about the cellular retention kinetics and, thus, it is impossible to take the cellular retention rigorously into account in permeability estimates. Anyhow, it has been suggested that poor recovery could be taken into account in $P_{app,sink}$ estimate based on recovery calculation at a single time point, in practice at the end of the experiment (Youdim et al., 2003). However, because the cellular retention time profiles are concentration and directions dependent (Figure 6.1), correcting the permeability estimates with a single time point recovery may lead into apparent concentration dependency and directionality although the transfer of the test compound were solely due to passive diffusion.

Sampling of both receiver and donor compartments has been suggested for more rigorous correction for poor recovery (Tran et al., 2004). When there is no significant cellular retention involved (ibuprofen and simulation K=4), $P_{app,Tran}$ works perfectly in estimating the passive permeability although sink conditions are nor maintained. However, when significant cellular retention is involved (propranolol, testosterone and simulations K=100 and K=400), this approach encounters similar type of errors than another single barrier approach $P_{app,Palm}$ (Figure 6.5 and Figure 6.6). More the compound is retained in the cells larger is the apparent direction dependence of

permeability. $P_{app,Tran}$ is based on assumption of a single barrier and the amount of compound lost (due to any mechanism) from the solutions is assumed to 'vanish' from the system and, thus, assumed not to contribute to the transfer by any means. If this assumption would strictly hold true, it would mean that if the solution at the both apical and basal compartments would be replaced with fresh buffer, none of the compound retained in the cells would flux out from the cells. There are several examples in the literature showing that this is not usually true if metabolism or other degradation of the compound is not involved (Ho et al., 1999). When the amount of compound retained in the cells is affecting the transfer, the cellular 'volume of distribution' and the amount of compound in the cell monolayer should be taken into account to obtain correct 'average system concentration' <C>. However, taking the cellular compartment into account in <C> calculation would not be applicable to single barrier model the rest of the calculations are based on.

The data shown in this report suggests that considering the cell monolayer as a single barrier is in some cases an over simplified view even when studying passive transfer of the solutes through the cell monolayer. Further, flaws of applying single barrier view in mechanistic studies, such as studies to elucidate active transporter function, have recently been reported (Bentz et al., 2005; Korjamo et al., 2007; Sun and Pang, 2008). Thus, it seems evident that more sophisticated data analysis and interpretation approaches than traditional single barrier view should be employed when detailed insight into solute transfer is to be obtained.

Often in cell monolayer permeation studies the conclusions are drawn based on the assumption that the cell monolayer is a single barrier which does not significantly retain the compound studied. This approach has been shown to be applicable for screening for transporter interactions (Polli et al., 2001) and prediction of intestinal absorption of passively absorbed compounds (Artursson et al., 2001). However, it has been suggested that as good predictions of intestinal absorption of passively absorbed compounds can be obtained even by computational methods (Linnankoski et al., 2008). The use of the cell monolayer permeability studies to predict the in vivo absorption have been justified with the presence of relevant transfer routes, which are absent in artificial membranes and are not necessarily taken into account in computational approaches, such as paracellular space and active transporters (Artursson et al., 2001). However, the relative role of different transfer routes in in vitro cell models tend to differ from the in vivo setting. Therefore, successful scaling from in vitro data to in vivo setting is likely to require detailed mechanistic insight.

7 Distribution of permeation resistance in in vitro cell permeation experiments[3]

Abstract. The results of cell monolayer permeation experiments are often affected by concentration dependent cellular processes, such as active transport and metabolism. The rigorous analysis of the concentration dependence of these processes is often limited by the lack of knowledge of the actual concentration at the site of action because the measurement of the local concentration is seldom feasible. However, the local concentrations can be estimated if the rates into and out of a particular location are known. Thus, an insight into the distribution of the permeation resistance in the *in vitro* cell monolayer permeation experiments would enable the estimation of local concentrations during the permeation experiments and, consequently, a more thorough analysis of the concentration dependent processes involved in the transepithelial transfer of compounds. In this study, a compartmental model was constructed applicable for dissecting the roles of apical and basal side aqueous boundary layers and the cell membranes in the total permeation barrier for weakly acidic and basic compounds. The model was applied for the analysis of the Caco-2 permeation data of three high permeability compounds, propranolol, metoprolol and ibuprofen. Furthermore, the effects of extracellular pH and the agitation conditions on the local concentrations of these compounds were evaluated.

[3] Adapted from: Heikkinen A.T., Mönkkönen J., Korjamo T.: Determination of permeation resistance distribution in *in vitro* cell monolayer permeation experiments. Eur J Pharm Sci 40: 132-142, 2010.

7.1 INTRODUCTION

Mechanistic cell permeation studies are often focused on some concentration dependent mechanism(s) involved in the transfer of the studied compound, such as active transport and/or metabolism. The site of action is rarely ever in the bulk phase of the donor or receiver compartment in such studies. Rather, the site of action lies at some specific cellular substructure, such as on the cell surface for uptake transporters (Balakrishnan et al., 2007), within the inner leaflet of the cell membrane for efflux transporters (Ambudkar et al., 2006) or at the endoplasmic reticulum for cytochrome P450 enzymes (Szczesna-Skorupa and Kemper, 2008). Although the location of the site of action is often known, the local substrate concentration is usually not readily measurable from intact cells. Consequently, the initial donor concentration is often used as a surrogate for the true local concentration (Maier-Salamon et al., 2006; Troutman and Thakker, 2003a). In the permeation setting, there is a concentration gradient from the donor to the receiver chamber and the cellular structures are downstream from the donor compartment. Furthermore, in practice the donor concentration always declines during the permeation experiment to some extent. Thus, the use of initial donor concentration in kinetic analyses biases the results because intracellular and extracellular concentrations are neither constant nor in constant proportion to each other during the whole experiment. On the other hand, the concentration of the compound studied at any location during the experiments is dictated by the 'rate in' to and the 'rate out' from the particular site. Consequently, theoretically the local concentration can be estimated without direct measurements if the above mentioned rates are known.

The permeation barrier in the cell monolayer permeation experiments consists of several individual barriers; the ABLs and the cell membranes at both apical and basal sides of the cell cytosol (Figure 2.2). Consistent to the low fluidity of the exofacial leaflet of the apical cell membrane (Lande et al., 1995; Simons and van Meer, 1988), early reports suggest that for low permeability compounds digoxin and vinblastine (Ito et al., 1999) and the ciprofloxacin derivative, CNV 97100 (Gonzalez-Alvarez et al., 2005) the passive permeability across the permeation barrier at the apical side is less than that across the barrier at the basal side. In contrast, the results presented in the Chapter 6 suggested that the total passive permeation barrier at the basal side is two to three times greater than the barrier at the apical side for high permeability compounds propranolol, ibuprofen and testosterone. The ABL is a significant part of the permeation barrier for the high permeability compounds (Korjamo et al., 2009). Therefore, the distribution of permeation resistance for high permeability compounds into apical and basal sides of the cell monolayer is more likely to reflect the distribution

of ABL than the differential permeabilities through the apical and basolateral cell membranes. Thus, it seems that the distribution of the permeation barrier to the apical and basal sides depends both on the compound, apparatus used for the experiments and on the experimental conditions.

Several experimental approaches have been proposed to distinguish the permeation resistance of ABL from the resistance of the biological or artificial barrier of interest (reviewed in Korjamo et al., 2009). However, generally these methods are not able to distinguish the distribution of the ABL and cell monolayer into the apical and basal components. Thus, often some simplified assumption of the distribution of permeation barrier is applied. For example, ABL can be totally neglected and the permeability through both apical and basal cell membranes is assumed to be equal (Sun et al., 2008) or ABL may be postulated either to be negligible on the basal side because there is an extensive sink in the basal compartment or to be equally distributed into apical and basal sides (Nielsen and Avdeef, 2004). Furthermore, there is only one study reported in which the dissection of the distribution of UWL into apical and basal components has been attempted experimentally (Korjamo et al., 2008). However, in that study the cell monolayer was modeled as a single barrier. Thus, the analysis did not enable direct estimation of the intracellular concentrations or the local concentrations at the surfaces of the cell monolayer. Consequently, the results cannot be directly used for mechanistic analysis of concentration dependent processes, such as metabolism or active transport.

Compartmental model based analysis, without discrimination of ABLs from cell membranes, has been applied for estimating the distribution of the permeation barrier into the apical and basal components (Gonzalez-Alvarez et al., 2005; Ito et al., 1999). On the other hand, the so called pH shift method exploiting the different cell monolayer permeation, but similar ABL permeation characteristics of the ionized and unionized species has been applied for estimation of the distribution of the permeation barrier into the ABL and cell monolayer (Avdeef et al., 2005; Korjamo et al., 2009). However, apical and basal components were not discriminated. In this study these two approaches were combined in order to estimate the distribution of the permeation resistance into four components; apical and basal side ABLs and cell membranes. A compartmental model accounting for the cell membranes and apical and basal ABLs individually was constructed and used to analyze our earlier *in vitro* Caco-2 permeation data (Korjamo et al., 2008). This modeling exercise was conducted in order to assess the suitability and robustness of a compartmental modeling approach for estimating the relative contributions of individual barriers in the total permeation barrier. Additionally, the compartmental model constructed was further exploited to explore the effects of extracellular pH and agitation conditions on the distribution of

the permeation resistance in Caco-2 monolayer permeation experiments and the consequent effects on the estimated intracellular and cell surface concentrations.

7.2 MATERIALS AND METHODS

7.2.1 Experimental data

The experimental data were taken from (Korjamo et al., 2008). Briefly, the permeation experiments to both directions at four different pH values (5.8, 6.5, 7.0 and 7.4) and at four different shaking rates (250 rpm, 320 rpm, 370 rpm and 420 rpm) with and without vigorous magnetic stirring at the basal chamber were conducted using Caco-2 monolayers on an orbital shaker with orbit diameter of 1.5 mm (Titramax 1000, Heidolph, Germany). For clarification, in this text the terms shaking and stirring refer to the planar orbital shaking of the Transwell plate and to the magnetic stirring at the basal chamber, respectively, whereas the term agitation is used as a more general term covering both shaking and stirring. The studied compounds (atenolol, antipyrine, ibuprofen, metoprolol, propranolol and verapamil) were dosed as a mixture, each at 50 µM initial donor concentration. Atenolol was used as a cell monolayer integrity control in the study and the concentrations at the receiver compartment in successful experiments were partially below or at the detection limit. Thus, the atenolol data was not included in the analysis. The method applied to estimate aqueous boundary layer permeability is based on the change of ionization of the compound as a function of pH. Since the charge state of antipyrine is virtually zero throughout the entire pH range used, antipyrine data could not be used for this analysis. Earlier analysis of verapamil data pointed to apically directed active transport of verapamil (Korjamo et al., 2008). The compartmental model applied in this study assumes only passive diffusion based transfer of the compounds. Thus, the verapamil data was also omitted from the current analysis.

7.2.2 Kinetic modeling

Model 2 was applied for the analysis of the data, i.e. the disposition of the compounds in the cell monolayer permeation experiments was modeled as movement of the compound between five consecutive compartments; apical bulk, apical ABL, cell, basal ABL and basal bulk (Figure 4.1). The results reported in the Chapter 6 revealed that the cellular retention may be saturable. However, current data was only from single concentration experiments. Therefore, the data did not allow for fitting the concentration dependence of the cellular retention. Consequently, K was assumed to be concentration independent.

Due to differences in the apical and basal cell membrane composition (Simons and van Meer, 1988), the permeabilies through apical and basal cell membranes may differ from

each other. However, current data did not allow rigorous fitting apical and basal of cell membrane permeabilities separately (data not shown). Thus, for final model fitting both P_i and P_u were constrained to be equal across the apical and basal cell membranes.

7.2.3 Simulations and estimation of model parameters

The permeability and cellular distribution parameters were estimated by fitting the compartmental model individually to the data sets from different agitation schemes (each dataset containing data from experiments at 4 different pH values in both directions) using WinNonlin software, version 5.2.1 (Pharsight, Mountain View, CA) to estimate the permeabilities through the cell membranes and cellular distribution coefficients of propranolol, metoprolol and ibuprofen and the apical and basal ABL thickness at the different agitation schemes. A weighting scheme 1/predicted^2 was chosen for all data fittings based on residual plots (Figure 7.1) and S.E. of the parameter estimates. Otherwise, the default WinNonlin settings for minimization of error were applied.

Simulated concentrations from the best fits to the data were used to explore the estimated concentrations at the cell surfaces and within the cell cytosol during the experiments at different experimental conditions.

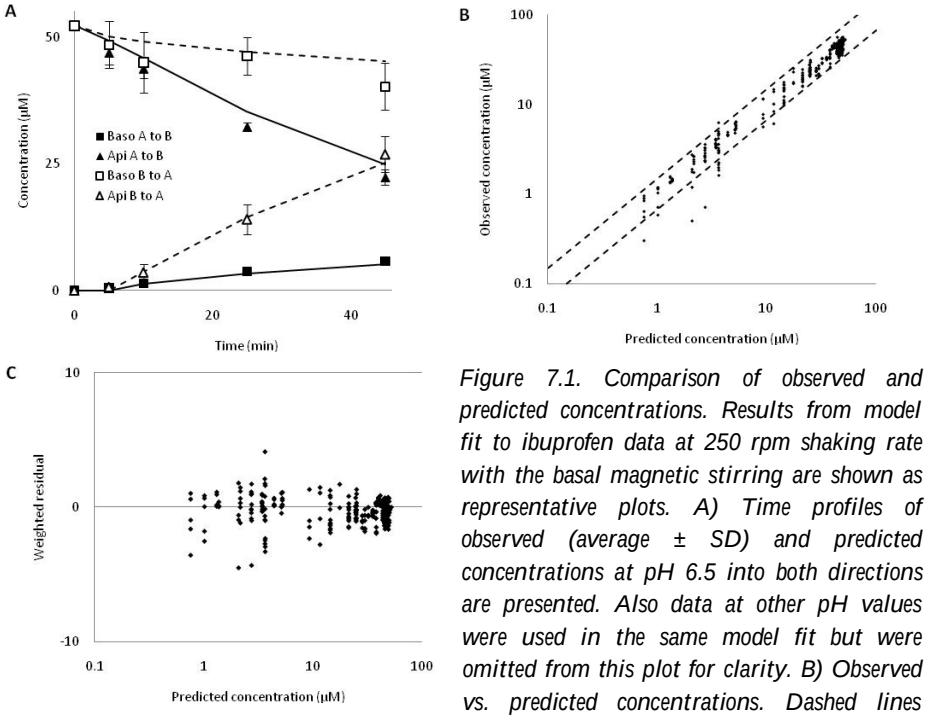

Figure 7.1. Comparison of observed and predicted concentrations. Results from model fit to ibuprofen data at 250 rpm shaking rate with the basal magnetic stirring are shown as representative plots. A) Time profiles of observed (average ± SD) and predicted concentrations at pH 6.5 into both directions are presented. Also data at other pH values were used in the same model fit but were omitted from this plot for clarity. B) Observed vs. predicted concentrations. Dashed lines depict the 1.5 fold error interval. C) Distribution of weighted residuals.

7.3 RESULTS

7.3.1 Estimation of the cell membrane permeabilities, cellular distribution and the effects of agitation on the ABL thickness

The five compartment model constructed was able to mimic the observed concentration profiles. In total, more than 85% and 97% of the observed concentrations were within 1.2 fold and 1.5 fold error intervals, respectively. Comparison of observed and predicted concentrations of a typical model fit is visualized in Figure 7.1.

As expected, the estimated cell membrane permeability of unionized species of all model compounds were significantly (2 to 4 orders of magnitude) higher than the cell membrane permeability of the corresponding ionized species (Figure 7.2). Furthermore, generally the best fit estimates of cell membrane permeability (Figure 7.2) or the cellular distribution coefficients (Figure 7.3) remained unaffected by the agitation applied. However, the estimates of cell membrane permeability ionized metoprolol as well as the cellular distribution coefficient of ibuprofen showed substantial variations. On the other hand, despite the considerable variation in the estimates the agitation applied exerted clear effects on the operational ABL thickness on both sides of the cell monolayer (Figure 7.4). Furthermore, the trends of ABL thickness were similar for all compounds studied. However, the estimated ABL thickness was generally slightly higher for metoprolol than for propranolol and ibuprofen. Without basal magnetic stirring, the ABL thickness decreases with higher shaking rates at both apical and basal sides. However, in the presence of basal magnetic stirring, the increase in shaking rate did not decrease the basal ABL. In contrast, the estimated basal ABL thickness was slightly higher at 420 rpm than with the lower shaking rates. Furthermore, the basal magnetic stirring did not exert any clear effects on the apical ABL thickness, whereas the basal ABL thickness was generally lower in the presence than in the absence of basal magnetic stirring. Overall, the operational ABL thickness, and consequently the ABL permeability, without basal magnetic stirring seem to be at an approximately similar level on both sides of the cell monolayer. However, due to the presence of the support filter, the ABL lies more at the basal side with higher than with lower shaking rates.

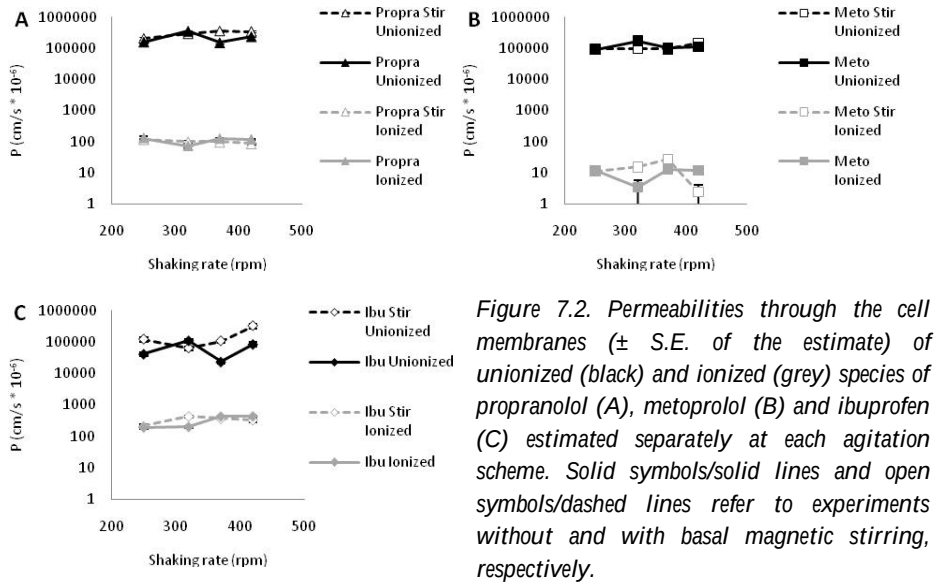

Figure 7.2. Permeabilities through the cell membranes (± S.E. of the estimate) of unionized (black) and ionized (grey) species of propranolol (A), metoprolol (B) and ibuprofen (C) estimated separately at each agitation scheme. Solid symbols/solid lines and open symbols/dashed lines refer to experiments without and with basal magnetic stirring, respectively.

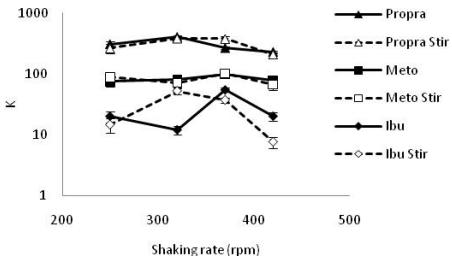

Figure 7.3. Cellular distribution coefficients (± S.E. of the estimate) of propranolol (triangles), metoprolol (squares) and ibuprofen (diamonds) estimated separately at each agitation scheme. Solid symbols/solid lines and open symbols/dashed lines refer to experiments without and with basal magnetic stirring, respectively.

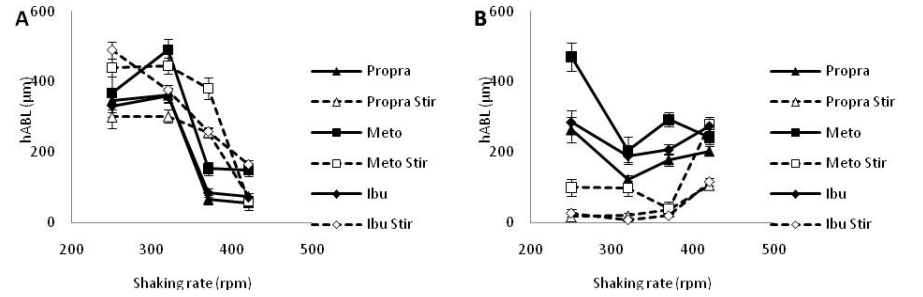

Figure 7.4. The estimated operational ABL thicknesses (± S.E. of the estimate) at apical (A) and basal (B) sides at different agitation schemes for propranolol (triangles), metoprolol (squares) and ibuprofen (diamonds). Solid symbols/solid lines and open symbols/dashed lines refer to experiments without and with basal magnetic stirring, respectively.

7.3.2 Effects of extracellular pH and shaking rate on the free cellular and cell surface concentrations during the cell permeation experiments

The simulated free intracellular and cell surface concentrations at different extracellular pH and shaking conditions were taken from the best fits of the model to the corresponding experimental data.

According to the simulations the cellular free concentrations of all model compounds reach approximately half of the initial donor concentration level at pH 7.4, when there is no pH gradient across the cell membranes (Figure 7.5). In contrast at a lower extracellular pH values, the basic metoprolol is rejected from the cytosol whereas acidic compound, ibuprofen is sequestered into the cytosol, resulting in low free cellular metoprolol concentrations and high free cellular ibuprofen concentrations at pH 5.8. Consequently, at low extracellular pH the metoprolol concentration in receiver compartment exceeds the intracellular free concentration during the late phases of the experiment, whereas the intracellular free ibuprofen concentration exceeds both the receiver and donor concentrations (Figure 7.5 and Figure 7.6). A change in the shaking rate affects the time profile of cellular concentration, but exerts only minor effect on the average cellular concentration level. Propranolol, the other basic model compound used, displayed a similar trends as seen with metoprolol (not shown).

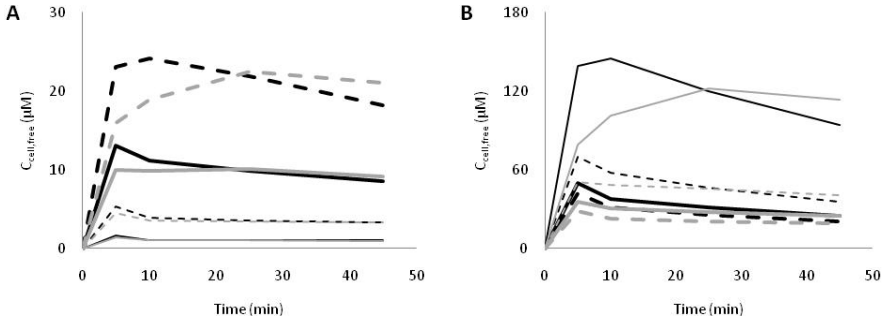

Figure 7.5. Simulated cellular free concentrations of metoprolol (A) and ibuprofen (B) in 250 rpm (grey lines) and 420 rpm (black lines) apical to basal direction experiments at different extracellular pH values. pH 5.8 thin solid line, pH 6.5 thin dashed line, pH 7.0 thick solid line and pH 7.4 thick dashed line. The cellular free concentrations reach approximately half of the initial donor concentration at pH 7.4, when there is no pH gradient across the cell membranes. At lower extracellular pH values the pH gradient across the cell membranes rejects the basic metoprolol from the cytosol and sequesters the acidic ibuprofen into the cytosol, resulting in low and high cellular metoprolol and ibuprofen concentrations at pH 5.8, respectively. The change in stirring rate affects the time profile of the cellular concentration but causes only a minor effect on the average cellular concentration level.

The effects of shaking rate and extracellular pH on the concentrations at the cell surfaces are illustrated in Figure 7.6. The concentration gradient across the cell

monolayer (from the cell surface to another) becomes smaller with a higher permeability through the cell monolayer, i.e. at high pH values for basic metoprolol and propranolol and at low pH for ibuprofen. Consequently, also the concentration difference between the bulk phase and the corresponding cell surface is more pronounced when the permeability through the cell monolayer is high. On the other hand, the concentration difference between bulk phase and the corresponding cell surface decreases as the shaking rate increases, whereas the concentration gradient across the cell monolayer increases slightly. Similar trends were observed also in the simulations of the propranolol and ibuprofen concentrations and also in the basal to apical direction experiments (not shown).

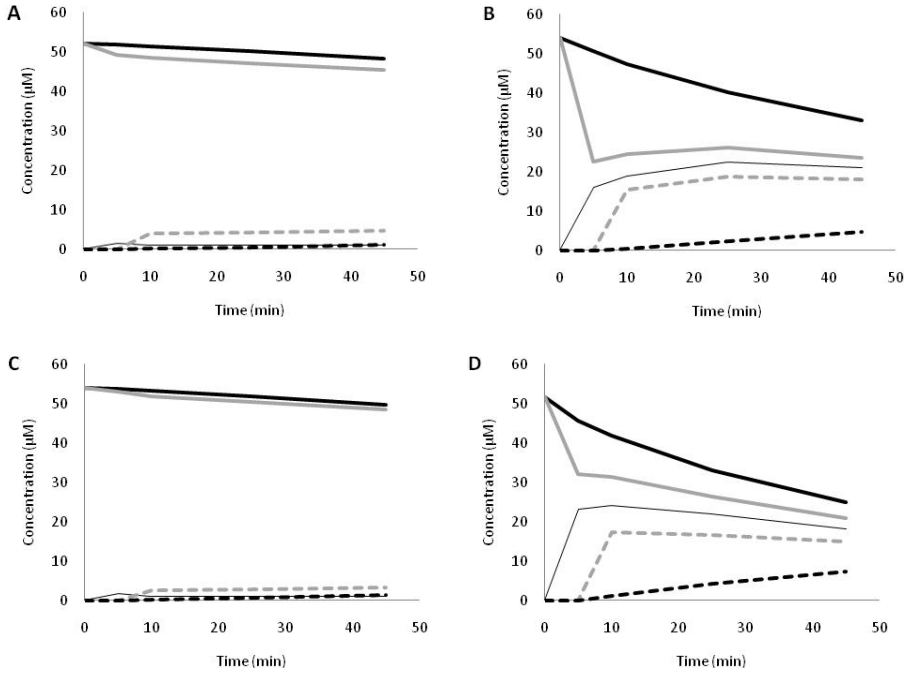

Figure 7.6. Simulated metoprolol concentrations at different locations during 250 rpm (A,B) and 420 rpm (C,D) apical to basal direction experiments at pH 5.8 (A,C) and pH 7.4 (B,D). Black and grey lines refer to bulk phases and cell surfaces, respectively. Solid and dashed lines represent the concentrations at the apical and basal sides of the cell monolayer, respectively. The thin line is the simulated cellular free concentration. The concentration gradient across the cell monolayer (from apical to basal cell surface) becomes smaller as the permeability through the cell monolayer becomes higher, i.e. at high pH values for the basic compound, metoprolol. The concentration gradient between the bulk phase and the corresponding cell surface becomes smaller with a higher stirring rate.

7.4 DISCUSSION

The present study evaluated the feasibility and robustness of compartmental model based data analysis to determine the distribution of the permeation resistance in *in vitro* cell permeation experiments. The five compartment model developed was further exploited to estimate the local concentrations at the cell surfaces as well as in the intracellular compartment during the time course of the experiments.

Theoretically, the cellular permeation and distribution should be independent of the agitation applied whereas the thickness and distribution of ABL are expected to be dependent on the agitation applied. On the other hand, ABL thickness and distribution should be similar for these similar sized molecules (Table 4.1) (Yu and Sinko, 1997), whereas the cellular permeation and distribution characteristics would be expected to be compound specific. Consequently, more accurate estimates of different parameters would be expected if all the available data were utilized in a single model fit, i.e. by fitting the model simultaneously to all data sets and estimating only one value for cell related parameters (P_u, P_i and K) for each compound and single values for apical and basal ABL thickness for each agitation scheme. Also, utilization of non-linear mixed-effects modeling approach could enable inclusion of covariate factors, such as shaking rate or molecule properties into the model and quantitative analysis of the effects of these covariates. However, there were two reasons why the parameter estimation was conducted individually for each compound at each agitation scheme rather than estimating the 'global' best fit values based on all the data sets: 1) For practical reasons, further applications of the approach used for the parameter estimation should not require such an extensive amount of experimental data as was conducted in this study. Consequently, one of the main goals of this study was to assess the robustness of the compartmental model based data analysis in the determination of the distribution of permeation resistance into apical and basal ABL and cell membranes in *in vitro* cell permeation experiments. 2) The amount of differential equations and data points handled simultaneously is limited in WinNonlin software thus creating a practical limitation for the model complexity and the amount of data used for simultaneous fitting when this software is used.

In general, the parameter estimates followed the above mentioned expectations: the parameters describing the cellular permeation and distribution (P_u, P_i and K) remained generally fairly stable and were not affected by the agitation applied (Figure 7.2 and Figure 7.3) whereas the ABLs were clearly dependent on the agitation. This suggests that the current five compartment model is able to distinguish the ABL and cell monolayer related processes from each other. The estimated distribution of ABL and UWL into apical and basal sides of the cell monolayer follows the same general trends

than obtained in the earlier analysis of these data (Korjamo et al., 2008). The ABL resistance is at an approximately similar level on both sides, but the contribution of UWL decreases with high shaking rates whereas the filter permeability is unaffected. Thus, an increase in orbital shaking rate of Transwell plate will decrease more efficiently the apical than the basolateral ABL. Furthermore, the operational ABL thickness at the basal side in the presence of basal magnetic stirring is generally in the level of <100µm. This is in accordance with the calculated permeability through the filter support (Korjamo et al., 2008), which would respond to approximately 80µm of operational ABL thickness. Additionally, this result also confirms the ability of our five compartment model to estimate the magnitude and distribution of ABL. However, there was considerable variation in some of the parameter estimates, which is probably partly a consequence of the fact that the experimental data used was obtained from an earlier study and, thus, the experimental setup was not designed for the purposes of the current analysis approach. In the compartmental model based analysis, the experimental data needs to contain information about the time profile of the compound transfer in each compartment included in the model; i.e., when there are no direct measurements of cellular retention available, the information about the concentration time profile in cellular compartment is based on the recovery of the drug from the aqueous compartments. Therefore, it would be advantageous if the cellular retention time profile would be readily observable from the recovery. However, the original data analysis and interpretation of this data set was based on the determination of apparent permeability (P_{app}) through the whole barrier at several experimental conditions (Korjamo et al., 2008). Poor recovery and variation in the recovery may disturb the P_{app} estimates (Hubatsch et al., 2007; Youdim et al., 2003). Therefore, the effects of cellular retention on the permeability estimates were minimized in the current experimental setting with a 5 minute initial accumulation phase into the cells before application of the receiver buffer (Korjamo et al., 2008). Consequently, there were no major changes in the recovery after the initial accumulation phase, which makes the compartmental model based analysis more vulnerable to experimental variation.

Although the current model was able, to some extent, to estimate the distribution of ABL into apical and basal sides of the cell monolayer, it was not able to distinguish the permeability coefficients through apical and basal cell membranes. The attempts to fit separate permeability values for apical and basal cell membranes resulted in similar permeability coefficients through both membranes accompanied by increased uncertainty and greated variation in the parameter estimates (data not shown). Consequently, in model fitting the permeabilities through apical and basal cell membranes were constrained to be equal. This contrasts to the generally accepted

assumption that the apical cell membrane is the primary barrier for transcellular permeation (Lennernäs, 2007), which is supported by the lower fluidity of the exofacial leaflet of the apical cell membrane (Lande et al., 1995) as well as the compartmental model based analysis of cell monolayer permeation kinetics of the low permeability compounds digoxin, vinblastine and CNV 97100 (Gonzalez-Alvarez et al., 2005; Ito et al., 1999). The failure to distinguish apical and basal cell membrane permeabilities may partly be related to the above discussed suboptimal experimental design for current analysis. However, similar results were obtained also for another high permeability compound, quinidine (Chapter 8), indicating that more thorough sampling from aqueous compartments does not solve this problem. Furthermore, analysis of the passive efflux rate of the highly permeable lipid antioxidant, U-78517F from MDCK cells suggested that the permeabilities through the apical and basal cell membranes are equivalent (Raub et al., 1993). Thus, a more plausible explanation for indistinguishable apparent permeability of high permeability compounds through the apical and basal cell membranes may be traced to the intracellular permeation and distribution kinetics. The current model assumes that the space between the cell membranes is well stirred without any resistance to compound transfer. For low permeability compounds, the relative permeation resistance of cytosol is likely to be negligible whereas for high permeability compounds, such as the molecules used in this study, the cytosol may represent a more significant part of the permeation barrier. If one assumes that the permeation barrier of cytosol is equal to a 20 µm thick water layer in between the cell membranes (equal to thickness of Caco-2 cell monolayer) it can be approximated that the proportion of cytosol in the total permeation resistance of the cell monolayer is 5-25% for the compounds used in this study (see sub-chapter 7.5 for the calculations). However, the viscosity of the cell cytosol is likely to be higher than that of bulk water (Luby-Phelps, 2000) and, thus, the role of cytosol in the cellular permeation barrier may be even more prominent. Nonetheless, it should be noted that effectively the overall *in vitro* permeation for such rapidly transported compounds is primarily controlled by ABL. Additionally, analysis of propranolol and metoprolol data may be confounded by lysosomal sequestration of these compounds. The previous analysis of the cellular retention kinetics of propranolol indicated that acidic cellular compartments such as lysosomes may behave as a 'slow' kinetic cellular compartment (Chapter 6). However, the current data do not include direct measurements of cellular retention and, thus, do not provide sufficient information about the cellular retention profile to allow inclusion of an additional cellular compartment into the model. Consequently, the possible effects of lysosomal sequestration on the cellular distribution kinetics are neglected. Thus, in the case of high permeability compounds, the P_u and P_i estimates may reflect

not only the permeability through the cell membranes but may also be limited by the permeation and distribution kinetics within the cells.

Although intracellular kinetics may limit the cell membrane permeability estimates, the P_i estimates, especially of ibuprofen and propranolol, were much higher than the paracellular permeability of mannitol suggesting that the ionized species of these molecules are able to permeate the cell membranes. The pH partition hypothesis suggests that only unionized molecules are able to diffuse through the cell membranes. Thus, our results do not agree with the pH partition hypothesis. The apparent transcellular permeability of ionized species in Caco-2 experiments has also been reported by others (Avdeef et al., 2005), though the exact mechanism underlying these findings remains to be clarified. The ionized species of lipophilic compounds have been shown to be able to distribute into artificial lipids and, thus, it has been suggested that passive diffusion based permeation of ionized molecules could contribute to membrane permeability (Austin et al., 1995; Duvvuri et al., 2004). Furthermore, there are also experimental results suggesting lipid bilayer permeability of anionic forms of weak acids has been reported (Thomae et al., 2005). However, these results are controversial and it has been suggested that they arise from an experimental artifact (Saparov et al., 2006). On the other hand, although there were no signs of polarization of transport through the whole cell monolayer, the possible involvement of transporters in the current study cannot be ruled out. It has been suggested that cell membrane permeation of ionized forms of metoprolol and propranolol is mediated by the organic cation transporter OCT2 rather than passive diffusion (Dudley et al., 2000). Furthermore, uptake experiments with *Xenopus laevis oocytes* have suggested that ibuprofen can inhibit the monocarboxylic acid transporter 1 (MCT1) mediated transport of lactic acid and OAT1 mediated transport of para-aminohippurate and, thus, it was proposed that ibuprofen might be transported by these proteins (Apiwattanakul et al., 1999; Tamai et al., 1995). Since there is some evidence for expression of these transporters in Caco-2 (Ahlin et al., 2009; Hilgendorf et al., 2007), it is possible that their involvement has interfered with the current results.

The five compartment model based data analysis allows estimation of the free concentration inside the cell monolayer as well as at both cell surfaces when only the bulk phase concentrations are measured (Figure 7.5 and Figure 7.6). However, due to above discussed limitations and uncertainties in estimating the contributions of different permeation barriers the estimates of local concentrations should be considered only as approximations. Nonetheless, these estimates are believed to follow the trends of the actual local concentrations and, thus, are likely to represent a better basis for analysis of concentration dependent cellular processes than the traditionally applied

initial donor concentration approach. Furthermore, the simulations highlight significant difference in the free intracellular concentrations of weak bases compared to weak acids when there is a pH gradient across the cell membranes (Figure 7.5). Since there is a pH gradient across the apical cell membrane in the intestine *in vivo* (acidic intestinal lumen vs. approximately neutral enterocyte interior) (Avdeef, 2003), this may have significant implications on the interpretation of concentration dependent intracellular processes observed in *in vitro* permeation experiments as well as on the extrapolation of these processes to the *in vivo* situation.

To conclude, this study demonstrated the applicability of compartmental models for the analysis of the permeation resistance distribution and as a way to estimate the local concentrations in *in vitro* cell permeation experiments. Furthermore, the compartmental model used can be further developed to incorporate other drug disposition mechanisms, such as active transport and metabolism. However, current analysis underlines the importance of high quality data and good experimental design when compartmental models are applied for data analysis. In addition, the limitations of using the experimental data to justify and estimate the parameters describing the mechanistic detail embedded in the model were demonstrated. Compartmental models will invariably represent simplifications of the system being modeled and, thus, dynamically minor mechanisms are not described in detail. Consequently, critical inspection of the underlying mechanisms is crucial for rigorous interpretation and application of the results obtained.

7.5 APPENDIX: APPROXIMATION OF THE PROPORTION OF CYTOSOL IN THE PERMEATION RESISTANCE OF CELL MONOLAYER

In the five compartment model used for analysis of the experimental data, the permeation through the cell monolayer was modeled as the passive permeation of ionized and unionized species through the cell membranes. The permeation barrier of the cell monolayer was assumed to consist of only apical and basal cell membranes, whereas the possible permeation barrier caused by the space in between the apical and basal cell membranes (i.e. cytosol) was neglected. Although the space in between the apical and basal cell membranes contains several other structures and is not only cytosol, for simplicity, in this text, the word cytosol refers to the space in between the apical and basal cell membranes unless indicated otherwise. However, when membrane permeability is high, it is possible that the cytosol constitutes a significant part of the cellular permeation barrier. The calculations to estimate the proportion of the cytosol in the permeation resistance of the cell monolayer are derived in this supplement. First, the total pH dependent cellular permeation resistance (R_{cell}) of each compound is calculated from the cell membrane permeability values of the ionized (P_i)

and unionized (P_u) species estimated by the five compartment model based analysis presented in the actual research report. Second, the permeation resistance of the cytosol (R_{cyto}) is estimated assuming that the cytosol is an aqueous space with the thickness equal to cell monolayer height. Finally, the proportion of the permeation barrier attributed to the cytosol (R_{cyto}%) is calculated from the estimated R_{cell} and R_{cyto}.

7.5.1 Calculation of R_{cell} from experimental data

The effective permeability for each compound through the whole cell monolayer (P_{cell}) is calculated from the average of the best fit values P_i and P_u from the fitting of the five compartment model.

First, let C_1, C_2, C_3 and C_4 be the concentrations at the donor side cell surface, cytosol facing donor side cell membrane, cytosol facing the receiver side cell membrane and receiver side cell surface, respectively (Figure 7.7). P_i and P_u values used for calculations are estimated using the five compartment model neglecting the cytosolic concentration gradient. Thus, C_2 is assumed to equal C_3. Subsequently let J1 and J2 be the flux rate of the compound from the donor to the cellular and from the cellular to the receiver compartments, respectively (Figure 7.7).

$$\mathbf{J1} = \mathbf{A} * \left[\left(\mathbf{f_u P_u} + \mathbf{f_i P_i} \right) \mathbf{C_1} - \left(\mathbf{f_{u,cell} P_u} + \mathbf{f_{i,cell} P_i} \right) \mathbf{C_2} \right] \qquad \textit{Equation 7.1}$$

$$\mathbf{J2} = \mathbf{A} * \left[\left(\mathbf{f_{u,cell} P_u} + \mathbf{f_{i,cell} P_i} \right) \mathbf{C_3} - \left(\mathbf{f_u P_u} + \mathbf{f_i P_i} \right) \mathbf{C_4} \right] \qquad \textit{Equation 7.2}$$

At steady state, the flux rate across each individual barrier equals the flux rate across the whole cell monolayer; therefore,

$$\mathbf{J} = \mathbf{J1} = \mathbf{J2} \qquad \textit{Equation 7.3}$$

By combining Equation 7.1, Equation 7.2 and Equation 7.3 and setting $C_{cell}=C_2=C_3$, we obtain

$$\left[\left(\mathbf{f_u P_u} + \mathbf{f_i P_i} \right) \mathbf{C_1} - \left(\mathbf{f_{u,cell} P_u} + \mathbf{f_{i,cell} P_i} \right) \mathbf{C_2} \right] = \left[\left(\mathbf{f_{u,cell} P_u} + \mathbf{f_{i,cell} P_i} \right) \mathbf{C_3} - \left(\mathbf{f_u P_u} + \mathbf{f_i P_i} \right) \mathbf{C_4} \right] \qquad \textit{Equation 7.4}$$

Subsequently, the cellular concentration can be solved

$$\mathbf{C_{cell}} = \frac{\left(\mathbf{f_u P_u} + \mathbf{f_i P_i} \right)}{2\left(\mathbf{f_{u,cell} P_u} + \mathbf{f_{i,cell} P_i} \right)} \left(\mathbf{C_1} + \mathbf{C_4} \right) \qquad \textit{Equation 7.5}$$

Thus, the flux rate through the whole cell monolayer is

$$\mathbf{J} = \mathbf{J1} = \mathbf{J2} = \mathbf{A} * \frac{\left(\mathbf{f_u P_u} + \mathbf{f_i P_i} \right)}{\mathbf{2}} \left(\mathbf{C_1} - \mathbf{C_4} \right) \qquad \textit{Equation 7.6}$$

Thus, the effective permeability through the cell monolayer is

$$\mathbf{P_{cell}} = \frac{\left(\mathbf{f_u P_u} + \mathbf{f_i P_i} \right)}{\mathbf{2}} \qquad \textit{Equation 7.7}$$

The P_{cell} estimates at different extracellular pH (Table *7.1*) are generally at similar level with the values reported earlier in the literature (Korjamo et al., 2008).

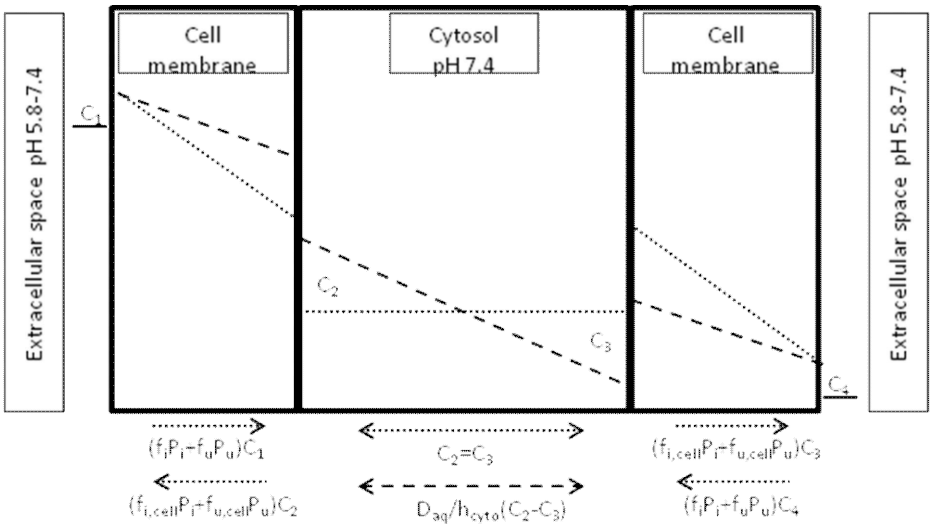

Figure 7.7. Schematic representation of the concentration gradient within the cell monolayer. The dotted line represents the approximated concentration profile based on the assumptions of the five compartment model used to analyze the experimental data; the cytosol is assumed to be a well stirred space and, thus, the cytosolic concentration facing the donor side cell membrane (C_2) is assumed to equal the cytosolic concentration facing the receiver side cell membrane (C_3). The cell membrane permeability values for ionized and unionized species estimated using this model were used for estimation of the total cellular permeation resistance (R_{cell}). The dashed line represents the approximated concentration profile when the cytosolic permeation resistance is accounted for, i.e. there is a concentration gradient in between the C_2 and C_3. This approach was used in order to estimate the cytosolic permeation resistance (R_{cyto}).

Table 7.1. The estimated permeabilities across the Caco-2 monolayer

		Metoprolol	Propranolol	Ibuprofen
	P_u (cm/s * 10^{-6}) [a]	110000	260000	110000
	P_i (cm/s * 10^{-6}) [a]	11	100	320
	pKa	9.56	9.53	4.45
	D_{aq} (cm^2/s *10^{-6})	7.91	7.80	7.90
	R_{cyto}% [b]	10 %	26 %	6 %
pH 5.8	f_u	0.017 %	0.019 %	4.276 %
	P_{cell} (cm/s * 10^{-6}) [c]	15	74	2500
pH 6.5	f_u	0.087 %	0.093 %	0.883 %
	P_{cell} (cm/s * 10^{-6}) [c]	53	170	640
pH 7.0	f_u	0.275 %	0.294 %	0.281 %
	P_{cell} (cm/s * 10^{-6}) [c]	160	430	310
pH 7.4	f_u (= $f_{u,cell}$)	0.687 %	0.736 %	0.112 %
	P_{cell} (cm/s * 10^{-6}) [c]	380	1000	220

[a] The average of best fit estimates of the permeabilities of unionized and ionized species across the cell membrane

[b] The estimated proportion of the cytosol in the cellular permeation barrier is independent of extracellular pH. Calculated according to Equation 7.17

[c] The apparent permeability across the cell monolayer. Calculated according to Equation 7.7

The permeation resistance is defined as the reciprocal of permeability (Flynn et al., 1974), consequently the permeation resistance of the cell monolayer is

$$\mathbf{R_{cell}} = \frac{\mathbf{2}}{\left(\mathbf{f_u P_u} + \mathbf{f_i P_i}\right)} \qquad \textit{Equation 7.8}$$

7.5.2 Calculation of R_{cyto} from theoretical considerations

The permeation resistance of the j^{th} barrier in the series of barriers is

$$\mathbf{R_j} = \frac{\mathbf{h_j}}{\mathbf{D_j * K_j}} \qquad \textit{Equation 7.9}$$

where h_j is the thickness of the of the j^{th} barrier, D_j is the diffusion coefficient within the j^{th} barrier and K_j represent the distribution coefficient to the j^{th} barrier in respect to the external phase (Flynn et al., 1974). For the approximation of cytosolic permeation resistance, it is assumed that the diffusion rate in the cytosol equals the diffusion rate in water and the thickness of the cytosol is equal to the height of the Caco-2 cell monolayer (20 µm). The effective distribution coefficient between the cytosol and the extracellular aqueous phase at donor or receiver ($K_{cell,1}$ or $K_{cell,2}$, respectively) is assumed to be constant throughout the experiment and, thus, equal to the distribution at equilibrium. At equilibrium, the effective flux rate J equals zero, i.e.

$$\mathbf{J1} = \mathbf{A} * \left[\left(\mathbf{f_u}\overline{\mathbf{P}}_{\mathbf{u}} + \mathbf{f_i}\overline{\mathbf{P}}_{\mathbf{i}}\right)\mathbf{C_1} - \left(\mathbf{f_{u,cell}}\overline{\mathbf{P}}_{\mathbf{u}} + \mathbf{f_{i,cell}}\overline{\mathbf{P}}_{\mathbf{i}}\right)\mathbf{C_2}\right] = \mathbf{0} \qquad \textit{Equation 7.10}$$

$$\mathbf{J2 = A * \left[\left(f_{u,cell}\tilde{P}_u + f_{i,cell}\tilde{P}_i\right)C_3 - \left(f_u\tilde{P}_u + f_i\tilde{P}_i\right)C_4\right] = 0} \qquad \textit{Equation 7.11}$$

where $\bar{P}_u$ and $\bar{P}_i$ are the permeabilities of unionized and ionized species through the donor side cell membrane when the cytosolic concentration gradient is accounted for whereas $\tilde{P}_u$ and $\tilde{P}_i$ refer to permeabilities through the receiver side cell membrane, respectively. Consequently,

$$\mathbf{K_{cyto,1} = \frac{C_2}{C_1} = \frac{\left(f_u\bar{P}_u + f_i\bar{P}_i\right)}{\left(f_{u,cell}\bar{P}_u + f_{i,cell}\bar{P}_i\right)}} \qquad \textit{Equation 7.12}$$

$$\mathbf{K_{cyto,2} = \frac{C_3}{C_4} = \frac{\left(f_u\tilde{P}_u + f_i\tilde{P}_i\right)}{\left(f_{u,cell}\tilde{P}_u + f_{i,cell}\tilde{P}_i\right)}} \qquad \textit{Equation 7.13}$$

The ratio of cell membrane permeabilities of ionized and unionized species is assumed to equal the ratio of P_i and P_u estimated using five compartment model, i.e.

$$\mathbf{P_i \big/ P_u = \bar{P}_i \big/ \bar{P}_u = \tilde{P}_i \big/ \tilde{P}_u} \qquad \textit{Equation 7.14}$$

This is a reasonable approximation, because if $\bar{P}_i/\bar{P}_u$ would be significantly different than $\tilde{P}_i/\tilde{P}_u$ it would result in polarization of the transcellular flux in the presence of a pH gradient across the cell membranes, whereas there were no indications of this kind of polarization of the transcellular flux in the experimental data.

By combining Equation 7.12, Equation 7.13 and Equation 7.14 we obtain

$$\mathbf{K_{cyto} = K_{cyto,1} = K_{cyto,2} = \frac{\left(f_uP_u + f_iP_i\right)}{\left(f_{u,cell}P_u + f_{i,cell}P_i\right)}} \qquad \textit{Equation 7.15}$$

Thus, the effective distribution coefficient between the extracellular aqueous phase and the cytosol is dictated by the ionization states of the compound in the extracellular and cytosolic compartments and the ratio of cell membrane permeabilities of ionized and unionized species.

By combining Equation 7.9 and Equation 7.15, the permeation resistance of the cytosol is estimated to be

$$\mathbf{R_{cyto} = \frac{h_{cyto}}{D_{aq} * K_{cyto}} = \frac{h_{cyto}\left(f_{u,cell}P_u + f_{i,cell}P_i\right)}{D_{aq}\left(f_uP_u + f_iP_i\right)}} \qquad \textit{Equation 7.16}$$

7.5.3 Calculation of R_{cyto}%

When the permeation resistances of the whole cell monolayer as well as of the cytosol are estimated, the proportion of cytosol in the permeation resistance of cell monolayer can be approximated to be

$$\mathbf{R_{cyto}\% = \frac{R_{cyto}}{R_{cell}} = \frac{h_{cyto}\left(f_{u,cell}P_u + f_{i,cell}P_i\right)}{2 * D_{aq}}} \qquad \textit{Equation 7.17}$$

From Equation 7.17, we can see that the proportion of the cytosol in the permeation

resistance of cytosol is not affected by the extracellular pH conditions. Based on the average of the best fit values of P_i and P_u, the relative contribution of the cytosol in the cellular permeation barrier was approximated to be 10%, 26% and 6% for metoprolol, propranolol and ibuprofen, respectively (Table 7.1). However, the cytosol is not pure water and it has been estimated that the cytosol viscosity may be significantly higher than that of bulk water (Luby-Phelps, 2000). Consequently, the diffusion rate in the cytosol could be significantly less than diffusion rate in water. Furthermore, our approximation of cytosol permeability completely neglects the possible diffusion via the lateral cell membrane and the existence of cellular organelles. Thus, the contribution of space between the apical and basal cell membranes in the permeation barrier may be more significant than approximated above. However, because of this relatively crude estimation of the cytosolic permeation barrier, it was considered that these approximations would be too arbitrary to be included into the compartmental model. Thus, these estimates are used only as suggestive values to illustrate that the space in between the cell membranes may indeed play a role in the cellular permeation barrier and interfere with the determination of P_i and P_u.

8 Concentration dependency of active efflux transport in in vitro cell permeation experiments[4]

Abstract. P-gp mediated efflux is one of the barriers limiting drug absorption from the intestine. Predictions of the intestinal P-gp function need to take into account the concentration dependency because high intestinal drug concentrations may saturate P-gp. However, the substrate binding site of P-gp lies inside the cells and the drug concentration at the binding site cannot be measured directly. Therefore, rigorous determination of concentration dependent P-gp kinetics is challenging. In this study, the effects of the aqueous boundary layers, extracellular pH and cellular retention on the apparent saturation kinetics of P-glycoprotein mediated transport of quinidine in an *in vitro* cell permeation setting were explored. The changes in the experimental conditions caused one order of magnitude variation in the apparent affinity to P-gp ($K_{m,app}$) and a five-fold difference in the maximum effective P-gp mediated transport rate of quinidine ($V_{max,app}$). However, fitting the concentration data into a compartmental model which accounted for the aqueous boundary layers, cell membranes and cellular retention suggested that the P-gp function *per se* was not altered, it was the differences in the passive transfer of quinidine which changed the apparent transport kinetics. These results provide further insight into the dynamics of the P-gp mediated transport and on the roles of several confounding factors involved in *in vitro* experimental setting.

[4] Adapted with permission of the American Chemical Society from: Heikkinen A.T., Korjamo T., Lepikkö V., Mönkkönen J.: Effects of experimental setup on the apparent concentration dependency of active efflux transport in *in vitro* cell permeation experiments. Mol Pharmaceutics 7: 605-617, 2010.

8.1 INTRODUCTION

One of the key characteristics of P-gp mediated transport is its saturability; this is especially the case in the intestine where the drug concentrations are relatively high (Li et al., 2008; Saitoh et al., 2007; Tubic et al., 2006). Thus, reasonable predictions of P-gp function *in vivo* must include the possibility of P-gp saturation. Usually the concentration dependency of P-gp mediated transport in *in vitro* cell permeation experiments is described via Michaelis-Menten type kinetics, i.e. with $V_{max,app}$ and $K_{m,app}$ parameters. In cell monolayer permeability experiments, these parameters have traditionally been estimated based on the observed apparent permeability (P_{app}) or the flux rate through the cell monolayer as a function of initial donor concentration (C_{d0}). However, the $V_{max,app}$ and $K_{m,app}$ parameters reported in the literature tend to vary significantly. This variability can partly be attributed to the fact that the binding site of P-gp lies within the cell monolayer (Ambudkar et al., 2006), whereas the concentration dependency is estimated on the basis of the initial donor concentration. Several factors in the experimental setup, in addition to initial donor concentration, can affect the local intracellular concentrations in the permeation experiments. Thus, it is reasonable to predict that these factors may affect also the apparent P-gp mediated transport.

Indeed, the effects of several factors on apparent P-gp mediated transport in permeation experiments have been discussed in the recent literature:

A) In contrast to Michaelis-Menten theory, the $K_{m,app}$ values in the cell monolayer permeability assays have been reported to correlate with the $V_{max,app}$ value and, thus, also with the P-gp expression levels of the cells used (Korjamo et al., 2007; Shirasaka et al., 2008b). This has been attributed to decreased substrate concentration at the binding site of P-gp due to the transporter function. Thus, the extracellular substrate concentration needed to saturate the pump will be higher if more functional P-gp is being expressed in the cell monolayer used (Bentz et al., 2005; Korjamo et al., 2007; Sun and Pang, 2008).

B) The pH of extracellular buffer has been shown to affect the apparent P-gp mediated transport of basic P-gp substrate quinidine in the rat *in situ* intestinal permeability assay (Varma and Panchagnula, 2005). As the pH of extracellular buffer decreases, the apparent $V_{max,app}$ and $K_{m,app}$ increases because quinidine is more ionized at lower pH and consequently the ability to traverse the cell membrane to the binding site of P-gp is decreased.

C) In addition to the cell monolayer, the aqueous boundary layer (ABL) on both sides of the cell monolayer may play a prominent role in the permeability barrier for high permeability compounds (Avdeef et al., 2005; Korjamo et al., 2009). The effects of ABL on the apparent human apical sodium-dependent bile acid transporter (hASBT)

kinetics have been examined recently (Balakrishnan et al., 2007). Thus, it is likely that also apparent P-gp mediated efflux kinetics of high permeability substrates are affected by ABL (Korjamo et al., 2007). However, no definitive data detailing this effect have been published.

D) The majority of the P-gp substrates drugs are weak bases and thus, it is possible that they are sequestered into the acidic intracellular compartments such as lysosomes (Asokan and Cho, 2002; Duvvuri and Krise, 2005b). Recently, it has been shown that lysosomal sequestration may significantly affect the apparent permeability of amodiaquine (Hayeshi et al., 2008b) Furthermore, lysosomal sequestration may affect the substrate concentration at the interaction site of P-gp. Thus, lysosomal sequestration is likely to affect the apparent P-gp mediated transport. Indeed, it has been reported that some lysosomotrophic agents can affect the apparent P-gp mediated transport in *in vitro* permeability experiments (Lacave et al., 1999). However, no definitive conclusions about the mechanism(s) underlying this finding can be drawn based on the data reported.

Although several factors affecting the apparent permeability of P-gp substrates and the apparent P-gp mediated transport are known, the relative contributions of these various factors are not fully understood. Consequently, it is not known how these factors should be taken into account when determining the concentration dependent P-gp function *in vitro* so that the parameters obtained could be used for valid prediction of saturation of intestinal P-gp *in vivo* (Bolger et al., 2009; Del Amo et al., 2009). However, a detailed dissection of the concentration dependent P-gp mediated transport would play a vital role in the successful IVIVE of intestinal P-gp function (Badhan et al., 2009; Bolger et al., 2009; Tachibana et al., 2010).

In this study, the effects of aqueous boundary layer, extracellular pH and lysosomal sequestration on the apparent P-gp mediated transport of quinidine were examined. All these factors were demonstrated to affect the apparent P-gp mediated transport. Thereafter, a compartmental model was exploited to determine the concentration dependent P-gp mediated transport *'in situ'*. This model takes into account the apical and basal cell membranes and aqueous boundary layers (ABL) separately and allows the discrimination of P-gp mediated transport from passive disposition processes. The current analysis provides further insight into the dynamics of the interplay of active transport and passive disposition through several barriers in cell monolayer permeation experiments. Furthermore, the implications on the IVIVE of active transport, especially in the context of intestinal absorption, are discussed.

8.2 EXPERIMENTAL SECTION

8.2.1 Permeation experiments and sample analysis

The donor solutions with unlabeled quinidine at the concentrations indicated were prepared in the corresponding transport buffer, HBSS buffered either with 25 mM Hepes (pH ≥ 7.0) or MES (pH < 7.0) with or without 5 µM GF120918, P-gp inhibitor, and/or 100 nM bafilomycin A1, a specific inhibitor of vacuolar type H^+ -ATPase (Bowman et al., 1988), that inhibits the acidification of lysosomes (Yoshimori et al., 1991) and, thus, reduces the cellular retention of lysosomotrophic compounds. The donor solutions were spiked with ^{3}H-quinidine. The stock solutions were prepared in DMSO but the DMSO concentration did not exceed 1 % in final donor solutions.

The experiments were started by replacing the preincubation buffer with fresh transport buffer into the receiver chamber and donor solution into the donor chamber. At each sampling time point (5, 15, 30, 45, 60, 90 and 120 minutes), 25 µl samples were withdrawn from both chambers simultaneously. Additionally, the amount of quinidine retained in the cell monolayers was sampled at 120 minutes according to the procedure presented in Chapter 6.2.1.

The permeation experiments were conducted at 37 °C in a humidified incubator on an orbital shaker with an orbit diameter of 3 mm or 1.5 mm (small) as indicated (Titramax 101 or Titramax 1000, respectively; Heidolph, Schwabach, Germany). The shaking rate was 320 rpm in all experiments.

8.2.2 Selection of compounds

Quinidine was chosen as the model compound for these studies because it is a well known P-gp substrate that is stable in the cell monolayer permeation setting and it can readily be used in such experiments in the concentration range where a full saturation curve of the apparent P-gp mediated transport is observed. GF120918 is an effective inhibitor of both P-gp and breast cancer resistance protein BCRP. However, the evidence available in the literature suggests that quinidine does not interact with BCRP or MRP2 (Matsson et al., 2009), the other major ABC transporters expressed in the Caco-2 cells as well as in the intestinal epithelia. Moreover, in the presence of GF120918 the polarization of quinidine disposition through the cell monolayer is abolished in both cell lines used (Korjamo et al., 2007). Thus, although several other transporters are expressed in the cell lines used (Ahlin et al., 2009; Goh et al., 2002) and quinidine has been suggested to be transported by OCTN2 transporter (Ohashi et al., 1999), the data in this study is not expected to be significantly confounded by the involvement of other transporters than P-gp. However, a minor contribution of additional transporters cannot be ruled out totally.

8.2.3 Determination of the apparent permeability and apparent P-gp function

To study the effects of different factors on the apparent P-gp mediated transport as well as on the apparent passive permeability of quinidine, the permeation experiments were conducted with six different donor concentrations ranging from 1 to 300 µM in MDCKII-MDR1 or from 0.3 to 100 µM in Caco-2 in the absorptive direction (apical to basal) with and without the P-gp inhibitor, GF120918 (5 µM) at eight different experimental conditions. The experimental approaches to probe the effects of aqueous boundary layer, cell membrane permeability and cellular retention are summarized in Table 8.1.

Table 8.1. Summary of permeation experiments conducted to experimentally dissect the roles of different factors affecting the apparent P-gp mediated transport of quinidine. The experiments were conducted only in the absorptive direction (apical to basal).

Factor probed	Experimental approach used	Extracellular pH[a]	Orbit diameter[b]	Cell line	Treatment
None		7.4	3 mm	MDCKII-MDR1	None
Aqueous boundary layer	Change of agitation scheme	7.4	1.5 mm	MDCKII-MDR1	None
Cell membrane permeability	Change of extracellular pH	6.4	3 mm	MDCKII-MDR1	None
		6.4	1.5 mm	MDCKII-MDR1	None
Cellular retention	Inhibition of lysosomal sequestration	7.4	3 mm	MDCKII-MDR1	BAF[c]
		6.4	3 mm	MDCKII-MDR1	BAF[c]
Expression level of P-gp	Use of cell lines with different P-gp expression levels	7.4	3 mm	Caco-2[d]	None
		6.4	3 mm	Caco-2[d]	None

[a] Same pH was used in both apical and basal compartments.

[b] Orbital shaking rate in all experiments was 320 rpm.

[c] Lysosomal acidification and consequent lysosomal sequestration of quinidine was inhibited by treating the cells with 100 nM bafilomycin A1.

[d] The P-gp expression level in Caco-2 cells is significantly lower than in MDCKII-MDR1 cells (Korjamo et al 2007).

The concentration dependency of the effective P-gp mediated transport in permeation setting has often been described with Equation 2.7. To solve the concentration dependency of P_{app} (in absorptive direction), the Equation 2.7 is modified to

$$\mathbf{P_{app} = P_{pass} - \frac{V_{max,app}}{K_{m,app} + C_{d0}}} \qquad \textit{Equation 8.1}$$

When P-gp is involved in the permeation kinetics the transcellular transport is polarized. Thus, $P_{app,Palm}$ (Equation 2.4) or $P_{app,Tran}$ (Equation 2.5) would not be applicable. Therefore, $P_{app,sink}$ (Equation 2.3) was used for determination of P_{app}. Subsequently, Equation 8.1 was fitted to the P_{app} at six quinidine concentrations without P-gp inhibitor to estimate P_{pass}, $V_{max,app}$ and $K_{m,app}$ parameters under different experimental conditions using GraphPad Prism software, version 4.03 (GraphPad Software Inc., San Diego, CA). In order to avoid unreasonably high P_{pass} estimates in data fitting, P_{pass} was constrained not to be higher than the highest apparent permeability observed at the corresponding experimental conditions (with or without P-gp inhibitor GF120918). Extra sum-of squares F test was used for comparison of $V_{max,app}$ and $K_{m,app}$ at different experimental conditions and P values lower than 0.05 were considered to signify statistically significant difference.

8.2.4 Parameter estimation

The estimation of parameters describing the quinidine disposition in cell permeation experiments was done by sequential fitting the compartmental models to apical and basal chamber concentration data of several permeation experiments using WinNonlin software, version 5.2.1 (Pharsight, Mountain View, CA). A weighting scheme 1/predicted^2 was chosen based on residual plots and S.E. of the parameter estimates. Otherwise, the default WinNonlin settings for minimization of error were applied.

In the first fitting step, the parameters describing the concentration dependency of cellular binding of quinidine (K_{max}, K_{min} and EC_{50}) to MDCKII-MDR1 and Caco-2, and to MDCKII-MDR1 in the presence of 100 nM bafilomycin A1 were estimated by fitting the three compartment model (Figure 4.1) to the data from corresponding experiments with six different quinidine concentrations in the presence of 5 µM GF120918 at pH 7.4. When the disposition through individual permeation barriers is symmetric (i.e. when pH gradient across membranes or active transporters are not involved) the apical and basal permeation barriers (including ABL and cell membrane each) can be described as single barriers. Furthermore, at this step there were no separate estimates of ABL and cell membrane permeabilities available. Therefore, the three compartment model was exploited in this parameter estimation step.

In the second fitting step, the cellular binding parameters were fixed to the best fit values of the first fitting step. Subsequently, the parameters describing the passive permeation through the cell membranes (P_u and P_i) and ABLs ($P_{ABL,api}$ and $P_{ABL,baso}$) were estimated by fitting the five compartment model (Figure 1B) into the concentration data from permeation experiments through MDCKII-MDR1 conducted with 30 µM quinidine into both directions at five different pH (5.6, 6.0. 6.4, 7.0 and 7.4). The initial donor quinidine concentration was 30 µM and 5 µM GF120918 was present in both

donor and receiver compartments. Equal permeability values were assumed for apical and basal cell membranes, because determination of separate was not possible with the current data. P_u and P_i were constrained to be independent of agitation, whereas separate values for $P_{ABL,api}$ and $P_{ABL,baso}$ were estimated for experiments conducted under different agitation conditions. Quinidine is a diprotic base with pKa values of 4.32 and 8.51 (Table 4.1), i.e. there are two ionized species of quinidine present at the pH conditions applied. However, current data does not allow determination of permeation characteristics of these two ionized species separately (not shown). Thus, the membrane permeability of both ionized species were approximated to be equal and only the pKa value of 8.51 was used to calculate the unionized and ionized fractions (f_u, f_i and $f_{u,cell}$, $f_{i,cell}$ in extra- and intracellular spaces, respectively).

In the final, third, fitting step, the passive permeability parameters were fixed to the best fit values of the second fitting step and the cellular binding parameters remained fixed to the corresponding best fit values of the first fitting step. Subsequently, the parameters describing the concentration dependent P-gp mediated transport *in situ* (V_{max} and K_m) were estimated by fitting the five compartment model to data from experiments with six different quinidine concentrations in the absence of GF120918 at each experimental condition (Table 8.1).

8.3 RESULTS

8.3.1 Effects of passive permeability on the apparent P-gp mediated transport

Figure 8.1 illustrates the effects of extracellular pH and ABL on the concentration dependence of the apparent permeability of quinidine. Quinidine is more ionized at pH 6.4 than at pH 7.4 and, consequently, the permeability through the cell monolayer was lower at pH 6.4 than at pH 7.4, whereas the permeability through ABLs is assumed to be unaffected. Additionally, the change of pH from 7.4 to 6.4 also shifted the P-gp saturation curve to the right (i.e. to higher concentrations). This shift was manifested as the higher apparent $K_{m,app}$. In addition, the apparent $V_{max,app}$ was higher at pH 6.4 than in pH 7.4 (Table 8.2). Similar pH effects in $K_{m,app}$ and $V_{max,app}$ were observed at both shaking orbits (3 mm and 1.5 mm) and with both cell lines.

Reduced agitation (change of shaking orbit diameter from 3 mm to 1.5 mm) reduced the permeability through ABLs, whereas the permeability through the cell monolayer was assumed to be unaffected. Additionally, the P-gp saturation curve shifted slightly to the right. However, although the apparent passive permeability through the whole system was reduced virtually to the same extent by the change in the cell monolayer permeability (the pH effect at 3 mm shaker) and by the change in ABL permeability

(the agitation effect at pH 7.4), the shift in the P-gp saturation curve was less pronounced in the latter case (Figure 8.1). Consequently, $V_{max,app}$ remained virtually unaffected by the agitation and there was a tendency towards the higher $K_{m,app}$ values at reduced agitation. Similar effects in $K_{m,app}$ and $V_{max,app}$ due to agitation applied were observed at both pH conditions (6.4 and 7.4). However, the effect on $K_{m,app}$ reached statistical significance only at pH 6.4 (Table 8.2).

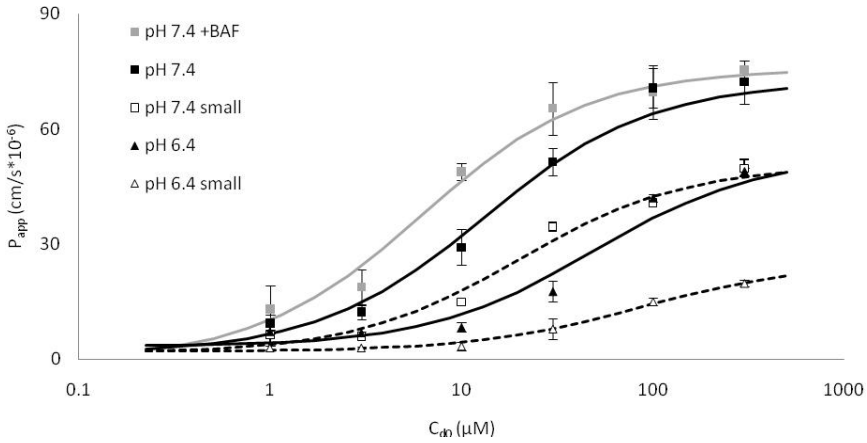

Figure 8.1. Effect of extracellular pH, aqueous boundary layer and cellular retention on the apparent P-gp mediated transport of quinidine through MDCKII-MDR1 cell monolayers. The symbols refer to the average of three to six measurements (± standard deviation) and the predicted curves are simulated with the best fit values of Equation 8.1. Squares are for pH 7.4 and triangles for pH 6.4. Solid and open symbols represent the experiments on the shakers with 3 mm and 1.5 mm (small) orbit diameter, respectively. Grey color refers to experiments with inhibition of lysosomal sequestration (100 nM bafilomycin A). The results of the experiments in the presence of bafilomycin A at pH 6.4 are omitted for clarity.

Table 8.2. Summary of fitted parameters (± S.E.) from fitting the Equation 8.1 to apparent permeability data and from the compartmental modeling

Setup	P_{pass}[c] ($cm/s*10^{-6}$)	$V_{max,app}$[c] ($fmol/s/cm^2$)	$K_{m,app}$[c] (μM)	$P_{ABL,api}$[d] ($cm/s*10^{-6}$)	$P_{ABL,baso}$[d] ($cm/s*10^{-6}$)	P_u[d] ($cm/s*10^{-6}$)	P_l[d] ($cm/s*10^{-6}$)	K_{max}[e]	K_{min}[e]	$EC_{50,K}$[e] (μM)	V_{max}[f] ($fmol/s/cm^2$)	K_m[f] (μM)
		MDCKII-MDR1										
pH 7.4	72 ±2	920 ±90[g]	13 ±2[g]	440 ±40	170 ±8	26700 ±1300	21 ±3	538 ±12	89 ±5	1.2 ±0.1	5670 ±300	0.23 ±0.02
pH 6.4	53 ±3	2450 ±240[g,h]	49 ±5[g,h]								4910 ±190	0.28 ±0.01
pH 7.4 +BAF[a]	76 ±2	470 ±60[i]	6 ±1[i]					53 ±3	47 ±6	16 ±62	4710 ±220	0.22 ±0.02
pH 6.4 +BAF[a]	59 ±3	2080 ±220[h]	40 ±5[h]								3930 ±230	0.36 ±0.03
pH 7.4 small[b]	50 ±2	980 ±110	20 ±3	200 ±12	87 ±2			538 ±12	89 ±5	1.2 ±0.1	7490 ±550	0.28 ±0.03
pH 6.4 small[b]	25 ±1	1960 ±110[h]	85 ±6[h,j]								8090 ±420	0.27 ±0.03
		Caco-2										
pH 7.4	69 ±2	470 ±40	9 ±1	440 ±40	170 ±8			233 ±6	77 ±4	0.6 ±0.1	1970 ±120	0.28 ±0.02
pH 6.4	56 ±5	1340 ±160[h]	31 ±4[h]								3210 ±140	0.30 ±0.03

[a] Lysosomal sequestration was inhibited by neutralizing the lysosomes with 100 nM bafilomycin A1. [b] Small refers to the experiments conducted on the orbital shaker with 1.5 mm orbit diameter. All the other experiments were on the orbital shaker with 3 mm orbit diameter. [c] Parameters describing the apparent passive permeability through the cell membrane and concentration dependence of apparent effective P-gp mediated transport were estimated by fitting the apparent permeability data into Equation 8.1. [d] Parameters describing the passive permeation of ionized and unionized quinidine through ABLs and cell membranes were estimated on the 2nd step of sequential compartmental model fitting. [e] Parameters describing the concentration dependence of cellular binding were estimated on the 1st step of sequential compartmental model fitting. [f] Parameters describing the concentration dependence of P-gp mediated transport in situ were estimated on the 3rd step of sequential compartmental model fitting. [g] Significantly higher for MDCKII-MDR1 than for Caco-2 at similar experimental conditions. [h] Significantly higher values at pH 6.4 than at pH 7.4 at otherwise similar experimental conditions. [i] Significantly lower than the corresponding value without bafilomycin A. [j] Significantly higher at small shaker.

8.3.2 Effects of lysosomal sequestration on the apparent P-gp mediated transport

Weak bases, such as quinidine, are susceptible to lysosomal sequestration during permeation experiments. Consequently, the inhibition of the acidification of lysosomes by bafilomycin A1 reduced the extent of cellular retention of quinidine at pH 7.4 (Figure 8.2).

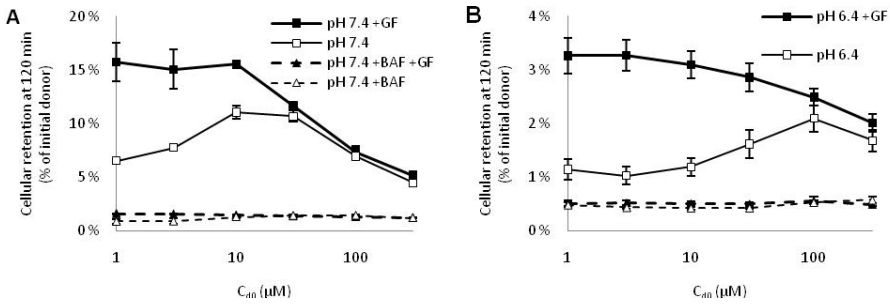

Figure 8.2. The effects of P-gp mediated efflux, lysosomal sequestration and extracellular pH on the extent of cellular retention of quinidine in permeation experiments. The symbols refer to the amount of quinidine recovered from the MDCKII-MDR1 cell monolayer at the end of the permeation experiments (at 120 min) at pH 7.4 (A) and at pH 6.4 (B) (average of three to six measurements ± standard deviation). Solid symbols/thick lines refer to experiments with 5 µM GF120918 (P-gp inhibitor) and open symbols/thin lines refer to experiments without GF120918. Triangles/dashed lines refer to experiments with 100 nM bafilomycin A (inhibition of lysosomal sequestration) and squares/solid lines refer to experiments without bafilomycin A.

At low quinidine concentrations P-gp efficiently reduced the cellular retention of quinidine. At intermediate quinidine concentrations, the P-gp starts to saturate and the cellular retention increased, whereas at high quinidine concentrations, the cellular retention again decreased probably because of the saturation of cellular binding and saturation of lysosomal sequestration of quinidine (Figure 8.2). A similar bell shape trend in cellular retention as a function of quinidine concentrations was observed with each experimental setup. However, this trend was less pronounced in the presence of bafilomycin A and in the pH 6.4 experiments because of the lower cellular retention (Figure 8.2B). Consequently, quinidine was retained in the cells to a greater extent at intermediate concentrations than at low or high concentrations and the effect of bafilomycin A on cellular retention was most pronounced at intermediate concentrations. Cellular retention decreases the appearance rate into the receiver compartment and, thus, decreases the apparent permeability. Consequently, the inhibition of lysosomal sequestration caused an increase in P_{app} at the intermediate quinidine concentrations whereas the P_{app} at high and low quinidine was affected to a

significantly lesser extent. Consequently, at pH 7.4 the apparent P-gp saturation curve shifted to the left in the presence of bafilomycin A1 (Figure 8.1). This was reflected as significantly lower apparent $K_{m,app}$ and $V_{max,app}$ values (Table 8.2).

At pH 6.4, the extent of cellular retention was significantly lower than at pH 7.4 (Figure 8.2). Therefore, the cellular retention and the effect on the cellular retention by bafilomycin A1 did not significantly affect the apparent permeability of quinidine. Consequently, the $K_{m,app}$ and $V_{max,app}$ values were not significantly affected by bafilomycin A1 at pH 6.4 (Table 2). This suggests that bafilomycin A1 did not have any direct effect on P-gp function but, rather, the effect seen at pH 7.4 was caused by the changes in the cellular retention.

8.3.3 Effects of P-gp expression level on the apparent P-gp mediated transport

Comparison of the concentration dependent apparent permeability through MDCKII-MDR1 and Caco-2 monolayers is shown in Figure 8.3. Caco-2 cells have a lower P-gp expression level than MDCKII-MDR1 cells, whereas the passive permeability of quinidine is apparently rather similar in both of these cell lines (Korjamo et al., 2007) (Figure 8.3, Table 8.2). The effect of P-gp mediated transport on the apparent permeability of quinidine was more pronounced in MDCKII-MDR1 cells than in Caco-2 cells as expected based on P-gp expression levels. This was reflected as higher $V_{max,app}$ and $K_{m,app}$ values in MDCKII-MDR1 cells compared to Caco-2 cells (Table 8.2).

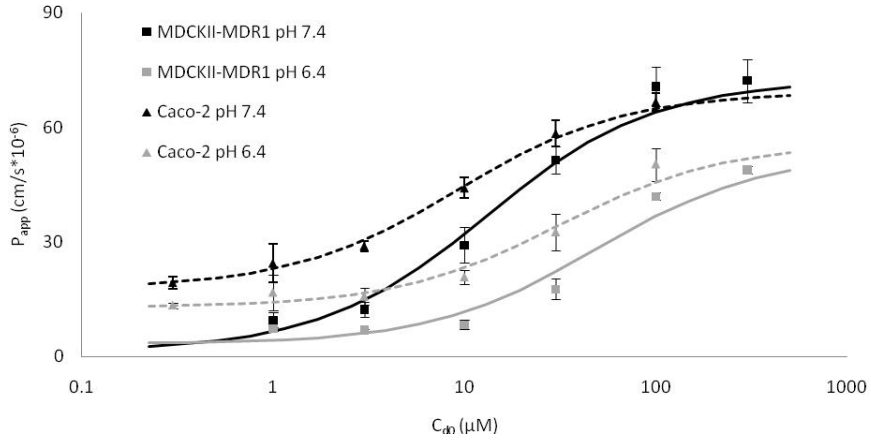

Figure 8.3. Effect of P-gp expression level on the apparent P-gp mediated transport of quinidine. The symbols refer to average of three to six measurements (±standard deviation) and the predicted curves are simulated with the best fit values of Equation 8.1. Squares/solid lines and triangles/dashed lines refer to MDCKII-MDR1 and Caco-2, respectively. Black and grey color refer to pH 7.4 and 6.4, respectively.

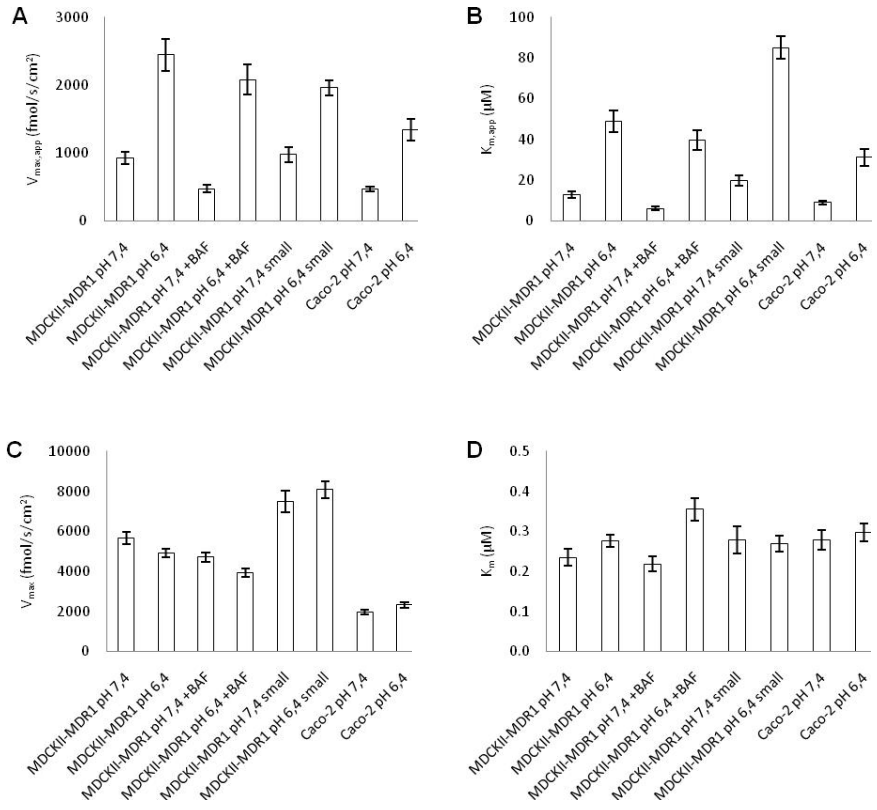

Figure 8.4. The apparent (A, B) and in situ (C, D) parameters describing the concentration dependent P-gp mediated transport of quinidine at different experimental conditions.

8.3.4 Compartmental modeling and determination of K_m and V_{max} of P-gp mediated transport in situ

The estimated parameters from sequential compartmental model fitting are summarized in Table 8.2. Additionally, comparison of $K_{m,app}$ and $V_{max,app}$ and *in situ* K_m and V_{max} values of P-gp mediated transport of quinidine at different experimental setups are visualized in Figure 8.4. The K_m values at different setups were all at a similar level, the average being 0.3 µM with 1.6 fold difference between the lowest and highest estimates, whereas the $K_{m,app}$ values varied by more than one order of magnitude. The relative variation in V_{max} estimates between different experimental settings was larger than in K_m estimates and, thus, partly masking the presumed difference in V_{max} between Caco-2 and MDCKII-MDR1. However, on average, the V_{max} estimates in MDCKII-MDR1 (5800 fmol/s/cm^2) were almost 3 fold higher than those obtained with Caco-2 (2100 fmol/s/cm^2). Furthermore, the $K_{m,app}$ estimates were significantly higher than *in situ* K_m values whereas $V_{max,app}$ values were significantly

lower than their *in situ* V_{max} couterparts. The difference between $K_{m,app}$ and K_m values was more pronounced at pH 6.4 than at pH 7.4 and also slightly more pronounced in experiments with the 1.5 mm shaker than in experiments with the 3 mm shaker, whereas the difference between $V_{max,app}$ and V_{max} was more pronounced at pH 7.4 than at pH 6.4 and at a similar level with both agitation conditions.

8.4 DISCUSSION

The apparent active transporter kinetics in *in vitro* permeation experiments are usually biased by the experimental setup and the combination of both active and passive permeation. This study examined the effects of the experimental setup on the apparent kinetic parameters of the P-gp mediated transport. The expression level of P-gp and, consequently, the P-gp mediated transport rate has been reported to be higher in MDCKII-MDR1 cells than in Caco-2 cells (Korjamo et al., 2007; Shirasaka et al., 2008b). Furthermore, the P-gp mediated transport decreases the substrate concentration at the intracellular binding site of P-gp and, thus, the higher the level of expression is the higher an initial donor concentration is needed to saturate the pump, i.e. a higher $K_{m,app}$ (Korjamo et al., 2007; Sun and Pang, 2008). The values of both $V_{max,app}$ and $K_{m,app}$ observed in this study under similar experimental conditions were higher in MDCKII-MDR1 cells than their counterparts in Caco-2, thus supporting the results reported earlier. Furthermore, both $V_{max,app}$ and $K_{m,app}$ observed in this study were higher at extracellular pH 6.4 than at pH 7.4. Thus, the effects of the extracellular pH on the apparent concentration dependent P-gp mediated transport of quinidine are also in line with the results reported earlier in the literature (Varma and Panchagnula, 2005). Additionally, the permeation resistance of ABL and the cellular retention were demonstrated to play a role in the apparent concentration dependent P-gp mediated transport of quinidine. However, the compartmental modeling results indicate that the P-gp function *per se* was not affected by the experimental conditions but, rather, the changes seen in the apparent P-gp kinetics were due to the modulation of the access of the substrate to the binding site of the transporter protein.

P-gp transports the substrate molecules out of the cell across the apical cell membrane. Thus, P-gp mediated transport reduces the permeation rate through the cell monolayer in absorptive direction permeation experiments by maintaining the concentration gradient across the apical cell membrane. In contrast, the permeabilities across the other permeation barriers (i.e. ABL at both sides of the cell monolayer and the basal cell membrane) are not affected by P-gp. The magnitude of the concentration gradient across the apical cell membrane maintained by P-gp and, consequently, the effective P-gp mediated transport rate is dictated by the actual P-gp mediated transport rate and the passive permeation rate from the apical cell surface to the intracellular binding site

of P-gp. Thus, the maximum effective transport rate ($V_{max,app}$) is increased by the increase in maximum actual transport rate (i.e. V_{max}) and decreased by the increase in passive permeability through the apical cell membrane from the cell surface into the cell (i.e. $f_iP_i+f_uP_u$). Consequently, $V_{max,app}$ is bound to be lower than V_{max}. Lowering the extracellular pH decreases the passive permeability of quinidine from the cell surface into the cell whereas the P-gp function *per se* is believed not to be affected by the pH conditions (Altenberg et al., 1993; Neuhoff et al., 2003). This is seen as higher Vmax,app at 6.4 compared to the situation at 7.4 (Table 8.2, Figure 8.4). In contrast, decreasing the permeability through the whole cell monolayer by decreasing the agitation (i.e. decreasing the ABL permeability) does not affect the passive permeability from the cell surface into the cell nor the P-gp function. Consequently, the $V_{max,app}$ is not significantly affected by the agitation applied (Table 8.2, Figure 8.4).

$K_{m,app}$ represents the initial donor concentration resulting in 50% of $V_{max,app}$. Thus, $K_{m,app}$ is a composite parameter representing the actual K_m as well as the relationship of the initial donor concentration and the concentration at the intracellular binding site of P-gp. $K_{m,app}$ is bound to be higher than K_m because the intracellular binding site of P-gp is downstream from the donor compartment in the concentration gradient. The changes applied in the experimental setup are assumed not to affect the actual K_m. Thus, all the variation in $K_{m,app}$ can be attributed to the changes in the access to the intracellular binding site of P-gp. The decrease in the permeability from the donor bulk phase into the intracellular binding site of P-gp by either lowering the extracellular pH or by decreasing the agitation reduces the access rate of the substrate to the binding site of P-gp. Consequently, the initial donor concentration needed to saturate the pump is increased, i.e. the $K_{m,app}$ is increased. However, the decrease in the extracellular pH also increases the effective P-gp mediated transport rate from the binding site. Thus, the concentration gradient in between the donor bulk phase and the intracellular binding site of P-gp is more increased by the decrease in the extracellular pH than by the decrease in the agitation. Consequently, the effect of extracellular pH on the $K_{m,app}$ value is more pronounced than the effect of agitation.

The estimation of $V_{max,app}$ and $K_{m,app}$ is based on P_{app} determined at several substrate concentrations. Since the determination of P_{app} is based on the assumption of 100% recovery, the P_{app} estimates are affected by the recovery. Low recovery (due to e.g. cellular retention) leads to the underestimation of the actual permeability. Consequently, the changes in the recovery as a function of concentration result in concentration dependency of P_{app}. At pH 7.4, the changes in the cellular retention of quinidine, caused by the saturation of P-gp followed by the saturation of apparent cellular binding, were sufficient to cause a shift in the concentration dependence of

quinidine P_{app} (Figure 8.1 and Figure 8.2). The inhibition of the lysosomal sequestration decreases significantly the cellular retention of quinidine, thus virtually abolishing the concentration dependence of cellular retention and consequently the bias in the apparent saturation of the effective P-gp mediated transport. Although the effects of poor recovery on the P_{app} estimates are generally acknowledged, there are no universal correction terms available for accounting for poor recovery in the determination of P_{app} (Hubatsch et al., 2007). If there is no evidence of major recovery problems, the effects of recovery are often neglected in the data analysis. However, the results of this study demonstrate that neglecting the role of recovery may bias the interpretation of the apparent concentration dependent transporter function.

It is evident that the single-barrier view based analysis of the apparent concentration dependency of P-gp mediated transport is biased by the passive disposition of the compound. Therefore, compartmental modeling was applied to account for the passive disposition and to estimate the P-gp kinetics *in situ*. The estimation of the parameter values embedded in the compartmental model was conducted by sequential fitting of the models to the experimental data. One major drawback of this approach is the fact that the possible misspecifications of the model in the early fitting steps may be reflected in the later fitting steps. On the other hand, the possible misspecifications of the model in the late fitting steps will not confound the early fitting steps. More importantly, for the further application of compartmental models to quantify the concentration dependent transporter function, it would not be feasible to perform all the experiments performed in this study. For instance, the estimates of ABL permeabilities can theoretically be derived from the results of calibrator molecule(s) (Yu and Sinko, 1997) or the parameters describing the distribution/binding into cellular structures could be derived from separate, simpler experiments (Sun et al., 2008; Tran et al., 2005). This kind of approach would be essentially similar to the current sequential fitting approach. However, determining the optimal study design will require further research.

The *in situ* V_{max} and K_m are considered to reflect the actual P-gp mediated transport kinetics through the apical cell membrane from the intracellular aqueous phase to the cell surface. Thus, V_{max} would be expected to correlate with the expression level of functional P-gp in the cell line used, whereas K_m should be independent of the P-gp expression level. Furthermore, it is assumed that the experimental conditions will not affect the P-gp function *per se*, i.e. K_m and V_{max} should be independent of the experimental conditions. However, the determination of *in situ* K_m is based on the estimated intracellular free concentration of the substrate, i.e unbound concentration in the cellular aqueous phase, whereas the binding site(s) of P-gp are generally considered

to lie within the inner leaflet of the cell membrane (Ambudkar et al., 2006). Assuming the association and dissociation rates between the lipid and aqueous phases are much faster than the rate of transmembrane transfer (Tran et al., 2005), the consentration at the binding site of P-gp is at constant proportion to the unbound aqueous concentration. Consequently, the current model is consistent with the substrate binding from the lipid phase. However, the K_m determined actually represents the product of the cytosol – cell membrane distribution coefficient and the actual 'lipid-phase K_m'. There are differences in the cell membrane lipid composition between cells from different tissues (Avdeef, 2003). Thus, it can be hypothesized that K_m values might be cell type specific if there are significant differences in the cytosol-cell membrane distribution of the P-gp substrate in different cell types. However, there were no signs of this kind of difference between MDCKII-MDR1 and Caco-2 cell lines.

The K_m estimates were at the same level regardless of the experimental conditions or the cell line utilized (Figure 8.4, Table 8.2), thus fulfilling the above mentioned expectations and providing further confidence on the interpretation of this parameter. In addition, the V_{max} estimates within both cell lines were approximately at the same level irrespective of the experimental conditions. However, there was a substantial variation in V_{max} estimates probably partly masking the expected difference between V_{max} in MDCKII-MDR1 and Caco-2. Earlier western blot results in our lab suggest that the P-gp expression level in MDCKII-MDR1 is about one order of magnitude higher than in Caco-2 (Korjamo et al., 2007) whereas the difference was on average only about 3 fold in V_{max} estimated in this study. The reason(s) for this discrepancy are not known but several possible explanations can be hypothesized. A) The P-gp expression levels were not quantified from the cell batches used in this study. Furthermore, for practical reasons, the serum batch used in the cell culture during this study was not the same as utilized in our earlier study. Consequently, the P-gp expression levels reported earlier may not exactly reflect the expression levels in the cells used here. The difference in $K_{m,app}$ and $V_{max,app}$ between MDCKII-MDR1 and Caco-2 in this study was not as significant as in our previous study (Korjamo et al., 2007), thus favoring this explanation. B) The expression levels quantified by western blot measures the total expression level of P-gp protein whereas some of the P-gp expressed may not be localized on the cell membrane (Porcelli et al., 2009). Thus, the difference in the P-gp expression levels detected by western blot may not directly reflect the difference in the expression of active P-gp. C) There are indications that the permeability is lower across the apical than the basal cell membrane (Gonzalez-Alvarez et al., 2005; Ito et al., 1999). However, the passive permeability coefficients through the apical and basal cell membranes were assumed to be equivalent because the experimental data did not

allow for fitting of separate permeability coefficients for the apical and basal cell membranes. Thus, the interplay of passive permeation and P-gp mediated transport through the apical cell membrane may be inaccurately described in the current analysis. D) The analysis in the current compartmental model was based on the assumption that the passive permeability parameters determined using MDCKII-MDR1 data describe the passive permeation also in Caco-2. This is a reasonable approximation because there were no significant differences between these cell lines in the apparent passive permeabilities at different pH conditions (Figure 8.3, Table 8.2). Similar permeation characteristics of Caco-2 and MDCK cell lines have also been reported by others (Crespi et al., 2000; Irvine et al., 1999). However, the composition of cell membranes as well as other cellular structures is different in these cell lines. Consequently, the assumption of exactly same permeability coefficients may not be totally correct and this inaccuracy may be translated into the estimated parameters describing the P-gp function.

The pharmacokinetics is a result of the interplay of several mechanisms, such as passive permeability, active transport by several transporters and metabolism in the enterocytes in the case of intestinal absorption. Consequently, successful prediction of the *in vivo* pharmacokinetics based on *in vitro* data, i.e. IVIVE, requires inclusion of all the clinically significant mechanisms and their interplay into a single prediction in both physiological and mechanistically reasonable way. In practice, several studies aiming for physiologically based IVIVE with varying levels of mechanistic detail have been published in the recent literature (Badhan et al., 2009; Bolger et al., 2009; De Buck and Mackie, 2007; Yang et al., 2007). Some of these studies have utilized commercial software designed for this purpose, such as GastroPlus™ (Simulations Plus Inc, Lancaster, CA, USA) and Simcyp® Population-based ADME Simulator (Simcyp Ltd, Sheffield, UK). Physiologically based IVIVE of hepatic metabolism have resulted in predictions with sufficient reliability to have practical utility in the drug development (Fagerholm, 2007a; Rostami-Hodjegan and Tucker, 2007), whereas there are still no success stories published of the IVIVE of concentration dependent efflux transporter kinetics.

The virtually linear correlation between P-gp expression level and both $V_{max,app}$ and $K_{m,app}$, in constant experimental conditions, has been reported recently (Korjamo et al., 2007; Shirasaka et al., 2008b). Consequently, it was suggested that the $V_{max,app}$ and $K_{m,app}$ determined using at least three cell lines with different P-gp expression levels in combination with a scaling factor derived from the apparent passive permeabilities *in vitro* and *in vivo* could be exploited for predicting *in vivo* $V_{max,app}$ and $K_{m,app}$. Subsequently, these estimates could be used for prediction of concentration dependent

intestinal wall permeability *in vivo* (Shirasaka et al., 2008a). However, the results shown in the current study suggest that when the data analysis is based on the apparent permeability as a function of the initial donor concentration, the interpretation of the relationship between passive permeation and P-gp mediated transport is not always straightforward, thus making the extrapolation less reliable. Secondly, and more importantly, there are often more than one saturable process affecting the overall permeation through the intestinal wall, such as different transporters and metabolic enzymes. The local concentration at the binding site of an individual transporter may be significantly affected by the interplay with the other transporters and metabolic enzymes. Thus, the applicability of this single-barrier view based scaling of $V_{max,app}$ and $K_{m,app}$ values is limited. For more general applicability of IVIVE, the models used for simulation of *in vivo* kinetics should enable prediction of the interplay of passive diffusion, transporters, metabolic enzymes etc. in the intestinal absorption. Consequently, many recent physiologically based intestinal absorption models have included enterocytes as a distinct kinetic compartment in between the intestinal lumen and the mesenteric circulation (Badhan et al., 2009; Huang et al., 2009; Jamei et al., 2009b). However, one of the major challenges of using these models for IVIVE is obtaining suitable input parameters which accurately describe the active transporter kinetics (Badhan et al., 2009; Bolger et al., 2009; Tubic et al., 2006).

It is clear that the *in situ* K_m and V_{max} values obtained in this study are to some extent composite parameters that may partly reflect the passive disposition kinetics of the substrate rather than exclusively P-gp mediated transport. However, the robustness against the changes in the experimental conditions suggests that the *in situ* K_m and V_{max} values are not significantly biased by the passive disposition of the substrate. Therefore, compartmental model based quantification of active transporter kinetics seems a promising approach for handling the *in vitro* component of physiologically based IVIVE.

In addition to current compartmental model based approach, also another approach for analyzing the concentration dependent permeability data in order to estimate *in situ* K_m and V_{max} for P-gp mediated transport has been published just recently (Tachibana et al., 2010). This model and the results obtained have some similarities with the current compartmental model. Distingt permeation barriers at apical and basal sides of the cell monolayer and concentration dependent P-gp mediated efflux through the apical barrier with intracellular binding site are accounted for. Consequently, similar correlation between $K_{m,app}$ and $V_{max,app}$ is predicted and also the K_m estimates obtained are consistently lower than $K_{m,app}$ and at the same level with several cell lines with different P-gp expression levels. However, despite the similarities in the results, there

are also fundamental differences between these approaches. In the Tachibana approach, compartmental model structure is used to derive steady state flux rates and, consequently, P_{app} values through the whole cell monolayer at different donor concentrations. Thereafter, the K_m and V_{max} values are estimated by fitting the model to observed P_{app} values. Thus, Tachibana approach is applicaple only for experimental data where P_{app} ($P_{app,sink}$ to be precise) can be reliably determined, i.e. concentration gradient from donor to receiver compartment and recovery from aqueous chambers should be virtually constant throughout the experiments. Consequently, the applicability of the current compartmental model based approach to experiments where these assumptions are violated provides a significant advantage over the Tachibana approach. On the other hand, Tachibana approach does not involve fitting complex model(s) consisting group of differential equations and may thus be more easily implemented. Furthermore, the contribution of ABL in the permeation barrier is neglected in Tachibana model, i.e. the model assumes that P-gp transports the substrate from the intracellular binding site all the way to apical bulk compartment. Consequently, when ABL is a significant part of the permeation barrier, V_{max} estimates using Tachibana model are bound to be lower than V_{max} estimates obtained with current five compartment model, whereas K_m estimates seems to end up at similar level (average K_m for quinidine in Tachibana paper was 0.25 µM). However, the Tachibana approach should be possible to refine in order to take ABL into account provided that there is *a priori* information of the contribution of ABL. However, further research is needed in order to evaluate the practical value of both of these approaches in analysis of concentration dependent transporter function for IVIVE.

9 Summary and future perspectives

The rapid technological development of computer science during the past few decades has provided enormous advancements in computing power generally available. One field of pharmaceutical research that has effectively exploited this progress has been PBPK modeling and physiologically based IVIVE. Successful utilization of *in silico* and *in vitro* methods to predict drug behavior *in vivo* would reduce the need for *in vivo* animal and clinical testing and, thus, be an advantage from both ethical and economical point of views. Consequently, modeling and simulation has become an integral part of the drug discovery – development process.

In order to achieve successful IVIVE the *in vitro* model exploited has to 1) be biologically and mechanistically relevant for obtaining the desired information and 2) thoroughly understood in order to adequately interpret the data obtained. The current study aimed mainly at this latter aspect in the context of *in vitro* models for gut wall permeation.

Membrane based assays, such as the ATPase activation assay, can be used to gain insight into active transporter kinetics. However, it is currently not known in detail how the observed ATPase activity translates into actual transport rates in living cells or tissues (Giacomini et al., 2010). Therefore, in the drug development process the ATPase activation assay should be considered primarily as a screening method for identifyig transporter interacting compounds, whereas cell permeation experiments are more suitable for detailed analysis of transport kinetics.

The total permeation barrier in cell monolayer permeation experiments is made up of several individual barriers. However, the single barrier view based determination of apparent permeability has been the cornerstone of permeation data analysis and still remains suitable for classification of high and low permeability compounds according to the Biopharmaceutical Classification System (Thiel-Demby et al., 2009; Volpe, 2004) and also for the prediction of the extent of intestinal absorption of passively absorbed compounds (Artursson et al., 2001). On the other hand, the single barrier view in permeation data analysis suffers some clear disadvantages; including the fact that the assumptions about sink conditions and recovery may be experimentally impossible to meet adequately. Moreover, there are no universal correction terms available for violations of these assumptions (Chapter 6). Therefore, the results of single barrier analysis of *in vitro* data are not always suitable for the quantitative uncoupling of the different mechanisms involved or mechanism based *in vitro – in vivo* extrapolation (Chapter 8). Consequently, more sophisticated data analysis approaches are required.

Compared to single barrier models, compartmental models provide a possibility to describe the transport phenomena during the *in vitro* permeation experiments in a more mechanistic manner and, thus, to give additional insights into the mechanisms involved in drug disposition (Chapters 6, 7 and 8). The rationale in using *in vitro* experiments as a model for the *in vivo* situation is based on the assumption that the drug behaviour *in vitro* is mechanistically similar to that occurring *in vivo*. Therefore, it is reasonable to expect that mechanistic modeling of the *in vitro* experiments could propose partial model structures feasible for simulating the *in vivo* situation. Simultaneously, modeling of the *in vitro* experiments seems a promising approach for determination of input parameters for *in vivo* simulations (Chapter 8). In addition to the interplay of passive and active transport kinetics in the intestinal epithelia, the focus of the current study, similar data analysis approaches have been applied for gaining insights into 'local kinetics' comprising metabolism coupled with transport kinetics in liver (Hallifax and Houston, 2006; Pelkonen et al., 2008; Poirier et al., 2008).

Although compartmental modeling seems a feasible and promising approach for analysing *in vitro* data for IVIVE, the performance can and should still be improved and also the validity of this approach still requires further verification. On the one hand, more rigorous modeling of *in vitro* experiments would benefit from more detailed experimental local and temporal concentration data within the system. On the other hand, as a routine approach collecting all the possible experimental detail would not be feasible in practice. Finding the balance between the extent of experimental detail and practical feasibility however requires a thorough insight into the system, i.e. what is crucial and what is trivial. In addition to the improvements in obtaining meaningful data from *in vitro* systems, also high quality physiological data, such as expression levels and population variation of transporters and enzymes in clinical setting are of major importance in improving the performance of physiologically based IVIVE (Sugano, 2009b).

In conclusion, the potential of physiologically based IVIVE is yet to be fully harnessed. There have been some clear advances, but nonetheless, the models involved can and should be further developed at both *in vitro* and *in vivo* ends of IVIVE so as to obtain more accurate, precise and reliable predictions. Moreover, if and when successful, physiologically based IVIVE should not be restricted to pharmacokinetics, but should be extended also to the interplay between pharmacokinetics and pharmacodynamics. At the end of the day, if pharmacokinetics is not coupled with pharmacodynamics it is only 'kinetics' without 'pharmaco'.

10 Conclusions

The present studies were conducted in order to understand how passive disposition kinetics affects the observed P-gp transporter kinetics in *in vitro* experiments. Alterations which are expected to affect the passive disposition kinetics but not the P-gp function *per se*, were experimentally tested in order to tease out the effects of the passive disposition. Furthermore, because active transport cannot be studied in the absence of passive disposition, a rigorous analysis of active transport must be based on a thorough understanding of the interplay between these two. Thus, the main focus of these studies was placed upon modeling initially of the kinetics of passive disposition only and, subsequently on passive disposition accompanied with active transport during cell permeation experiments. The modeling aimed also to determine kinetic parameters that might be applicable for *in vitro – in vivo* extrapolation. Furthermore, the pitfalls of the traditional *in vitro* permeation data analysis approaches were explored. The main conclusions that can be drawn from these studes are:

1. Minor alterations in the experimental setup affecting the passive disposition of the P-gp substrates may have a significant effect on the apparent concentration dependency of P-gp function and thus may hamper the correct interpretation of the data.
2. Single barrier assumption based data analysis is often an over-simplified view in cell monolayer permeation data analysis, especially when a detailed mechanistic insight is to be obtained.
3. Compartmental model based analysis of cell permeation data seems a promising approach for determining the active and passive drug disposition kinetics *in vitro*.

11 References

Adachi Y, Suzuki H, Sugiyama Y. (2001) Comparative studies on in vitro methods for evaluating in vivo function of MDR1 P-glycoprotein. *Pharm Res* 18:1660-1668.

Adson A, Burton PS, Raub TJ, Barsuhn CL, Audus KL, Ho NF. (1995) Passive diffusion of weak organic electrolytes across Caco-2 cell monolayers: Uncoupling the contributions of hydrodynamic, transcellular, and paracellular barriers. *J Pharm Sci* 84:1197-1204.

Agoram B, Woltosz WS, Bolger MB. (2001) Predicting the impact of physiological and biochemical processes on oral drug bioavailability. *Adv Drug Deliv Rev* 50 Suppl 1:S41-67.

Ahlin G, Hilgendorf C, Al-Khalili Szigyarto C, Uhlen M, Karlsson JE, Artursson P. (2009) Endogenous gene and protein expression of drug transporting proteins in cell lines routinely used in drug discovery programs. *Drug Metab Dispos* 37:2275-2283.

Al-Awqati Q. (1999) One hundred years of membrane permeability: Does overton still rule? *Nat Cell Biol* 1:E201-2.

Altenberg GA, Young G, Horton JK, Glass D, Belli JA, Reuss L. (1993) Changes in intra- or extracellular pH do not mediate P-glycoprotein-dependent multidrug resistance. *Proc Natl Acad Sci U S A* 90:9735-9738.

Ambudkar SV, Cardarelli CO, Pashinsky I, Stein WD. (1997) Relation between the turnover number for vinblastine transport and for vinblastine-stimulated ATP hydrolysis by human P-glycoprotein. *J Biol Chem* 272:21160-21166.

Ambudkar SV, Dey S, Hrycyna CA, Ramachandra M, Pastan I, Gottesman MM. (1999) Biochemical, cellular, and pharmacological aspects of the multidrug transporter. *Annu Rev Pharmacol Toxicol* 39:361-398.

Ambudkar SV, Kim IW, Sauna ZE. (2006) The power of the pump: Mechanisms of action of P-glycoprotein (ABCB1). *Eur J Pharm Sci* 27:392-400.

Apiwattanakul N, Sekine T, Chairoungdua A, Kanai Y, Nakajima N, Sophasan S, Endou H. (1999) Transport properties of nonsteroidal anti-inflammatory drugs by organic anion transporter 1 expressed in xenopus laevis oocytes. *Mol Pharmacol* 55:847-854.

Artursson P, Palm K, Luthman K. (2001) Caco-2 monolayers in experimental and theoretical predictions of drug transport. *Adv Drug Deliv Rev* 46:27-43.

Asokan A and Cho MJ. (2002) Exploitation of intracellular pH gradients in the cellular delivery of macromolecules. *J Pharm Sci* 91:903-913.

Austin RP, Davis AM, Manners CN. (1995) Partitioning of ionizing molecules between aqueous buffers and phospholipid vesicles. *J Pharm Sci* 84:1180-1183.

Avdeef A. (2010) Leakiness and size exclusion of paracellular channels in cultured epithelial cell monolayers-interlaboratory comparison. *Pharm Res 27:480-489*.

Avdeef A. (2003) Absorption and drug development: Solubility, permeability and charge state, Wiley-Interscience, Hoboken, NJ.

Avdeef A, Artursson P, Neuhoff S, Lazorova L, Gråsjö J, Tavelin S. (2005) Caco-2 permeability of weakly basic drugs predicted with the double-sink PAMPA pKa(flux) method. *Eur J Pharm Sci* 24:333-349.

Avdeef A and Box KJ. (1995) Sirius technical application notes (STAN), Sirius Analytical Instruments Ltd., Forest Row, UK.

Avdeef A and Tam KY. (2010) How well can the caco-2/Madin-darby canine kidney models predict effective human jejunal permeability? (dagger). *J Med Chem* DOI: 10.1021/jm901846t.

Badhan R, Penny J, Galetin A, Houston JB. (2009) Methodology for development of a physiological model incorporating CYP3A and P-glycoprotein for the prediction of intestinal drug absorption. *J Pharm Sci* 98:2180-2197.

Balakrishnan A, Hussainzada N, Gonzalez P, Bermejo M, Swaan PW, Polli JE. (2007) Bias in estimation of transporter kinetic parameters from overexpression systems: Interplay of transporter expression level and substrate affinity. *J Pharmacol Exp Ther* 320:133-144.

Balayssac D, Authier N, Cayre A, Coudore F. (2005) Does inhibition of P-glycoprotein lead to drug-drug interactions? *Toxicol Lett* 156:319-329.

Balimane PV and Chong S. (2005) Cell culture-based models for intestinal permeability: A critique. *Drug Discov Today* 10:335-343.

Balimane PV, Han YH, Chong S. (2006) Current industrial practices of assessing permeability and P-glycoprotein interaction. *AAPS J* 8:E1-13.

Barry PH and Diamond JM. (1984) Effects of unstirred layers on membrane phenomena. *Physiol Rev* 64:763-872.

Bartholome K, Rius M, Letschert K, Keller D, Timmer J, Keppler D. (2007) Data-based mathematical modeling of vectorial transport across double-transfected polarized cells. *Drug Metab Dispos* 35:1476-1481.

Bentz J, Tran TT, Polli JW, Ayrton A, Ellens H. (2005) The steady-state michaelis-menten analysis of P-glycoprotein mediated transport through a confluent cell monolayer cannot predict the correct michaelis constant km. *Pharm Res* 22:1667-1677.

Berggren S, Gall C, Wollnitz N, Ekelund M, Karlbom U, Hoogstraate J, Schrenk D, Lennernäs H. (2007) Gene and protein expression of P-glycoprotein, MRP1, MRP2, and CYP3A4 in the small and large human intestine. *Mol Pharm* 4:252-257.

Bogner P, Skehan P, Kenney S, Sainz E, Akeson MA, Friedman SJ. (1992) Stabilization of intercellular contacts in MDCK cells during Ca2+ deprivation. selective effects of monocarboxylic acids on desmosomes. *J Cell Sci* 103 (Pt 2):463-473.

Bolger MB, Lukacova V, Woltosz WS. (2009) Simulations of the nonlinear dose dependence for substrates of influx and efflux transporters in the human intestine. *AAPS J* 11:353-363.

Boobis A, Gundert-Remy U, Kremers P, Macheras P, Pelkonen O. (2002) In silico prediction of ADME and pharmacokinetics. report of an expert meeting organised by COST B15. *Eur J Pharm Sci* 17:183-193.

Borgnia MJ, Eytan GD, Assaraf YG. (1996) Competition of hydrophobic peptides, cytotoxic drugs, and chemosensitizers on a common P-glycoprotein pharmacophore as revealed by its ATPase activity. *J Biol Chem* 271:3163-3171.

Bourdet DL, Pollack GM, Thakker DR. (2006) Intestinal absorptive transport of the hydrophilic cation ranitidine: A kinetic modeling approach to elucidate the role of uptake and efflux transporters and paracellular vs. transcellular transport in caco-2 cells. *Pharm Res* 23:1178-1187.

Bowman EJ, Siebers A, Altendorf K. (1988) Bafilomycins: A class of inhibitors of membrane ATPases from microorganisms, animal cells, and plant cells. *Proc Natl Acad Sci U S A* 85:7972-7976.

Braun A, Hammerle S, Suda K, Rothen-Rutishauser B, Gunthert M, Kramer SD, Wunderli-Allenspach H. (2000) Cell cultures as tools in biopharmacy. *Eur J Pharm Sci* 11 Suppl 2:S51-60.

Chan LM, Lowes S, Hirst BH. (2004) The ABCs of drug transport in intestine and liver: Efflux proteins limiting drug absorption and bioavailability. *Eur J Pharm Sci* 21:25-51.

Chang G. (2003) Multidrug resistance ABC transporters. *FEBS Lett* 555:102.

Cong D, Doherty M, Pang KS. (2000) A new physiologically based, segregated-flow model to explain route-dependent intestinal metabolism. *Drug Metab Dispos* 28:224-235.

Cordon-Cardo C, O'Brien JP, Casals D, Rittman-Grauer L, Biedler JL, Melamed MR, Bertino JR. (1989) Multidrug-resistance gene (P-glycoprotein) is expressed by endothelial cells at blood-brain barrier sites. *Proc Natl Acad Sci U S A* 86:695-698.

Crespi CL, Fox L, Stocker P, Hu M, Steimel DT. (2000) Analysis of drug transport and metabolism in cell monolayer systems that have been modified by cytochrome P4503A4 cDNA-expression. *Eur J Pharm Sci* 12:63-68.

Dahan A, Sabit H, Amidon GL. (2009) Multiple efflux pumps are involved in the transepithelial transport of colchicine: Combined effect of p-glycoprotein and multidrug resistance-associated protein 2 leads to decreased intestinal absorption throughout the entire small intestine. *Drug Metab Dispos* 37:2028-2036.

Dahl SG, Aarons L, Gundert-Remy U, Karlsson MO, Schneider YJ, Steimer JL, Troconiz IF. (2009) Incorporating physiological and biochemical mechanisms into pharmacokinetic-pharmacodynamic models: A conceptual framework*. *Basic Clin Pharmacol Toxicol* .

Daniel H, Neugebauer B, Kratz A, Rehner G. (1985) Localization of acid microclimate along intestinal villi of rat jejunum. *Am J Physiol* 248:G293-8.

De Buck SS and Mackie CE. (2007) Physiologically based approaches towards the prediction of pharmacokinetics: In vitro-in vivo extrapolation. *Expert Opin Drug Metab Toxicol* 3:865-878.

Del Amo EM, Heikkinen AT, Mönkkönen J. (2009) In vitro-in vivo correlation in p-glycoprotein mediated transport in intestinal absorption. *Eur J Pharm Sci* 36:200-211.

DiMasi JA, Hansen RW, Grabowski HG. (2003) The price of innovation: New estimates of drug development costs. *J Health Econ* 22:151-185.

Dressman JB, Amidon GL, Reppas C, Shah VP. (1998) Dissolution testing as a prognostic tool for oral drug absorption: Immediate release dosage forms. *Pharm Res* 15:11-22.

Dudley AJ, Bleasby K, Brown CD. (2000) The organic cation transporter OCT2 mediates the uptake of beta-adrenoceptor antagonists across the apical membrane of renal LLC-PK(1) cell monolayers. *Br J Pharmacol* 131:71-79.

Duvvuri M, Gong Y, Chatterji D, Krise JP. (2004) Weak base permeability characteristics influence the intracellular sequestration site in the multidrug-resistant human leukemic cell line HL-60. *J Biol Chem* 279:32367-32372.

Duvvuri M and Krise JP. (2005a) Intracellular drug sequestration events associated with the emergence of multidrug resistance: A mechanistic review. *Front Biosci* 10:1499-1509.

Duvvuri M and Krise JP. (2005b) A novel assay reveals that weakly basic model compounds concentrate in lysosomes to an extent greater than pH-partitioning theory would predict. *Mol Pharm* 2:440-448.

Englund G, Hallberg P, Artursson P, Michaelsson K, Melhus H. (2004) Association between the number of coadministered P-glycoprotein inhibitors and serum digoxin levels in patients on therapeutic drug monitoring. *BMC Med* 2:8.

Englund G, Rorsman F, Ronnblom A, Karlbom U, Lazorova L, Gråsjö J, Kindmark A, Artursson P. (2006) Regional levels of drug transporters along the human intestinal tract: Co-expression of ABC and SLC transporters and comparison with caco-2 cells. *Eur J Pharm Sci* 29:269-277.

Engman HA, Lennernäs H, Taipalensuu J, Otter C, Leidvik B, Artursson P. (2001) CYP3A4, CYP3A5, and MDR1 in human small and large intestinal cell lines suitable for drug transport studies. *J Pharm Sci* 90:1736-1751.

Fagerholm U. (2007a) Prediction of human pharmacokinetics--evaluation of methods for prediction of hepatic metabolic clearance. *J Pharm Pharmacol* 59:803-828.

Fagerholm U. (2007b) Prediction of human pharmacokinetics--gastrointestinal absorption. *J Pharm Pharmacol* 59:905-916.

Fagerholm U and Lennernäs H. (1995) Experimental estimation of the effective unstirred water layer thickness in the human jejunum, and its importance in oral drug absorption. *European Journal of Pharmaceutical Sciences* 3:247-253.

FDA. (2006) Draft guidance for industry: Drug interaction studies — study design, data dnalysis, and implications for dosing and labeling. .

Feng B, Mills JB, Davidson RE, Mireles RJ, Janiszewski JS, Troutman MD, de Morais SM. (2008) In vitro P-glycoprotein assays to predict the in vivo interactions of P-glycoprotein with drugs in the central nervous system. *Drug Metab Dispos* 36:268-275.

Fihn BM, Sjoqvist A, Jodal M. (2000) Permeability of the rat small intestinal epithelium along the villus-crypt axis: Effects of glucose transport. *Gastroenterology* 119:1029-1036.

Fisher JM, Wrighton SA, Watkins PB, Schmiedlin-Ren P, Calamia JC, Shen DD, Kunze KL, Thummel KE. (1999) First-pass midazolam metabolism catalyzed by 1alpha,25-dihydroxy vitamin D3-modified caco-2 cell monolayers. *J Pharmacol Exp Ther* 289:1134-1142.

Flynn GL, Yalkowsky SH, Roseman TJ. (1974) Mass transport phenomena and models: Theoretical concepts. *J Pharm Sci* 63:479-510.

Fromm MF. (2003) Importance of P-glycoprotein for drug disposition in humans. *Eur J Clin Invest* 33 Suppl 2:6.

Giacomini KM, Huang SM, Tweedie DJ, Benet LZ, Brouwer KL, Chu X, Dahlin A, Evers R, Fischer V, Hillgren KM, Hoffmaster KA, Ishikawa T, Keppler D, Kim RB, Lee CA, Niemi M, Polli JW, Sugiyama Y, Swaan PW, Ware JA, Wright SH, Wah Yee S, Zamek-Gliszczynski MJ, Zhang L. (2010) Membrane transporters in drug development. *Nat Rev Drug Discov* 9:215-236.

Glavinas H, Mehn D, Jani M, Oosterhuis B, Heredi-Szabo K, Krajcsi P. (2008) Utilization of membrane vesicle preparations to study drug-ABC transporter interactions. *Expert Opin Drug Metab Toxicol* 4:721-732.

Goh LB, Spears KJ, Yao D, Ayrton A, Morgan P, Roland Wolf C, Friedberg T. (2002) Endogenous drug transporters in in vitro and in vivo models for the prediction of drug disposition in man. *Biochem Pharmacol* 64:1569-1578.

Gonzalez-Alvarez I, Fernandez-Teruel C, Garrigues TM, Casabo VG, Ruiz-Garcia A, Bermejo M. (2005) Kinetic modelling of passive transport and active efflux of a fluoroquinolone across caco-2 cells using a compartmental approach in NONMEM. *Xenobiotica* 35:1067-1088.

Hallifax D and Houston JB. (2006) Uptake and intracellular binding of lipophilic amine drugs by isolated rat hepatocytes and implications for prediction of in vivo metabolic clearance. *Drug Metab Dispos* 34:1829-1836.

Hayeshi R, Hilgendorf C, Artursson P, Augustijns P, Brodin B, Dehertogh P, Fisher K, Fossati L, Hovenkamp E, Korjamo T, Masungi C, Maubon N, Mols R, Mullertz A, Monkkonen J, O'Driscoll C, Oppers-Tiemissen HM, Ragnarsson EG, Rooseboom M, Ungell AL. (2008a) Comparison of drug transporter gene expression and functionality in caco-2 cells from 10 different laboratories. *Eur J Pharm Sci* 35:383-396.

Hayeshi R, Masimirembwa C, Mukanganyama S, Ungell AL. (2008b) Lysosomal trapping of amodiaquine: Impact on transport across intestinal epithelia models. *Biopharm Drug Dispos* 29:324-334.

Hidalgo IJ. (2001) Assessing the absorption of new pharmaceuticals. *Curr Top Med Chem* 1:385-401.

Hilgendorf C, Ahlin G, Seithel A, Artursson P, Ungell AL, Karlsson J. (2007) Expression of thirty-six drug transporter genes in human intestine, liver, kidney, and organotypic cell lines. *Drug Metab Dispos* 35:1333-1340.

Ho NFH, Raub TJ, Burton PS, Barsuhn CL, Adson A, Audus KL, Borchardt RT. (1999) Quantitative approaches to delineate passive transport mechanisms in cell culture monolayers, in *Transport Processes in Pharmaceutical Systems.* (Amidon GL, Lee PI and Topp EM eds) pp 219-316, Marcel Dekker Incorporated, New York, Basel.

Hollander D. (1992) The intestinal permeability barrier. A hypothesis as to its regulation and involvement in crohn's disease. *Scand J Gastroenterol* 27:721-726.

Huang W, Lee SL, Yu LX. (2009) Mechanistic approaches to predicting oral drug absorption. *AAPS J* 11:217-224.

Hubatsch I, Ragnarsson EG, Artursson P. (2007) Determination of drug permeability and prediction of drug absorption in caco-2 monolayers. *Nat Protoc* 2:2111-2119.

Hyafil F, Vergely C, Du Vignaud P, Grand-Perret T. (1993) In vitro and in vivo reversal of multidrug resistance by GF120918, an acridonecarboxamide derivative. *Cancer Res* 53:4595-4602.

Irvine JD, Takahashi L, Lockhart K, Cheong J, Tolan JW, Selick HE, Grove JR. (1999) MDCK (madin-darby canine kidney) cells: A tool for membrane permeability screening. *J Pharm Sci* 88:28-33.

Ito S, Woodland C, Sarkadi B, Hockmann G, Walker SE, Koren G. (1999) Modeling of P-glycoprotein-involved epithelial drug transport in MDCK cells. *Am J Physiol* 277:F84-96.

Jamei M, Dickinson GL, Rostami-Hodjegan A. (2009a) A framework for assessing inter-individual variability in pharmacokinetics using virtual human populations and integrating general knowledge of physical chemistry, biology, anatomy, physiology and genetics: A tale of 'bottom-up' vs 'top-down' recognition of covariates. *Drug Metab Pharmacokinet* 24:53-75.

Jamei M, Turner D, Yang J, Neuhoff S, Polak S, Rostami-Hodjegan A, Tucker G. (2009b) Population-based mechanistic prediction of oral drug absorption. *AAPS J* 11:225-237.

Kalvass JC and Pollack GM. (2007) Kinetic considerations for the quantitative assessment of efflux activity and inhibition: Implications for understanding and predicting the effects of efflux inhibition. *Pharm Res* 24:265-276.

Kapitza SB, Michel BR, van Hoogevest P, Leigh ML, Imanidis G. (2007) Absorption of poorly water soluble drugs subject to apical efflux using phospholipids as solubilizers in the caco-2 cell model. *Eur J Pharm Biopharm* 66:146-158.

Karlsson J, Ungell A, Grasjo J, Artursson P. (1999) Paracellular drug transport across intestinal epithelia: Influence of charge and induced water flux. *Eur J Pharm Sci* 9:47-56.

Karlsson J and Artursson P. (1991) A method for the determination of cellular permeability coefficients and aqueous boundary layer thickness in monolayers of intestinal epithelial (caco-2) cells grown in permeable filter chambers. *Int J Pharm* 71:55-64.

Kaufmann AM and Krise JP. (2007) Lysosomal sequestration of amine-containing drugs: Analysis and therapeutic implications. *J Pharm Sci* 96:729-746.

Knight B, Troutman M, Thakker DR. (2006) Deconvoluting the effects of P-glycoprotein on intestinal CYP3A: A major challenge. *Curr Opin Pharmacol* 6:528-532.

Komin N and Toral R. (2009) Drug absorption through a cell monolayer: A theoretical work on a non-linear three-compartment model. *European Journal of Pharmaceutical Sciences* 37:106-114.

Korjamo T, Heikkinen AT, Mönkkönen J. (2009) Analysis of unstirred water layer in *in vitro* permeability experiments. *J Pharm Sci* 98:4469-4479.

Korjamo T, Heikkinen AT, Waltari P, Mönkkönen J. (2008) The asymmetry of the unstirred water layer in permeability experiments. *Pharm Res* 25:1714-1722.

Korjamo T, Honkakoski P, Toppinen MR, Niva S, Reinisalo M, Palmgren JJ, Mönkkönen J. (2005) Absorption properties and P-glycoprotein activity of modified caco-2 cell lines. *Eur J Pharm Sci* 26:266-279.

Korjamo T, Kemilainen H, Heikkinen AT, Mönkkönen J. (2007) Decrease in intracellular concentration causes the shift in km value of efflux pump substrates. *Drug Metab Dispos* 35:1574-1579.

Korjamo T, Mönkkönen J, Uusitalo J, Turpeinen M, Pelkonen O, Honkakoski P. (2006) Metabolic and efflux properties of caco-2 cells stably transfected with nuclear receptors. *Pharm Res* 23:1991-2001.

Lacave R, Ouar Z, Paulais M, Bens M, Ricci S, Cluzeaud F, Vandewalle A. (1999) Lysosomotropic agents increase vinblastine efflux from mouse MDR proximal kidney cells exhibiting vectorial drug transport. *J Cell Physiol* 178:247-257.

Lande MB, Donovan JM, Zeidel ML. (1995) The relationship between membrane fluidity and permeabilities to water, solutes, ammonia, and protons. *J Gen Physiol* 106:67-84.

Lau YY, Wu CY, Okochi H, Benet LZ. (2004) Ex situ inhibition of hepatic uptake and efflux significantly changes metabolism: Hepatic enzyme-transporter interplay. *J Pharmacol Exp Ther* 308:1040-1045.

Legen I and Kristl A. (2003) Factors affecting the microclimate pH of the rat jejunum in ringer bicarbonate buffer. *Biol Pharm Bull* 26:886-889.

Lennernäs H. (2007) Intestinal permeability and its relevance for absorption and elimination. *Xenobiotica* 37:1015-1051.

Li C, Liu T, Broske L, Brisson JM, Uss AS, Njoroge FG, Morrison RA, Cheng KC. (2008) Permeability evaluation of peptidic HCV protease inhibitors in caco-2 cells-correlation with in vivo absorption predicted in humans. *Biochem Pharmacol* 76:1757-1764.

Liang E, Liu P, Dinh S. (2007) Use of a pH-sensitive fluorescent probe for measuring intracellular pH of caco-2 cells. *Int J Pharm* 338:104-109.

Linnankoski J, Makela J, Palmgren J, Mauriala T, Vedin C, Ungell AL, Lazorova L, Artursson P, Urtti A, Yliperttula M. (2009) Paracellular porosity and pore size of the human intestinal epithelium in tissue and cell culture models. *J Pharm Sci* .

Linnankoski J, Ranta VP, Yliperttula M, Urtti A. (2008) Passive oral drug absorption can be predicted more reliably by experimental than computational models--fact or myth. *Eur J Pharm Sci* 34:129-139.

Litman T, Skovsgaard T, Stein WD. (2003) Pumping of drugs by P-glycoprotein: A two-step process? *J Pharmacol Exp Ther* 307:846.

Liu S, Tam D, Chen X, Pang KS. (2006) P-glycoprotein and an unstirred water layer barring digoxin absorption in the vascularly perfused rat small intestine preparation: Induction studies with pregnenolone-16alpha-carbonitrile. *Drug Metab Dispos* 34:1468-1479.

Loftsson T and Brewster ME. (2008) Physicochemical properties of water and its effect on drug delivery. A commentary. *Int J Pharm* 354:248-254.

Luby-Phelps K. (2000) Cytoarchitecture and physical properties of cytoplasm: Volume, viscosity, diffusion, intracellular surface area. *Int Rev Cytol* 192:189-221.

Maier-Salamon A, Hagenauer B, Wirth M, Gabor F, Szekeres T, Jager W. (2006) Increased transport of resveratrol across monolayers of the human intestinal caco-2 cells is mediated by inhibition and saturation of metabolites. *Pharm Res* 23:2107-2115.

Markov AG, Veshnyakova A, Fromm M, Amasheh M, Amasheh S. (2010) Segmental expression of claudin proteins correlates with tight junction barrier properties in rat intestine. *J Comp Physiol B* 180:591-598.

Matsson P. (2007) ATP-binding cassette efflux transporters and passive membrane permeability in drug absorption and disposition. *Digital Comprehensive Summaries of Uppsala Dissertations from the Faculty of Pharmacy* 67.

Matsson P, Bergstrom CA, Nagahara N, Tavelin S, Norinder U, Artursson P. (2005) Exploring the role of different drug transport routes in permeability screening. *J Med Chem* 48:604-613.

Matsson P, Pedersen JM, Norinder U, Bergstrom CA, Artursson P. (2009) Identification of novel specific and general inhibitors of the three major human ATP-binding cassette transporters P-gp, BCRP and MRP2 among registered drugs. *Pharm Res* 26:1816-1831.

Mouly S and Paine MF. (2003) P-glycoprotein increases from proximal to distal regions of human small intestine. *Pharm Res* 20:1595-1599.

Neuhoff S. (2005) Refined in vitro models for prediction of intestinal drug transport. *Digital Comprehensive Summaries of Uppsala Dissertations from the Faculty of Pharmacy* 14.

Neuhoff S, Ungell AL, Zamora I, Artursson P. (2003) pH-dependent bidirectional transport of weakly basic drugs across caco-2 monolayers: Implications for drug-drug interactions. *Pharm Res* 20:1141.

Nielsen CU, Amstrup J, Nielsen R, Steffansen B, Frokjaer S, Brodin B. (2003) Epidermal growth factor and insulin short-term increase hPepT1-mediated glycylsarcosine uptake in caco-2 cells. *Acta Physiol Scand* 178:139-148.

Nielsen PE and Avdeef A. (2004) PAMPA--a drug absorption in vitro model 8. apparent filter porosity and the unstirred water layer. *Eur J Pharm Sci* 22:33-41.

Ohashi R, Tamai I, Yabuuchi H, Nezu JI, Oku A, Sai Y, Shimane M, Tsuji A. (1999) Na(+)-dependent carnitine transport by organic cation transporter (OCTN2): Its pharmacological and toxicological relevance. *J Pharmacol Exp Ther* 291:778-784.

Ohkuma S and Poole B. (1981) Cytoplasmic vacuolation of mouse peritoneal macrophages and the uptake into lysosomes of weakly basic substances. *J Cell Biol* 90:656-664.

Omote H and Al-Shawi MK. (2006) Interaction of transported drugs with the lipid bilayer and P-glycoprotein through a solvation exchange mechanism. *Biophys J* 90:4046-4059.

Omote H and Al-Shawi MK. (2002) A novel electron paramagnetic resonance approach to determine the mechanism of drug transport by P-glycoprotein. *J Biol Chem* 277:45688-45694.

Owen A, Chandler B, Back DJ. (2005) The implications of P-glycoprotein in HIV: Friend or foe? *Fundam Clin Pharmacol* 19:283-296.

Pade V and Stavchansky S. (1997) Estimation of the relative contribution of the transcellular and paracellular pathway to the transport of passively absorbed drugs in the caco-2 cell culture model. *Pharm Res* 14:1210-1215.

Paine MF, Khalighi M, Fisher JM, Shen DD, Kunze KL, Marsh CL, Perkins JD, Thummel KE. (1997) Characterization of interintestinal and intraintestinal variations in human CYP3A-dependent metabolism. *J Pharmacol Exp Ther* 283:1552-1562.

Paine MF, Shen DD, Kunze KL, Perkins JD, Marsh CL, McVicar JP, Barr DM, Gillies BS, Thummel KE. (1996) First-pass metabolism of midazolam by the human intestine. *Clin Pharmacol Ther* 60:14-24.

Palm K, Luthman K, Ros J, Gråsjö J, Artursson P. (1999) Effect of molecular charge on intestinal epithelial drug transport: PH-dependent transport of cationic drugs. *J Pharmacol Exp Ther* 291:435-443.

Palmgren JJ, Mönkkönen J, Korjamo T, Hassinen A, Auriola S. (2006) Drug adsorption to plastic containers and retention of drugs in cultured cells under in vitro conditions. *Eur J Pharm Biopharm* 64:369-378.

Pang KS. (2003) Modeling of intestinal drug absorption: Roles of transporters and metabolic enzymes (for the gillette review series). *Drug Metab Dispos* 31:1507-1519.

Pedersen JM, Matsson P, Bergstrom CA, Norinder U, Hoogstraate J, Artursson P. (2008) Prediction and identification of drug interactions with the human ATP-binding cassette transporter multidrug-resistance associated protein 2 (MRP2; ABCC2). *J Med Chem* 51:3275-3287.

Pelkonen O, Kapitulnik J, Gundert-Remy U, Boobis AR, Stockis A. (2008) Local kinetics and dynamics of xenobiotics. *Crit Rev Toxicol* 38:697-720.

Pohl P, Saparov SM, Antonenko YN. (1998) The size of the unstirred layer as a function of the solute diffusion coefficient. *Biophys J* 75:1403-1409.

Poirier A, Lave T, Portmann R, Brun ME, Senner F, Kansy M, Grimm HP, Funk C. (2008) Design, data analysis, and simulation of in vitro drug transport kinetic experiments using a mechanistic in vitro model. *Drug Metab Dispos* 36:2434-2444.

Polgar O and Bates SE. (2005) ABC transporters in the balance: Is there a role in multidrug resistance? *Biochem Soc Trans* 33:241-245.

Polli JE, Yu LX, Cook JA, Amidon GL, Borchardt RT, Burnside BA, Burton PS, Chen ML, Conner DP, Faustino PJ, Hawi AA, Hussain AS, Joshi HN, Kwei G, Lee VH, Lesko LJ, Lipper RA, Loper AE, Nerurkar SG, Polli JW, Sanvordeker DR, Taneja R, Uppoor RS, Vattikonda CS, Wilding I, Zhang G. (2004) Summary workshop report: Biopharmaceutics classification system--implementation challenges and extension opportunities. *J Pharm Sci* 93:1375-1381.

Polli JW, Wring SA, Humphreys JE, Huang L, Morgan JB, Webster LO, Serabjit-Singh CS. (2001) Rational use of in vitro P-glycoprotein assays in drug discovery. *J Pharmacol Exp Ther* 299:620-628.

Poole B and Ohkuma S. (1981) Effect of weak bases on the intralysosomal pH in mouse peritoneal macrophages. *J Cell Biol* 90:665-669.

Porcelli L, Lemos C, Peters GJ, Paradiso A, Azzariti A. (2009) Intracellular trafficking of MDR transporters and relevance of SNPs. *Curr Top Med Chem* 9:197-208.

Prueksaritanont T, Gorham LM, Hochman JH, Tran LO, Vyas KP. (1996) Comparative studies of drug-metabolizing enzymes in dog, monkey, and human small intestines, and in caco-2 cells. *Drug Metab Dispos* 24:634-642.

Raub TJ, Barsuhn CL, Williams LR, Decker DE, Sawada GA, Ho NF. (1993) Use of a biophysical-kinetic model to understand the roles of protein binding and membrane partitioning on passive diffusion of highly lipophilic molecules across cellular barriers. *J Drug Target* 1:269-286.

Rostami-Hodjegan A and Tucker GT. (2007) Simulation and prediction of in vivo drug metabolism in human populations from in vitro data. *Nat Rev Drug Discov* 6:140-148.

Saitoh R, Miyayama T, Mitsui T, Akiba Y, Higashida A, Takata S, Kawanishi T, Aso Y, Itoh Z, Omura S. (2007) Nonlinear intestinal pharmacokinetics of mitemcinal, the first acid-resistant non-peptide motilin receptor agonist, in rats. *Xenobiotica* 37:1421-1432.

Sakurai A, Onishi Y, Hirano H, Seigneuret M, Obanayama K, Kim G, Liew EL, Sakaeda T, Yoshiura K, Niikawa N, Sakurai M, Ishikawa T. (2007) Quantitative structure--activity relationship analysis and molecular dynamics simulation to functionally validate nonsynonymous polymorphisms of human ABC transporter ABCB1 (P-glycoprotein/MDR1). *Biochemistry* 46:7678-7693.

Saparov SM, Antonenko YN, Pohl P. (2006) A new model of weak acid permeation through membranes revisited: Does overton still rule? *Biophys J* 90:L86-8.

Sarkadi B, Price EM, Boucher RC, Germann UA, Scarborough GA. (1992) Expression of the human multidrug resistance cDNA in insect cells generates a high activity drug-stimulated membrane ATPase. *J Biol Chem* 267:4854-4858.

Sawada GA, Barsuhn CL, Lutzke BS, Houghton ME, Padbury GE, Ho NF, Raub TJ. (1999) Increased lipophilicity and subsequent cell partitioning decrease passive transcellular diffusion of novel, highly lipophilic antioxidants. *J Pharmacol Exp Ther* 288:1317-1326.

Schellens JHM, Malingré MM, Kruijtzer CMF, Bardelmeijer HA, van Tellingen O, Schinkel AH, Beijnen JH. (2000) Modulation of oral bioavailability of anticancer drugs: From mouse to man. *European Journal of Pharmaceutical Sciences* 12:103-110.

Schwab D, Fischer H, Tabatabaei A, Poli S, Huwyler J. (2003) Comparison of in vitro P-glycoprotein screening assays: Recommendations for their use in drug discovery. *J Med Chem* 46:1716-1725.

Seelig A and Landwojtowicz E. (2000) Structure-activity relationship of P-glycoprotein substrates and modifiers. *Eur J Pharm Sci* 12:31-40.

Shapiro AB and Ling V. (1998) Stoichiometry of coupling of rhodamine 123 transport to ATP hydrolysis by P-glycoprotein. *Eur J Biochem* 254:189-193.

Sharom FJ, Yu X, Chu JW, Doige CA. (1995) Characterization of the ATPase activity of P-glycoprotein from multidrug-resistant chinese hamster ovary cells. *Biochem J* 308 (Pt 2):381-390.

Shiau YF, Fernandez P, Jackson MJ, McMonagle S. (1985) Mechanisms maintaining a low-pH microclimate in the intestine. *Am J Physiol* 248:G608-17.

Shirasaka Y, Masaoka Y, Kataoka M, Sakuma S, Yamashita S. (2008a) Scaling of in vitro membrane permeability to predict P-glycoprotein-mediated drug absorption in vivo. *Drug Metab Dispos* 36:916-922.

Shirasaka Y, Sakane T, Yamashita S. (2008b) Effect of P-glycoprotein expression levels on the concentration-dependent permeability of drugs to the cell membrane. *J Pharm Sci* 91:553-565.

Shore PA, Brodie BB, Hogben CA. (1957) The gastric secretion of drugs: A pH partition hypothesis. *J Pharmacol Exp Ther* 119:361-369.

Siissalo S, Laine L, Tolonen A, Kaukonen AM, Finel M, Hirvonen J. (2010) Caco-2 cell monolayers as a tool to study simultaneous phase II metabolism and metabolite efflux of indomethacin, paracetamol and 1-naphthol. *Int J Pharm* 383:24-29.

Simons K and van Meer G. (1988) Lipid sorting in epithelial cells. *Biochemistry* 27:6197-6202.

Steffansen B, Nielsen CU, Brodin B, Eriksson AH, Andersen R, Frokjaer S. (2004) Intestinal solute carriers: An overview of trends and strategies for improving oral drug absorption. *Eur J Pharm Sci* 21:3-16.

Strocchi A and Levitt MD. (1993) Role of villous surface area in absorption. science versus religion. *Dig Dis Sci* 38:385-387.

Sugano K. (2010) Possible reduction of effective thickness of intestinal unstirred water layer by particle drifting effect. *Int J Pharm* 387:103-109.

Sugano K. (2009a) Estimation of effective intestinal membrane permeability considering bile micelle solubilisation. *Int J Pharm* 368:116-122.

Sugano K. (2009b) Introduction to computational oral absorption simulation. *Expert Opin Drug Metab Toxicol* 5:259-293.

Sun H and Pang KS. (2008) Permeability, transport, and metabolism of solutes in caco-2 cell monolayers: A theoretical study. *Drug Metab Dispos* 36:102-123.

Sun H, Zhang L, Chow EC, Lin G, Zuo Z, Pang KS. (2008) A catenary model to study transport and conjugation of baicalein, a bioactive flavonoid, in the caco-2 cell monolayer: Demonstration of substrate inhibition. *J Pharmacol Exp Ther* 326:117-126.

Szczesna-Skorupa E and Kemper B. (2008) Influence of protein-protein interactions on the cellular localization of cytochrome P450. *Expert Opin Drug Metab Toxicol* 4:123-136.

Tachibana T, Kitamura S, Kato M, Mitsui T, Shirasaka Y, Yamashita S, Sugiyama Y. (2010) Model analysis of the concentration-dependent permeability of P-gp substrates. *Pharm Res* 27:442-6

Tam D, Sun H, Pang KS. (2003) Influence of P-glycoprotein, transfer clearances, and drug binding on intestinal metabolism in caco-2 cell monolayers or membrane preparations: A theoretical analysis. *Drug Metab Dispos* 31:1214-1226.

Tamai I, Takanaga H, Maeda H, Sai Y, Ogihara T, Higashida H, Tsuji A. (1995) Participation of a proton-cotransporter, MCT1, in the intestinal transport of monocarboxylic acids. *Biochem Biophys Res Commun* 214:482-489.

Thiebaut F, Tsuruo T, Hamada H, Gottesman MM, Pastan I, Willingham MC. (1987) Cellular localization of the multidrug-resistance gene product P-glycoprotein in normal human tissues. *Proc Natl Acad Sci U S A* 84:7735-7738.

Thiel-Demby VE, Humphreys JE, St John Williams LA, Ellens HM, Shah N, Ayrton AD, Polli JW. (2009) Biopharmaceutics classification system: Validation and learnings of an in vitro permeability assay. *Mol Pharm* 6:11-18.

Thomae AV, Wunderli-Allenspach H, Kramer SD. (2005) Permeation of aromatic carboxylic acids across lipid bilayers: The pH-partition hypothesis revisited. *Biophys J* 89:1802-1811.

Thummel KE, O'Shea D, Paine MF, Shen DD, Kunze KL, Perkins JD, Wilkinson GR. (1996) Oral first-pass elimination of midazolam involves both gastrointestinal and hepatic CYP3A-mediated metabolism. *Clin Pharmacol Ther* 59:491-502.

Tran TT, Mittal A, Aldinger T, Polli JW, Ayrton A, Ellens H, Bentz J. (2005) The elementary mass action rate constants of P-gp transport for a confluent monolayer of MDCKII-hMDR1 cells. *Biophys J* 88:715-738.

Tran TT, Mittal A, Gales T, Maleeff B, Aldinger T, Polli JW, Ayrton A, Ellens H, Bentz J. (2004) Exact kinetic analysis of passive transport across a polarized confluent MDCK cell monolayer modeled as a single barrier. *J Pharm Sci* 93:2108-2123.

Troutman MD and Thakker DR. (2003a) Efflux ratio cannot assess P-glycoprotein-mediated attenuation of absorptive transport: Asymmetric effect of P-glycoprotein on

absorptive and secretory transport across caco-2 cell monolayers. *Pharm Res* 20:1200-1209.

Troutman MD and Thakker DR. (2003b) Novel experimental parameters to quantify the modulation of absorptive and secretory transport of compounds by P-glycoprotein in cell culture models of intestinal epithelium. *Pharm Res* 20:1210-1224.

Tubic M, Wagner D, Spahn-Langguth H, Bolger MB, Langguth P. (2006) In silico modeling of non-linear drug absorption for the P-gp substrate talinolol and of consequences for the resulting pharmacodynamic effect. *Pharm Res* 23:1712-1720.

Ungell AB. (2004) Caco-2 replace or refine? *Drug Discovery Today: Technologies* 1:423-430.

Walsh C. (2003) Where will new antibiotics come from? *Nat Rev Microbiol* 1:65-70.

Varma MV and Panchagnula R. (2005) pH-dependent functional activity of P-glycoprotein in limiting intestinal absorption of protic drugs: Kinetic analysis of quinidine efflux in situ. *J Pharm Sci* 94:2632-2643.

Volpe DA. (2004) Permeability classification of representative fluoroquinolones by a cell culture method. *AAPS J* 6:1-6.

Xia CQ, Milton MN, Gan LS. (2007) Evaluation of drug-transporter interactions using in vitro and in vivo models. *Curr Drug Metab* 8:341-363.

Xia CQ, Xiao G, Liu N, Pimprale S, Fox L, Patten CJ, Crespi CL, Miwa G, Gan LS. (2006) Comparison of species differences of P-glycoproteins in beagle dog, rhesus monkey, and human using atpase activity assays. *Mol Pharm* 3:78-86.

Yang J, Jamei M, Yeo KR, Tucker GT, Rostami-Hodjegan A. (2007) Prediction of intestinal first-pass drug metabolism. *Curr Drug Metab* 8:676-684.

Yoshimori T, Yamamoto A, Moriyama Y, Futai M, Tashiro Y. (1991) Bafilomycin A1, a specific inhibitor of vacuolar-type H(+)-ATPase, inhibits acidification and protein degradation in lysosomes of cultured cells. *J Biol Chem* 266:17707-17712.

Youdim KA, Avdeef A, Abbott NJ. (2003) In vitro trans-monolayer permeability calculations: Often forgotten assumptions. *Drug Discov Today* 8:997-1003.

Yu H and Sinko PJ. (1997) Influence of the microporous substratum and hydrodynamics on resistances to drug transport in cell culture systems: Calculation of intrinsic transport parameters. *J Pharm Sci* 86:1448-1457.

Yu LX and Amidon GL. (1999) A compartmental absorption and transit model for estimating oral drug absorption. *Int J Pharm* 186:119-125.

Zhang W, Han Y, Lim SL, Lim LY. (2009) Dietary regulation of P-gp function and expression. *Expert Opin Drug Metab Toxicol* 5:789-801.

Zhang X, Shedden K, Rosania GR. (2006) A cell-based molecular transport simulator for pharmacokinetic prediction and cheminformatic exploration. *Mol Pharm* 3:704-716.

Zhang X, Zheng N, Zou P, Zhu H, Hinestroza JP, Rosania GR. (2010) Cells on pores: A simulation-driven analysis of transcellular small molecule transport. *Mol Pharm* 7:456-467.

Östh K, Gråsjö J, Björk E. (2002) A new method for drug transport studies on pig nasal mucosa using a horizontal ussing chamber. *J Pharm Sci* 91:1259-1273.

Aki T. Heikkinen

Interplay of Passive and Active Drug Disposition in in vitro Models of Drug Absorption and Distribution

In vitro models are often used for prediction of intestinal absorption during the drug development process. However, because of the complexity of the factors affecting permeation through the intestinal epithelia there still are gaps in our capabilities of translating the *in vitro* observed permeation characteristics to the *in vivo* situation. This thesis provides further insights into the dynamics of the drug disposition kinetics in epithelial permeation as well as on the confounding factors involved in *in vitro* experimental settings.

UNIVERSITY OF
EASTERN FINLAND

Publications of the University of Eastern Finland
Dissertations in Health Sciences

ISBN 978-952-61-0139-2